ACCURATE LOCATION OF HYPOCENTERS USING DOUBLE DIFFERENCE AND ACTIVE FAULT STRUCTURES IN GÖKOVA BAY

by

Figen Eskiköy

B.S., Geophysics Engineering, Istanbul University, 2009

Submitted to the Institute for Graduate Studies in
Science and Engineering in partial fulfillment of
the requirements for the degree of
Master of Science

Graduate Program in Geophysics

Boğaziçi University

2014

ACCURATE LOCATION OF HYPOCENTERS USING DOUBLE DIFFERENCE AND ACTIVE FAULT STRUCTURES IN GÖKOVA BAY

APPROVED BY:

Prof. Dr. Mustafa Aktar ……...

(Thesis Supervisor)

Prof. Dr. Semih Ergintav ……

Asst. Prof. Özgün Konca ……..

DATE OF APPROVAL: 14.08.2014

TABLE OF CONTENTS

ACKNOWLEDGEMENTS

First of all, I would like to express my deepest gratitude to my advisor, Prof. Dr. Mustafa Aktar, for his excellent guidance and patience. It has been a great pleasure for me to be one of his students and work with him.

I would like to thank all of my friends and members of Kandilli Observatory and Earthquake Research Institute for their support and contributions.

I would like to acknowledge the REAKT Project for the supports during this thesis.

I would like to thank the National Earthquake Monitoring Center and the administration at KOERI-BU as well as the Department of Earth and Marine Sciences at TUBITAK.

Finally, I would like to thank my parents, Mustafa Eskiköy and Sevim Eskiköy for their unconditional love and understanding. My dear brother, Erman Eskiköy, I appreciate him not only for all his advices and support but also for sharing difficult times and trying to make me happy. I would not be able to complete this study, without their support.

ABSTRACT

ACCURATE LOCATION OF HYPOCENTERS USING DOUBLE DIFFERENCE AND ACTIVE FAULT STRUCTURES IN GÖKOVA BAY

Double Difference Algorithm, HYPODD, is used for relocating the earthquakes in the Gökova Bay. The aim of this thesis is two folds: first we look for the best choice of inversion parameters which determine the performance of HYPODD at local scale, and second, as a by product of the test data used in the study, we determined the active faults in the Gökova Bay. We used four year (April 2006-December 2009) seismic earthquake recordings and relocated 972 events with magnitudes between 1.5 and 4.5.

The inversion part of HYPODD package can be run by using both catalog and cross-correlation data. In this study both methods were used. We have observed that correlation based inversion gives a better picture only if the events in the cluster are very close to each other (<3km). When stations are sufficiently high in number (>4 stations) and well scattered around the seismic zone at moderate distances (i.e. <60 km), we observed that the performance is high, and do not critically depends on the control parameters. The improvement in using hypoDD and in particular correlation based applications is mostly apparent when depth sections are analyzed. The other important observation is that the choice parameters and therefore the final performance entirely depend on the geometry and the distance of event pairs. The parameters MAXSEP, MINLNK, MINOBS are very critical and a conservative selection of these parameters will lead to a drastic reduction of the data set. Separating the data into clusters or not is a matter which entirely depends on the data. If data shows isolated clusters with distinct character each, it would be unrealistic to use a single set of control parameters for all of them, and clustering is recommended.

In term of active fault geometry of the faults in Gökova, it is clear that an offshore fault parallel to the northern boundary is well confirmed. The fault extends from midway

between Ören and Çökertme to land close to Akyazı, roughly $27^0$45'W to $28^0$20'W. The depth section of this fault is vertical in the central part, but shows a possible south dipping in the east. At the western end the fault shows a change in strike and turns south with a strike direction of roughly 36^0. This fault continues to $36^0$45'N, midway between Cos Islands and Datça Peninsula.

ÖZET

ÇİFTLER ARASI FARK YÖNTEMİYLE DEPREMLERİN KESİN KONUMLARININ BELİRLENMESİ VE GÖKOVA KÖRFEZİ AKTİF FAY YAPISI

Çiftler arası fark yöntemi, HYPODD kullanılarak Gökova Körfezi'nde meydana gelen depremlerin konumları yeniden belirlendi. Bu tezin amacı, lokal ölçekte ters çözüm parametre seçimlerinin HYPODD'nin performansına etkilerini anlamak ve Gökova Körfezi'ndeki aktif fayların yerini belirlemektir. Bu amaçla, Nisan 2006-Aralık 2009 döneminde kaydedilmiş depremler kullanılmış ve büyüklükleri 1.5-4.5 arasında değişen bu depremlerden 972 tanesinin lokasyonu yeniden belirlenebilmiştir.

HYPODD'nin ters çözüm kısmı, katalog ve korelasyon olmak üzere iki farklı data üzerinde çalıştırılabilir. Bu çalışmada her iki yöntem de kullanılmıştır. Korelasyon datasına bağlı yürütülen ters çözümün, yalnızca depremlerin birbirine yakın olduğu bölgelerde iyi sonuç vermekte olduğu gözlenmiştir (<3km). İstasyon sayısının yeterince yüksek olduğu (>4 istasyon) ve depremlerin oluştuğu bölgeye orta mesafede (<60km) iyi dağılım gösterdiği durumlarda; kontrol parametrelerinden bağımsız olarak, sonuçların iyileştiği gözlenmiştir. Derinlik kesitleri incelendiğinde; HYPODD kullanımının özellikle de korelasyon verisi kullanımının etkisi açıkça görülmektedir. Önemli bir diğer gözlem ise, parametreler ve bunlara bağlı sonuçların geometri ve deprem çiftleri arasındaki uzaklığa bağlı olduğudur. MAXSEP, MINLNK, MINOBS parametreleri uygun aralıkta seçilmemeleri durumunda; veri setinde aşırı azalmaya sebep olabileceği için oldukça kritiktir. Verilerin kümelere ayrılması, tamamen veri seti özelliklerine bağlı bir durumdur. Eğer veri içerisinde birbirinden farklı özellikler gösteren kümeler varsa, hepsi için aynı kontrol parametrelerinin kullanılması gerçekçi bir yaklaşım olmayacaktır. Bu sebeple veriyi kümelere ayırma, tavsiye edilen bir yöntemdir.

Gökova Körfezi içindeki aktif fayların, kuzey kıyıya paralel olduğu açıktır. Ören ve Çökertme arasında kalan bölgeden ($27^0$45'W) başlayan bu fay, Akyazı yakınlarına ($28^0$20'W) kadar uzanmaktadır. Derinlik kesitleri göstermektedir ki; fayın orta kısmı dik bir yapı gösterirken, doğu kısım güneye dalan bir yapı göstermektedir. Körfezin batısında, fay yönelimi değişerek güneye dönmüştür ve kabaca 36^0 lik bir açıya sahiptir. Bu fay, Datça Yarımadası ve Kos Adası arasında $36^0$45'N civarına kadar devam etmektedir.

LIST OF FIGURES

LIST OF TABLES

LIST OF SYMBOLS

i	Earthquake
j	Earthquake
k	Seismic station
Ml	Local magnitude
T	Travel time
τ	Origin time
t^{obs}	Observed travel time
t^{cal}	Calculated travel time
Δm	Hypocentral coordinates and origin time
Δx^i	Hypocenter parameter of earthquake (x Direction)
Δy^i	Hypocenter parameter of earthquake (y Direction)
Δz^i	Hypocenter parameter of earthquake (z Direction)
$\Delta \tau^i$	Origin time
Δm^{ij}	Relative hypocentral parameters
BLCB	Balçova Station
BODT	Bodrum Station
BU	Boğaziçi University
CETI	Çetibeli Station
DALT	Dalaman Station
DAT	Datça Station
ELL	Elmalı Station
EW	East-West
FETY	Fethiye Station
GPS	Global Positioning System
HYPODD	Software Package
HypoDD	Inversion process
Hista2ddsta	Subprogram of HYPODD
KOERI	Kandilli Observatory and Earthquake Research Institute
MAXDIST	Maximum distance
MAXSEP	Maximum separation

MAXNGH	Maximum neighbor
MINLNK	Minimum link
MINOBS	Minimum observation
MAXOBS	Maximum observation
MLSB	Milas Station
NCSN	Northern California Seismic Network
Ncsn2pha	NCSN to phase format (Subprogram of HYPODD)
NS	North-South
NW	North-West
NE-SW	Northeast Southwest
Nor2dd	Nordic to DD format (Subprogram of Seisan)
OZCA	Özcan Station
OREN	Ören Station
Ph2dt	Subprogram of HYPODD
PQL	PASSCAL Quick Look
SE	South-East
SEISAN	Earthquake Analysis Software
SVD	Singular value decomposition
TURG	Turgutlu Station
WNW-ESE	West NorthWest-East SouthEast
YER	Yerkesik Station

1. INTRODUCTION

The aim of this thesis is two folds: first we look for the best choice of inversion parameters when using hypoDD at local scale, and second, as a by product of the test data used in the study, we determine the active faults in the Gökova Bay.

In general tectonic modeling, the errors in the locations of the earthquakes are not an extremely important problem because the seismic activities occur generally along the plate boundaries so a few hundred meters even kilometers are not critical in the large scale. On the other hand exact location of the earthquakes is important for studying the detailed geometry of fault structures. Therefore the importance of the location errors changes with respect of the aim of the study. Turkey is one of the most seismically active countries in the World and determining the faults more precisely is very important for tracing their exact trajectories and therefore decreasing the damage.

Both systematic and relative location errors can be observed in the earthquake locations (Douglas, 1967; Dewey, 1971, 1972; Jordan and Sverdrup, 1981; Pavlis, 1986). The systematic errors should be considered statistically (Pavlis, 1986) while the relative location errors are often results of the nonlinearity, measurement and velocity model errors (Pavlis, 1986). So the eliminating the relative location errors are more difficult than the systematic errors because of its complex causes. One of the most important factors on the earthquake location is the Earth structure. The double difference location algorithm (HYPODD) is presented as a solution to the poor Earth structure knowledge problem. Waldhauser *et al*. (2000) suggests that if the two earthquakes are close to each other the ray paths can be considered as same at common stations, so by using this assumption we can eliminate most of the Earth structure effects besides the effects caused by the distance between two earthquakes. In the HYPODD relocation algorithm the most important goal is optimizing the distance between the earthquakes by using the relative time differences (from catalog or cross-correlation data). The effectiveness of the HYPODD has been proved on especially aftershock studies because the distance between these earthquakes are relatively small. The aim of this thesis is to apply the HYPODD on the close earthquakes

and understand the effectiveness of relocation control parameters on different types of data sets.

The method we used is to carry out a series of tests on a well recorded data, with sufficient number of events and stations, all situated within local distances. For this purpose we used the four year (April 2006 - December 2009) seismic earthquake recordings of the Gökova Bay. The Gökova Bay is located at the southwest of Turkey (Figure 1.1). The African Plate subducts beneath the Turkey along the Hellenic arc and this tectonic activity dominates the seismicity of the Aegean region. The Gökova Bay is a part of this region and has been subject of many researches but the number of studies by utilizing seismological data is limited. In addition, the exact location of active faults at this region and their mechanism is still been debated.

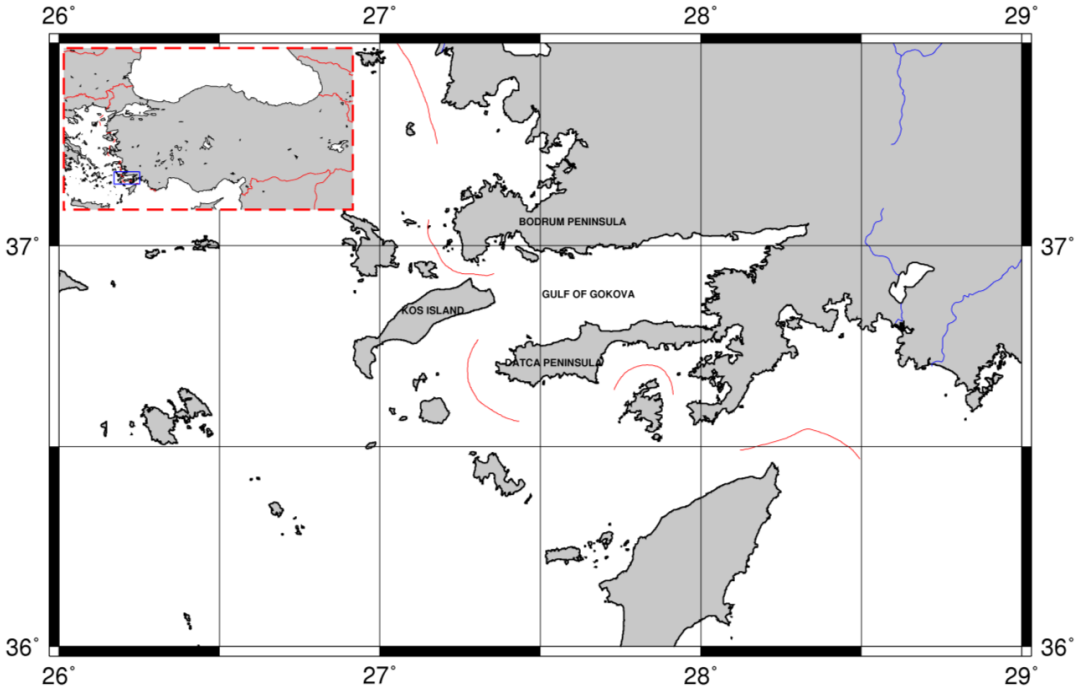

Figure 1.1. The map of the Gökova Bay.

1156 earthquakes were recorded at twelve seismic stations in four years time period (2006-2009). 972 of 1156 these earthquakes were picked by using PQL and the rest could not be picked because of the noise problems.

The study starts with an analysis of the effects of the selecting event pairs (ph2dt) and the effect of the inversion process parameters (hypoDD) upon the outputs. We have also tried to understand the effectiveness of the HYPODD on various data sets different in size and in density. All these test were done by using both catalog and cross-correlation approaches separately and together.

Before running the hypoDD program we have separated the data into four clusters according to the distribution of the earthquakes. Each cluster has different properties in term of geometrical shape, distance to stations, density of events, etc.

The first phase of the hypoDD (i.e. ph2dt) is to consider every possible combination of two events, check whether an event pair satisfies a given set of conditions and finally produce a list of events pairs which would be the ones to be used for the inversion. At this step it is crucial to choose the optimal conditions that will determine the best choice of event pairs. Much part of this thesis is dedicated to this problem.

We have then compared the effect of using catalog or cross-correlations for determining the travel time differences. And finally we have analyzed the final effect of processing the whole data together rather than in selected clusters.

Chapter 1 represents the introduction of the thesis, which includes a summary of the main topics followed by an outline of the presentation. The geology and tectonic settings of the study area and brief information about the previous studies are described in the Chapter 2. The method of the HYPODD and informations about the subprograms are presented at the Chapter 3. Chapter 4 includes the data preparation and the choice of the ph2dt and hypoDD input parameters. The results of the relocation of the earthquakes at the clusters separately by using catalog, cross-correlation and combination of both data sets and their comparisons are represented in the Chapter 5. Finally, the conclusions are given in the Chapter 6.

2. GEOLOGY AND TECTONIC SETTING

Turkey is located at the intersection of African, Arabian and Eurasian plates. East part of Turkey has crustal shortening and thickening regime as a result of the north directed movement of Arabian plate with respect to the Anatolia (Şengör and Yılmaz, 1981). These intense collisional events in the eastern part started with the closure of Neo-Tethyan Ocean (Şengör and Yılmaz, 1981). This compressional tectonic regime is still continuing, as part of the Alpine-Himalayan orogeny. Western Turkey and the Aegean Sea, which are bordered by the North Anatolian Fault to the north and the Hellenic Subduction Zone to the south, are characterized by an active extensional regime (McKenzie, 1970). GPS studies confirm that the Anatolian microplate has a counterclockwise rotation (Reilinger *et al.*, 2006). The speed of this movement increases gradually toward the Hellenic Arc. The speed of the rotation of Central Anatolia is 20-25 mm per year as a result of the movement of the Arabian plate (~20-30 mm/year) and the roll-back Hellenic Subduction regimes (Reilinger *et al.*, 2006) (Figure 2.1).

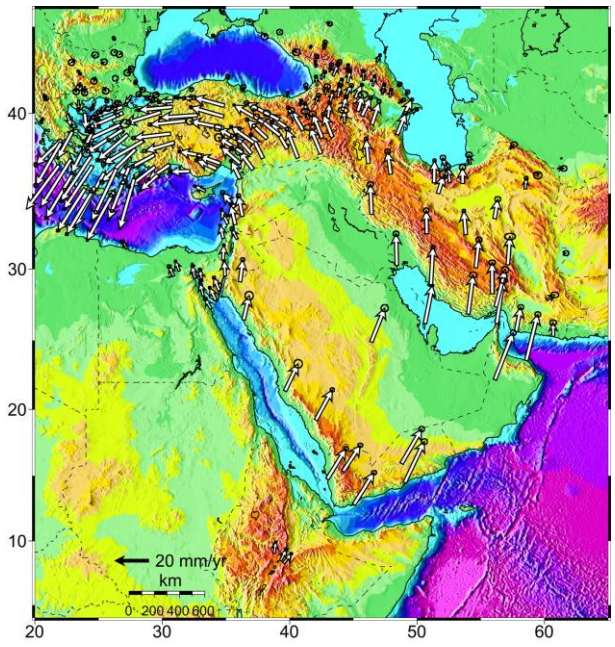

Figure 2.1. GPS velocities relative to Eurasia (Reilinger *et al.*, 2006).

The NS compression tectonic regime is well known to have started after the closure of the Tethyan Ocean during the late Cretaceous (Yılmaz, 2010). However, the compressive effect of the Arabian 'indenter' started to induce the extrusion process with a delay but before the Middle Miocene (maximum age: 16 Ma). The timing of the NS extension regime in the west of Turkey is still matter of debate (Gautier *et al.*, 1999). Some authors relating the extension directly to the extrusion tend to date the it later than the Middle Miocene (Le Pichon an Angelier, 1979; Dewey and Sengör, 1979) others using radiometric and stratigraphic data put the onset at an earlier time with a minimum age of 21 Ma (Gautier, 1999). The grabens and horsts at the Aegean region have occurred as a result of this new extensional tectonic regime. Our study area is located at the border of this complex system which is seismically active.

Geographically, the Gökova Bay is located at the southwest Turkey. It is bordered by Datça Peninsula from the south, Bodrum Peninsula from the north and the Cos Island from the west. Almost 120 km in length, the Gökova graben is neighbored by two active volcanoes to the southwest, namely Yalı and Nisyros (Dirik, 2007).

The first observational study in Datça Peninsula was made by Philippson in 1915 (Ersoy, 1991). Following this preliminary work, Datça peninsula had been the subject of many studies which are basically focused on the volcanism, geomorphology and the tectonics of the area (Dirik, 2007). The rock units of the Datça peninsula were formed in two main stages: Pre-Neogene (ophiolite, ophiolitic melange, blocky flysch and sediments) and Neogene-Post-Neogene (terresterial and marinal sediments, alluvium, beachsand, beachrock, talus, old terrace and volcanic deposits) (Ersoy, 1991). Ercan (1980) and Ercan *et al* (1984) studied on the volcanic activity of the region and Smith *et al.* (1996) proposed that the age of this volcanic activity is 161ka (Dirik, 2007). The pyroclastics remains were determined by Allen and Cas (2002) for Cos Island, Bodrum and Datça peninsula and the origin of these remains have shown more details of the volcanic activity around these regions (Dirik, 2007). As far as tectonic processes around Datça Peninsula are concerned, observations reveal the existence of two main episodes: compressional paleotectonic (NS and EW) followed by extensional neotectonic structures. The faults and other tectonic features observed today (i.e. symmetric and antisymmetric anticlinal and synclinals) were created by both the compressional and the subsequent extensional regimes (Ersoy, 1991).

The paleotectonic structures are mainly located at the western part of the Datça Graben contains both the trust and the reverse faults which are the evidence of the compressional regime (Ersoy, 1991) (Figure 2.2). The neotectonic structures are represented mainly by graben systems with different ages and orientations (Görür *et al.*, 1995) (Figure 2.3). The first one is NW-SE oriented Datça graben which contains sedimentary and volcanic rocks (Görür *et al.*, 1995). Datça graben is located at the middle of Reşadiye Peninsula (Datça Peninsula). It started to develop on the Lycian Nappes by NW trending fault as a half graben during early Pliocene. The second graben system is represented by the EW trending Gökova and Hisarönü grabens which cut the first one (Görür *et al.*, 1995). The evolution of the EW trending Gökova and Hisarönü grabens is based on NS directed extension which presently active. EW trending faults on the south edge of the Gökova graben and the north faults of the Hisarönü graben cut the late Pliocene deposits of Datça graben so the Reşadiye horst evolved between these two grabens (Dirik, 2007). Gökova and Hisarönü grabens are relatively young and started to develop from early Quaternary (Dirik, 2007).

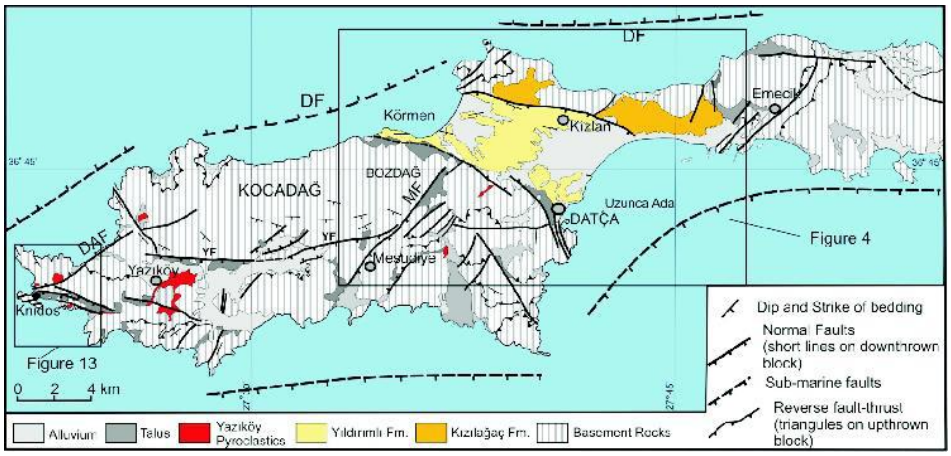

Figure 2.2. Geologic map of the western part of the Datça Peninsula. DF: Datça Fault, MF: Mesudiye Fault, YF: Yakaköy Fault, DAF: Damlaca Fault (Dirik, 2007).

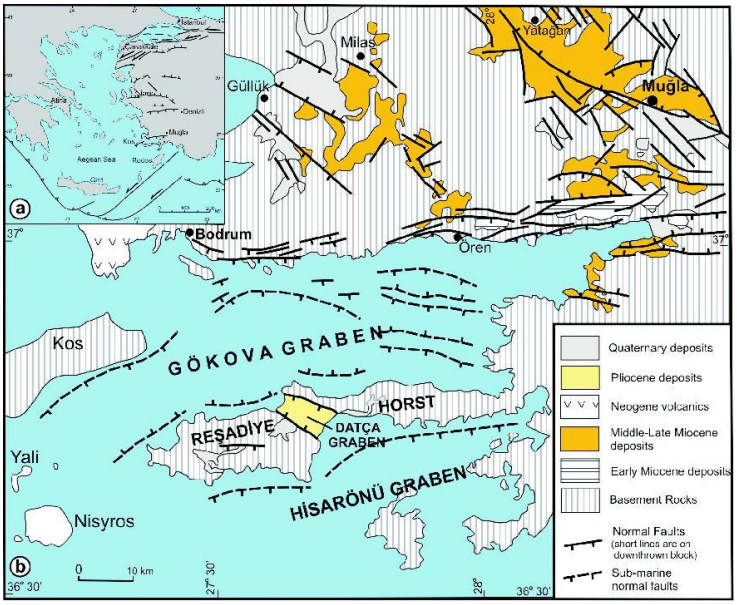

Figure 2.3. (a) Tectonic map of Aegean region (Dirik, 2007); (b) The general tectonic map of Gökova region (Dirik, 2007) (These maps were modified by Dirik (2007) from Görür *et al.* (1995) and Kurt *et al.* (1999).

The northern part of the Gökova Bay is represented by Lycian Nappes over which Muğla-Yatağan and Milas-Ören rift systems are developed (Görür *et al.*, 1995) (Figure 2.4). These NW-SE trending rift systems are cut by NE-SW trending short faults (Görür *et al.*, 1995). The original orientation of these rifts was NS and they rotated anticlockwise at the end of the Miocene (Görür *et al.*, 1995). The units of the NW-SE rifts can be grouped into three ages. The first one contains the Middle Miocene age clay-stone, sandstone and conglomerate and corresponds to the Eskihisar formation (320 m) (Görür *et al.*, 1995). The second sequence consists of Upper Miocene aged conglomerate, sandstone, siltstone, claystone, clayey limestone, limestone and tuff (350 m) which is called as Yatağan Formation (Görür *et al.*, 1995). The last section corresponds to the Quaternary sediments and the average thickness of these formation changes between 20 to 100 m (Görür *et al.*, 1995).

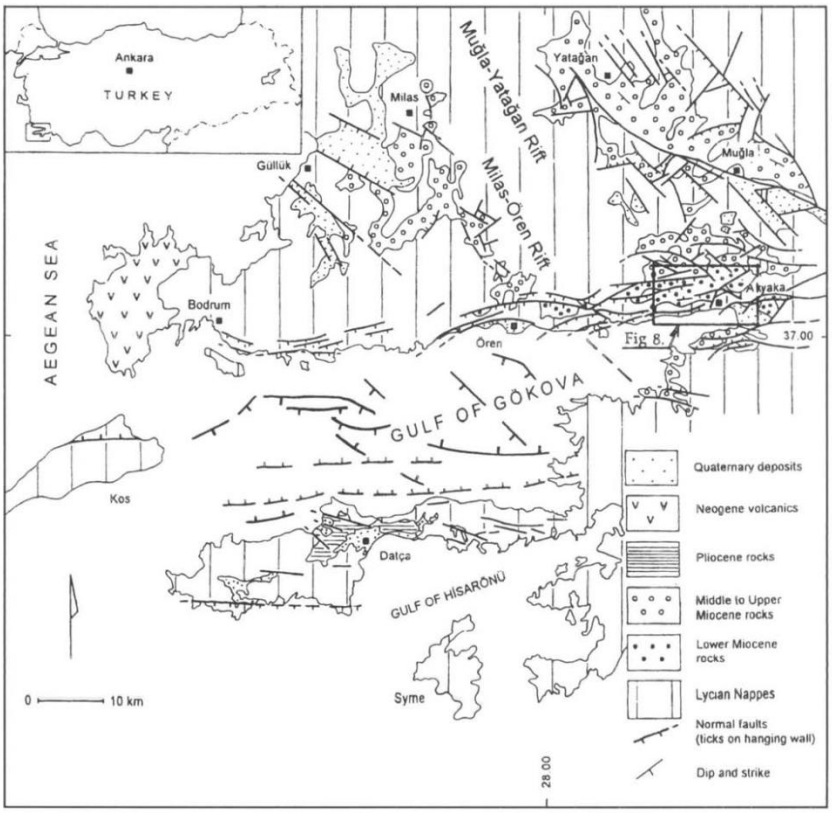

Figure 2.4. This geological map of the Gökova region illustrates the two rift systems (Görür *et al.*, 1995).

The geological units of Cos island are part of the Central Hellenic Nappes (Jacobshagen,1986; Drinia *et al.*, 2010). The oldest units are located at the central part towards the south coast (Units: Permocarboniferus marls, impure limestones, sandstones, phyllites and rare mafic intercalations) (Altherr *et al.*, 1972; Gralla, 1982; Drinia, 2010). Tilos and Nisyros (together with Yalı) islands are the members of the Hellenic Volcanic arc, which include Soussaki, Methana, Aegine and Paros islands at the western end and Milos, Santorini at the central part (Nomikou *et al.*, 2010) (Figure 2.5). The direction of the Hellenic arc at this region is parallel to morphological trend of Cos so it is ENE-WSW trending (Nomikou *et al.*, 2010).

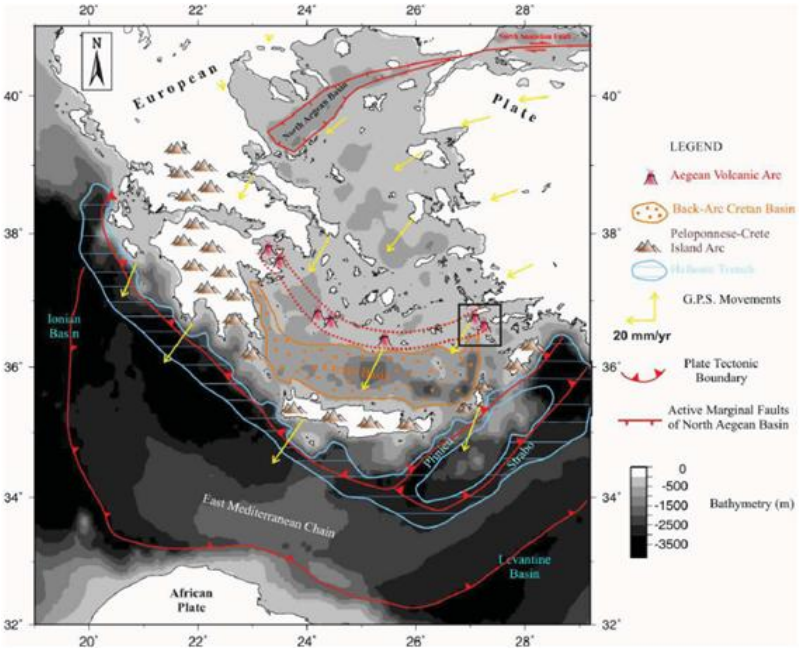

Figure 2.5. Present day geodynamic structure of the Hellenic Arc (Nomikou *et al.*, 2010).

Volcanic activity at the eastern sector of the Hellenic Volcanic Arc around the islands of Cos, Yalı and Nisyros started at in the Pliocene (approximately 2.6-2.8 my) and they were active during the Late Pleistocene-Holocene period (Nomikou *et al.*, 2010). The last magmatic eruptions were reported at the Nisyros island in 1871, 1873, 1888 (Georgalas, 1962; Papadopoulos *et al.*, 1998). The largest volcanic eruption of the Eastern Mediterranean occurred at Cos almost 0.16 my ago (Nomikou *et al.*, 2010). Ash, pyroclastics flows spread out 3000 km² area including Turkish mainland (Keller, 1969; Smith *et al.*, 1996; Allen *et al.*, 1999; Nomikou *et al.*, 2010).

The new studies have shown that the Methana, Milos, Santorini and Nisyros are the four active centers of volcanic arc (Nomikou *et al*., 2013). Each volcanic group geometry is different through time and so is the volume of the extruded rocks (Nomikou *et al*., 2013). Nisyros is an even younger volcanic group with the highest activity during Late Pleistocene–Holocene. Both onshore and offshore, post-dating the previous intense activity throughout Pliocene–Middle Pleistocene of Cos and the large marginal faults of the basins are usually normal in character (Nomikou *et al.*, 2013).

2.1. Previous Studies

The first mention of fault structures were done by Sieberg (1932) who suggested that Gökova Bay was bordered by two main faults from north and south and named the region as Cos Graben.

The Gökova fault was investigated in detail by Barka *et al*. (1985) for the purpose of site selection for Gökova Thermoelectric Power Plant (Barka *et al*., 1995). They indicated that Gökova Fault was located at the north coast of the bay and had normal mechanism (Barka *et al*., 1995). The western part of the fault continues offshore through the SW of Cos Island from Ören region. The east branch of the fault continues at land towards the Ula-Yerkesik-Gökova (Barka *et al*., 1995). Barka *et al*. (1995) argued that Gökova basin developed as a half graben because of this normal fault which has 120 km length in total. Several fault scarps around Ören region illustrate that the Gökova fault is an active zone and produced destructive earthquakes such as 1493 earthquake which destroyed the Bodrum city completely (Barka *et al*., 1995).

Ersoy (1991) made a study on geological structures of Datça Peninsula and asserted the two main faults which bound Gökova graben from the north and south (Figure 2.6).

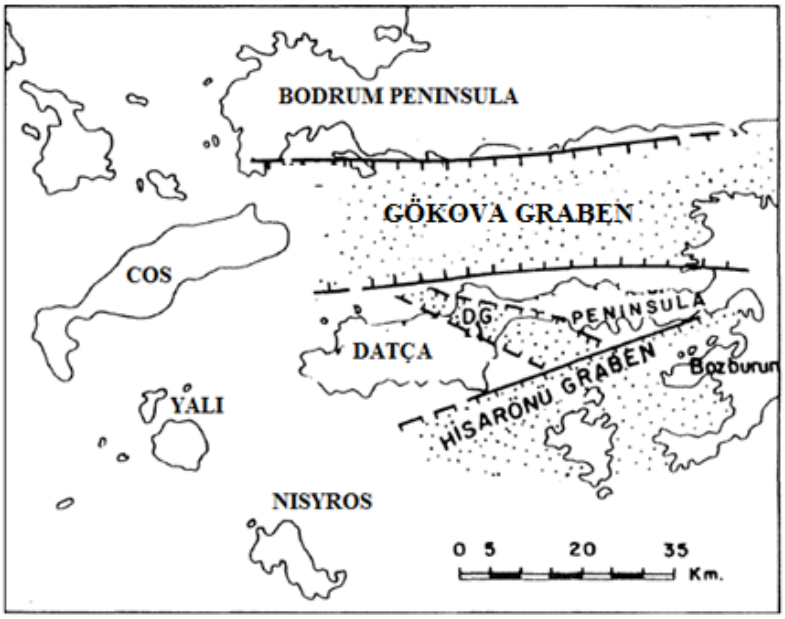

Figure 2.6. Map of the Gökova and Hisarönü Grabens and their main faults (Ersoy, 1991).

The offshore faults of Gökova Bay were studied by marine seismics (Uluğ *et al*., 1996, 1998; Ecevitoğlu *et al*., 1996). These first studies were inefficient for investigating deep structures because high seismic frequency signals are absorbed with depth rapidly and this limitation decreased the penetration depth (Ecevitoğlu *et al*., 1996). On the other hand these studies were important to explore the shallow structures for explaining the neotectonic regime of the bay (Ecevitoğlu *et al*., 1996). The results of the shallow seismic study of Uluğ *et al*. (1996) have illustrated that the NE region of Gökova Bay has several oblique deltaic layers. These delta structures were affected by sea level changes in the glacial and interglacial period (Uluğ *et al*., 1996). Uluğ *et al*. (1998) suggested that main part of the Gökova Bay was subsiding. The northwestern and western parts of Gökova Bay were bordered by WSW-ENE trending faults and south part of the bay was bordered by E-W trending fault (Uluğ *et al*., 1998).

Kurt *et al*. (1999) used multi-channel seismic reflection data and proposed the existence of The Datça Fault (1999) on the south of the bay. They claimed that the Gökova Bay opened by trough the vertical movement of this E-W directed, buried fault. The faults

at the northern part of the bay were identified as the antithetic faults of the Datça fault (Kurt *et al*., 1999) (Figure 2.7).

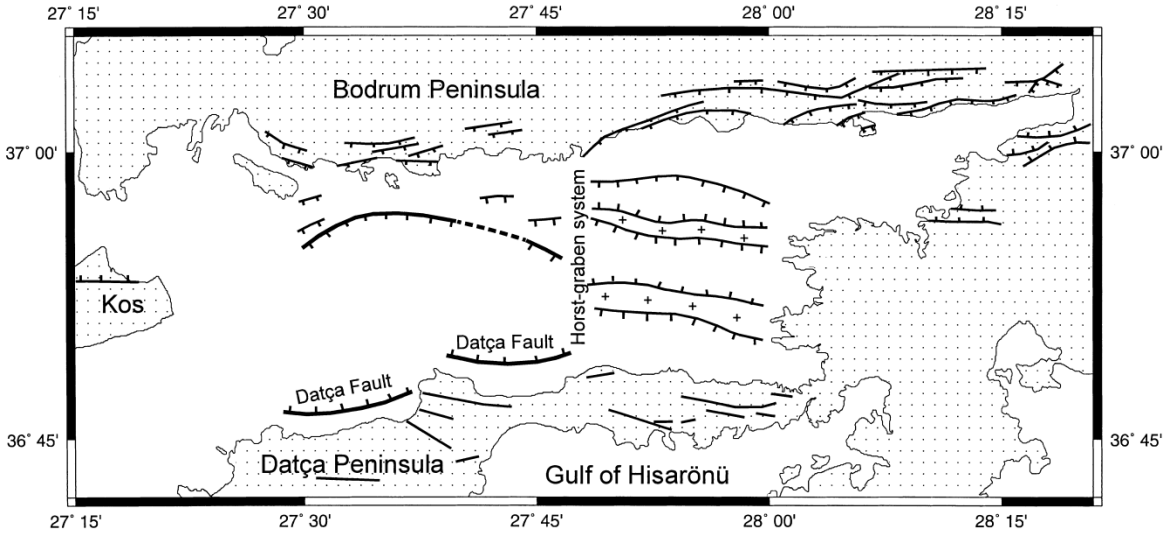

Figure 2.7. The fault map of the Gökova Bay (Kurt *et al*., 1999). The bold lines show the major faults and ticks are on hanging blocks. Kurt *et al*. (1999) adopted the on land faults from Görür *et al.* (1995).

EW trending opening regime of Gökova Bay as a result of Datça fault was also supported by Uluğ *et al*. (2005). In that study they used shallow seismic reflection. The most important outcome of the study of Uluğ *et al*. (2005) is NE-SW trending Gökova Transfer Fault is located at the central part of the bay. Uluğ *et al*. (2007) also used seismological data to support the existence of this fault (Figure 2.8).

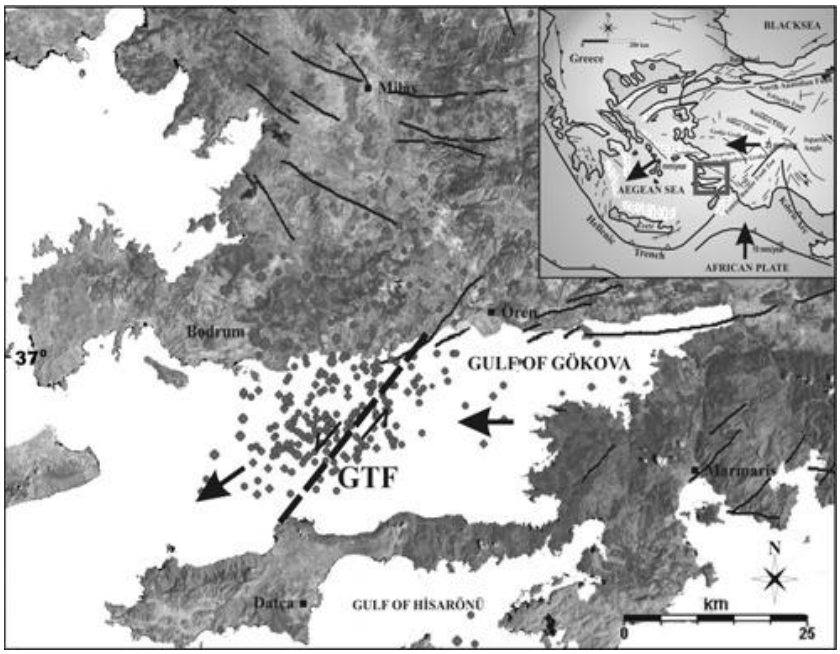

Figure 2.8. Seismotectonic map of Gökova Region (Uluğ *et al.*, 2007).

A recent seismic reflection study of Gökova Bay was made by İşcan *et al*. (2012). In contrary to earlier results, they claimed that the main structures of the Gökova Bay are strike-slip and reverse faults and folds (İşcan *et al*., 2012). According to their results, the young tectonic regime of Gökova Bay is characterized by NE-SW strike slip fault which intersects all WNW-ESE trending submarine structures. On the other hand the normal faults represents the old tectonic regime and at present they are inactive or less active (İşcan *et al*., 2012) (Figure 2.9).

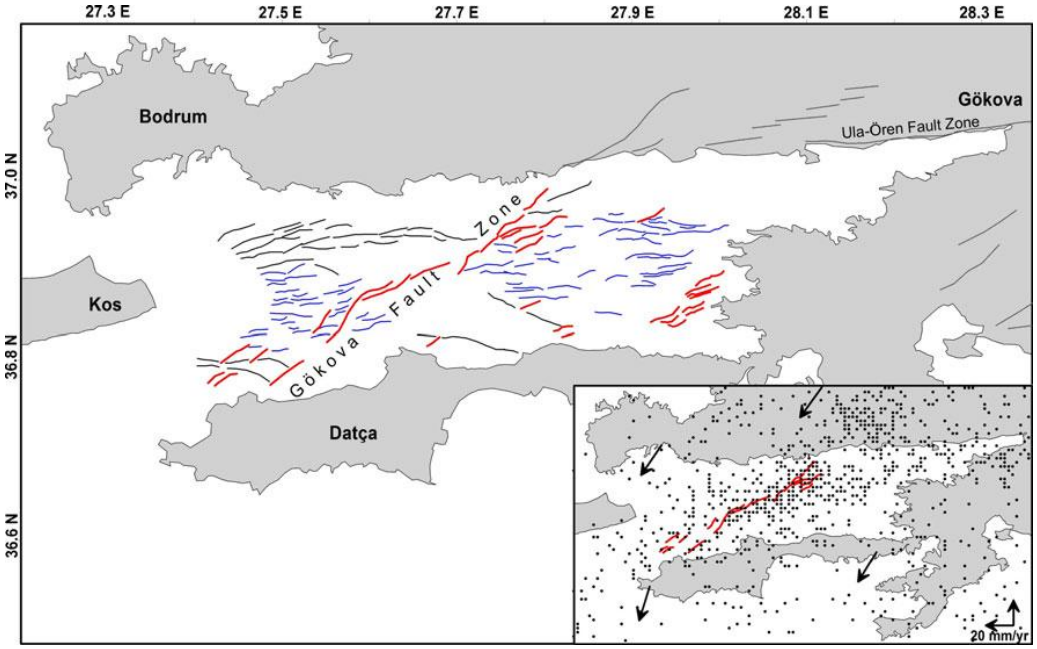

Figure 2.9. Active fault map of the Gökova Bay: red and black lines strike-slip and normal faults, respectively, blue lines reverse faults and folds (İşcan *et al*., 2012). In these maps the earthquakes (shown by dots) were used from the USGS and NEIC catalogs for the period 1973–2011, the Oland faults were used from Şaroğlu *et al.* (1992) and the GPS data were used from McClusky *et al.* (2000).

Most of the studies about the Gökova Bay are based on the seismic reflection or surface observational data. The number of studies utilizing seismological data is limited. The first seismological study was made by Eyidoğan *et al*. (1996) who studied 240 analog recordings of earthquakes recorded between 04/07/1995-05/08/1995. They suggested that the northern part of the bay was the active branch. The second study based on seismological data was made by Aktar *et al.* (2006). The results of that study has illustrated clearly that the northern part of the bay is seismologically active and several segments were identified. The total length of the fault between Ula-Ören is 40 km and the eastern part of this fault continued on land approximately 10-12 km (Aktar *et al*., 2006). An earthquake swarm occurred in 2004 at the western part of the fault which begins at Ören region and continues at the sea towards the west part of the bay (Aktar *et al*., 2006). In that study the earthquakes which are located at the southwest of Cos Island could not had been observed with accuracy, so the seismic activity of the fault beyond Cos Island remains

unclear (Aktar *et al*., 2006). The most important result of this study is about the Datça fault because Aktar *et al*. (2006) suggested that the Datça fault is a shallow antithetic fault and is not the main branch as was previously suggested by marine seismic studies (Kurt *et al*., 1999).

The latest seismological study is done by Yolsal *et al.* (2014). The aim of this study is determining the fault parameters and the deformation in the Aegean region by using P and SH waveform inversions. The important result of this study is the seismic activities of the bay are still controlled by NS extensional regime but they have small strike slip components.

2.2. Seismic Activity

The Gökova Bay is a part of the seismically active Aegean region. It is located at the southwest of Turkey and both historical and instrumental recordings show that the destructive earthquakes occurred at this region (Table 2.1).

Table 2.1. List of the earthquakes around the Gökova Bay.

DATE	LATITUDE	LONGITUDE	LOCATION	INTENSITY	REFERENCE
BC 222	36.50	28.00	RHODOS,CYPRUS(TSUNAMI)	X	KOERI
BC 185	36.00	28.00	RHODOS,CYPRUS	IX	KOERI
155	36.30	28.00	RHODOS,MUĞLA,FETHİYE	X	KOERI
08.08.1304	36.50	27.50	RHODOS,CRETE,CYPRUS	X	KOERI
03.10.1481	36.00	28.00	RHODOS,SW ANATOLIA(TSUNAMI)	IX	KOERI
18.08.1493	36.75	27.00	ISTANKOY(COS) ISLAND	IX	KOERI
1570	-	-	RHODOS	-	Ambraseys and Finkel, 2006
1571	-	-	COS ISLAND	-	Ambraseys and Finkel, 2006
1616	-	-	RHODOS	-	Ambraseys and Finkel, 2006
1660	-	-	RHODOS	-	Ambraseys and Finkel, 2006
1673	-	-	COS ISLAND	-	Ambraseys and Finkel, 2006
1685	-	-	RHODOS	-	Ambraseys and Finkel, 2006
1686	-	-	RHODOS	-	Ambraseys and Finkel, 2006
1714	-	-	RHODOS	-	Ambraseys and Finkel, 2006
1741	-	-	RHODOS	-	Ambraseys and Finkel, 2006
1776	-	-	RHODOS	-	Ambraseys and Finkel, 2006
18.10.1843	36.25	27.50	RHODOS,AEGEAN(6000 DEATHS)	IX	KOERI
28.02.1851	36.50		FETHİYE, MUĞLA, RHODOS	IX	KOERI
12.10.1856	36.25	28.00	RHODOS,CARPATOS,CRETE(TSUNAMI)	X	KOERI
22.04.1863	36.50	28.00	RHODOS	IX	KOERI
29.02.1885	37.20	27.20	AEGEAN SEA(18:30)	IX	KOERI
23.5.1941	-	-	MUĞLA (ML=6.0)	VIII	KOERI
25.4.1957	-	-	FETHİYE, RHODOS, MUĞLA (ML=7.1) (67 DEATHS)	IX	KOERI
25.4.1959	-	-	KÖYCEĞİZ, MUĞLA (Ml=5.9)	VIII	KOERI
23.5.1961	-	-	FETHİYE, RHODOS, MUĞLA	VIII	KOERI
January, 1987	-	-	RHODOS,MARMARİS (4.0 <Ml <4.4 The total number of earthquakes was 10)	-	KOERI
27.4.1989	-	-	GULF OF GÖKOVA (Ml=5.3)	-	KOERI
28.4.1989	-	-	GULF OF GÖKOVA (4.0 <Ml <5.1 The total number of earthquakes was 4)	-	KOERI
January, 1990	-	-	DATÇA,RHODOS,MARMARİS (4.0 <Ml <4.8 The total number of earthquakes was 21)	-	KOERI
26.8.1993	-	-	MARMARİS (Mb=5.3)	-	KOERI
12.4.1996	-	-	DATÇA (Ml= 5.4)	-	KOERI
1996	-	-	RHODOS (Ml= 5.2)	-	KOERI
5.10.1999	36.80	28.14	MARMARİS, MUĞLA (Ml=5.6)	-	KOERI
3.8.2004	-	-	GULF OF GÖKOVA (Ml=5.0)	-	KOERI
4.8.2004	-	-	GULF OF GÖKOVA (Ml=5.4)	-	KOERI
4.8.2004	-	-	GULF OF GÖKOVA (Ml=5.0) (The total number of earthquakes between 04.08.2004-08.08.2004 was 1308)	-	KOERI

The seismic activities of the bay have increased since 2004. According to the catalog data of KOERI (Figure 2.10) most of the seismic activities localize at the northern part of the bay. This part is dominated by EW trending normal faults and it is confirmed by many studies. The intense on-shore activities north of Ören represent the explosions of the quarries. On the other hand the Figure 2.10 illustrates the second earthquake cluster at the western part of the bay, nearly midway between Cos Island and Datça peninsula but this part is still debated.

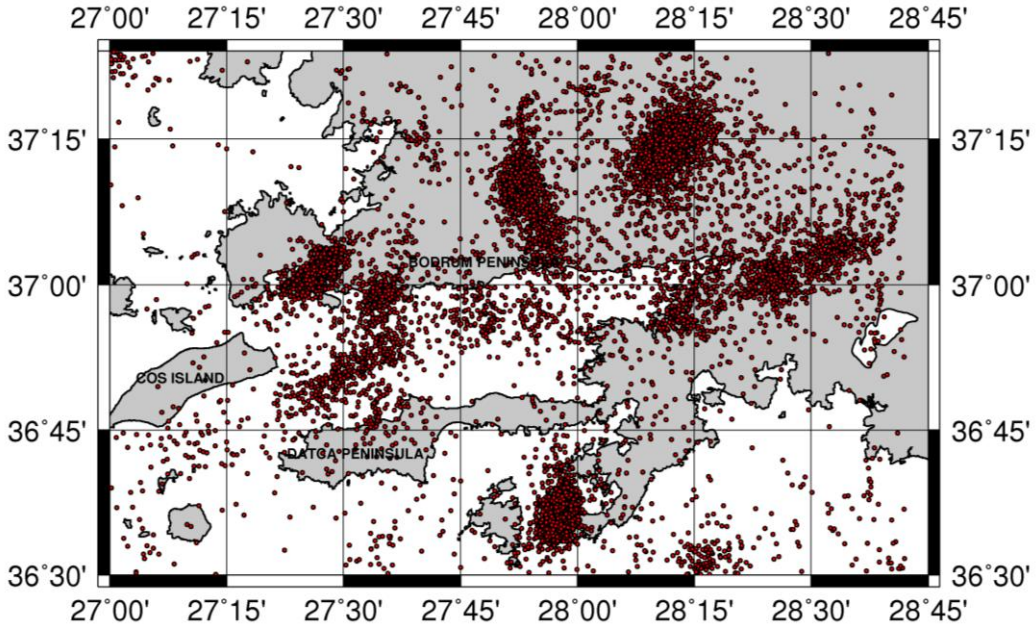

Figure 2.10. Seismic Activity in the Gökova Bay between 2009/07/10 and 2014/05/31 (0 <Ml< 9) KOERI.

3. HYPODD

3.1. Method

The earthquake location is an inverse problem where arrival times to stations are the data, the hypocenter coordinates and the origin time of each event are the unknowns. The observation vector is connected to the unknown vector by a matrix, of which the values depend on the unknowns in non-linear way. Therefore the hypocenter location problem is a complex inversion process. The errors in the earthquake location are basically due to the nonlinearity, measurement and velocity model errors. The main purpose of the earthquake location programs is to minimize these errors which mostly originate from the poor idea of the Earth structure. For most of the earthquake location programs Geiger's method is used for the iterative inversion. This method is based on least squares technique and linearizes the travel time equation locally by using Taylor series expansion. Iterative corrections are made depending on the difference between the observed and the predicted travel time.

A significant improvement in earthquake location is achieved when the relative position of earthquakes are also taken into account. Master event technique and Double Difference techniques are examples of such methods. In these latter approaches, if the hypocenter distance of two events is close to each other, the ray paths to the station may be accepted as the same. So the travel time difference between these two events depends only on their separation distance.

If the earthquakes are located with HYPODD, the common errors concerning the travel path to stations are eliminated practically. In the conventional approach, the travel time error between each hypocenter and stations are minimized individually. In HYPODD method, minimization is done over a number of events which are close to each other. In this method, relative positions of neighboring events are optimized by minimizing the travel time difference between all combinations of event pairs in the cluster. In this approach the relative positions of events are taken into account and therefore are more correct than the conventional approach. Furthermore, since the travel time difference of

event pairs only depends on the velocity structure around the epicenters, and not on the entire travel path to the station, the lack of knowledge of crustal velocities is a less serious problem.

The major problem in HYPODD is the fact that, since all hypocenters are solved simultaneously and since the observation vector (travel time difference of all event pairs) has a high dimension, the inversion process is difficult and tends to be ill conditioned. Therefore a number of measures need to be taken in order to guarantee the convergence of the inversion processes. This is done by properly limiting the number of event pairs to a useful minimum by an appropriate choice of filters. Furthermore the inversion algorithm needs to be selected using either least square or singular value methods. The damping factor in the recursive iteration also needs to be determined properly. In practice the inversion starts with a given set of parameters and these parameters are changed progressively as the iteration continues. In other word the success of HYODD method depends entirely on the choice of parameters which in turn depends on the data available. In practice, this requires a fine tuning in order to guarantee the best performance.

HYPODD software package contains four subprograms which are HypoDD, Ph2dt Hista2ddsta and Ncsn2pha. The hypoDD is the basic part of the double difference inversion algorithm. It locates the earthquakes either by independent creating groups or taking them as a whole. The travel time input data for the hypoDD (inversion process) is created by the ph2dt program form the catalog data. Ph2dt and hypoDD are the crucial parts of the HYPODD because hypoDD creates the relocated data file based on the ph2dt output. The other subprograms Hista2ddsta and Ncsn2pha basically convert the outputs of the earthquake location program to the double difference algorithm format for some specific seismic networks such as NCSN (Northern California Seismic Network). The outputs of Hista2ddsta and Ncsn2pha are the station and the phase files which are inputs of the Ph2dt program. In this study Hista2ddsta and Ncsn2pha were not used because these programs are not coherent with our data format. Instead, since our catalog is in SEISAN format, we have used Nor2dd which is a software tool of the SEISAN package.

Ph2dt program is the first step of HYPODD and calculates relatively the absolute and differential travel times for all event pairs from the catalog data (Waldhauser *et al.,* 2000;

Waldhauser, 2001). The output files of the ph2dt are dt.ct (selected pairs of travel times from catalog data), event.dat (a summary of all events), event.sel (selected events), ph2dt.log (reporting missing stations and outliers). In the case where differential times are calculated using waveform correlation rather than from catalog, we have written a software which produces dt.cc directly from the sac archive. At the second step of the program, the hypoDD locates groups by using the catalog or cross-correlation data (Waldhauser, 2001). We shall explain and discuss the parameters of both steps in the following chapters.

3.2. Ph2dt

The ph2dt program creates input file from the P and S phase catalog for the hypoDD as the first step of the double difference location process (Waldhauser, 2001). The output of this program includes the travel time information for all event pairs at common stations. However not all possible pairs are included, some are eliminated according to a filtering process set by the chosen input parameters. These parameters are: MINWGHT, MAXDIST, MAXSEP, MAXNGH, MINLNK, MINOBS, MAXOBS and are given in an input file (ph2dt.inp) (Waldhauser, 2001). The input parameters of ph2dt are important for creating qualified data set and connectivity of the events (Waldhauser, 2001).

When two events are close enough such that their differential time will be taken into account, they constitute an event pair. In this situation each event is considered to be the neighbor of the other. The input parameters to ph2dt determine the conditions for an event to be the neighbor of another. The above definitions are shown graphically in Figure 3.1.

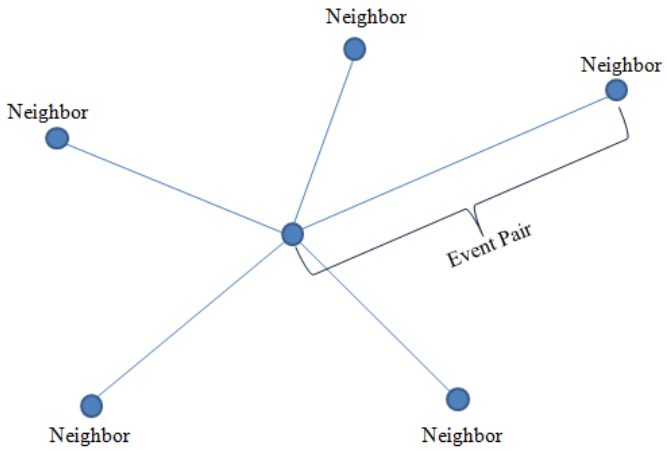

Figure 3.1. Sketch of the event pairs and the neighbors.

The parameter MINWGHT represents the picking weight when differential times are taken from catalogs. It determines how much the phase reading is accurate and therefore need to be taken account in the inversion. When inverting with waveform correlation case, this weighting corresponds to the correlation factor. MAXDIST is the maximum distance (km) between the events and the stations. This value should be chosen according to the study area. MAXDIST corresponds to the distance (km) above which phase readings are discarded. If the recordings are reliable, using small MAXDIST value is not recommended since it decreases the number of data or the redundant ones.

MAXSEP is defined as the search radius so that the distance between the event pairs cannot be larger. The distance between two events should be as small as possible for creating reliable data set. This parameter is illustrated in Figure 3.2.

Figure 3.2. Sketch of the event links according to the MAXSEP parameter.

The maximum number of neighbors of an event is limited by a parameter called MAXNGH. For each event number of neighbor events is limited to the closest MAXNGH events. Choosing MAXNGH too high leads to the unstability of the inversion. Choosing a low value leads to overlocalisation of the inversion, which in turn limits the performance. MINLNK is a parameters which concerns a given event pair. It determines the minimum number of phase readings that needs to exist for an event. P and S reading at one station are counted as two distinct phase readings. Strong and weak neigbors definitions are used based on this parameter. If the number of phase pairs of the neighbors is more than MINLNK, the event pair is named strongly linked events while the weakly linked events have less then MINLNK phase pairs and they are selected but not counted as strong neighbor. Finally MINOBS and MAXOBS are minimum and maximum number of the common stations for a given event pair, respectively.

3.3. HypoDD

HypoDD is the second step of double difference relocation program and any combination of catalog and cross-correlation data can be processed at this step (Waldhauser, 2001). The catalog or correlation data can be used separately or together and the weight input parameters can be changed according to the data sets (Waldhauser, 2001). The top of the hypoDD.inp file is associated with the input data type of the program and it can be changed. If only catalog data will be used, dt.cc file should be remove the hypoDD.inp file and the parameters should be changed according to the catalog data.

In HYPODD algorithm all earthquakes are first grouped into clusters so each one have link with the other one (Waldhauser, 2001). The links between the earthquakes create a chain into the cluster and the connectedness of this chain is related the minimum number of observations per event pair (Waldhauser, 2001). The minimum number of cross-correlation and catalog links is represented by OBSCC and OBSCT, respectively (Waldhauser, 2001). If the number of link for a given event is less than this value the chain is broken. This procedure creates a number of distinct clusters in one data set. In the limit, if the minimum number of link is chosen as zero, the whole data is considered to form a one single cluster. The hypoDD.inp parameters should be considered with the ph2dt.inp parameters for creating strong links within the events (Waldhauser, 2001).

Connectivity is one of the most important factor in hypoDD and it is controlled by weighting/cutoff parameters WDCT (for catalog data) and WDCC (for cross-correlation data) (Waldhauser, 2001). These parameters are similiar to MAXSEP parameter in ph2dt and control the distance between event pairs (Waldhauser, 2001).

3.4. Double Difference Algorithm

The arrival time (T) can be represented by the sum of the origin time (τ) and the travel time. The earthquake and the seismic station are represented by i and k respectively in the Equation 1.1. In this Equation u represents the slowness field and the path length element is *ds.*

$$T_k^i = \tau^i + \int_i^k u ds \tag{1.1}$$

The travel time and the event location has a nonlinear relationship which is lineralized by using Taylor expansion (Geiger, 1910) as mentioned above. The hypocentral coordinates and the origin time are implied with the Δm. These four hypocentral parameters have linear relationship with the travel time residuals (r).

$$\frac{dt_k^i}{dm} \Delta m^i = r_k^i \tag{1.2}$$

The difference between the observed and the theoretical travel time is represented by r_k^i ($r_k^i = (t^{obs} - t^{cal})_k^i$). The hypocentral parameters of an earthquake are symbolized by $\Delta x^i, \Delta y^i, \Delta z^i, \Delta \tau^i$.

The Equation 1.2 is not suitable for the double difference methods because it implies the residual for a single earthquake. Therefore the Equation 1.2 needs to be adapted for two events (*i* and *j*) (Frechet, 1985):

$$\frac{dt_k^{ij}}{dm} \Delta m^{ij} = dr_k^{ij} \tag{1.3}$$

In this new Equation 1.3, the unknowns Δm^{ij} represents the relative hypocentral parameters between two events i and j. The residual between observed and calculated differential travel time of two events is characterized by dr_k^{ij}.

The Equation 1.4 is two events form of the Equation 1.3.

$$dr_k^{ij} = (t_k^i - t_k^j)^{obs} - (t_k^i - t_k^j)^{cal} \quad (1.4)$$

The double difference algorithm is defined by using the Equation 1.4 and it is based on the difference between the travel times of the two events at a common station. The equation can be used for both absolute and relative travel times.

If the hypocentral distance between two events i and j is close to each other, the constant slowness vector assumption is valid since the major part of travel path is the same for both events. It is calculated by taking the difference between Equation 1.2 and using the appropriate slowness vector and origin time term for each event (Figure 3.3).

$$\frac{dt_k^i}{dm}\Delta m^i - \frac{dt_k^i}{dm}\Delta m^j = dr_k^{ij} \quad (1.5)$$

The full form of the Equation 1.5 is;

$$\frac{dt_k^i}{dx}\Delta x^i + \frac{dt_k^i}{dy}\Delta y^i + \frac{dt_k^i}{dz}\Delta z^i + \Delta\tau^i - \frac{dt_k^j}{dx}\Delta x^j - \frac{dt_k^j}{dy}\Delta y^j - \frac{dt_k^j}{dz}\Delta z^j - \Delta\tau^j = dr_k^{ij} \quad (1.6)$$

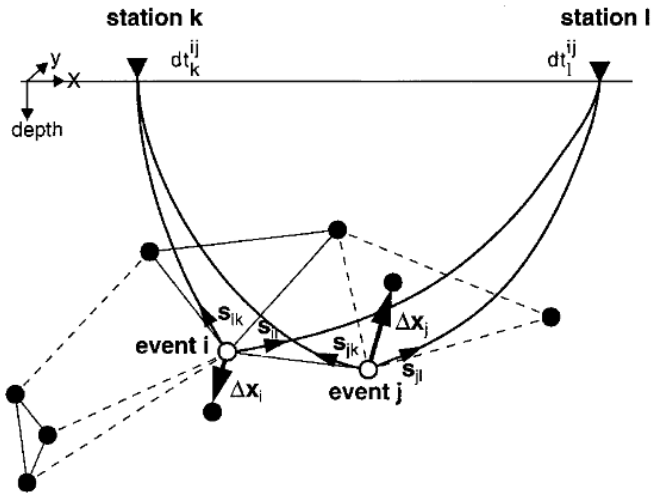

Figure 3.3. Double difference earthquake relocation algorithm (Waldhauser *et al.,* 2000).

The solid and open circles represent the hypocenters and they linked each other by cross-correlation (solid lines) or catalog (dashed lines) data. S is the slowness vector and i and j represents the two events. The stations are implied with k and l in this sketch. Relocation vectors of the events are represented by the thick arrows (Δx) and the dt is the travel time difference between the events at station k and l (Waldhauser *et al.,* 2000).

The generalized form of the Equation 1.6 can be written as;

$$WGm = Wd \tag{1.7}$$

Where G is Mx4N dimensional matrix (The number of the double difference observations and the events are symbolized by M and N respectively), d and m represent the data vector and hypocentral parameters vector W represents the weights.

$$\sum_{i=1}^{N} \Delta m_i = 0 \tag{1.8}$$

The Equation 1.7 may become numerically unstable. This problem can be solved by the elimination of the distant events by filtering suitably with the ph2dt and hypoDD input parameters or changing the damping factor.

$$\mathrm{W}\begin{bmatrix} G \\ \lambda I \end{bmatrix}\mathrm{m} = \mathrm{W}\begin{bmatrix} d \\ 0 \end{bmatrix} \tag{1.9}$$

The damping factor is characterized by λ in the Equation 1.9.

The least square or singular value decomposition can be used in double difference algorithm. SVD is more appropriate method for the small and the well conditioned systems on the other hand for large data set SVD is inefficient.

4. DATA

4.1. Data Preparation

In this thesis, the data were provided by 12 seismic stations which are located around the Gökova Bay. Four of these stations (OREN, OZCA, CETI, TURG) were temporary and installed within a TUBITAK project conducted by Aktar *et al*. (2006). The others are the permanent stations of Boğaziçi University Kandilli Observatory and Earthquake Research Institude (KOERI) (BLCB, BODT, DALT, DAT, ELL, FETY, MLSB, YER). Figure 4.1 illustrates the location of both temporary and the permanent stations. Although the ELL, FETY and BLCB do not take place on the map, they are used in the study. GURALP CMG-6T typed seismometers are used at all of the temporary stations and their frequency band is between 0.03-50 Hz, while the types of the permanent stations are GURALP CMG-3T ESP and their frequency band between is 0.012-25 Hz (Aktar *et al.*, 2006).

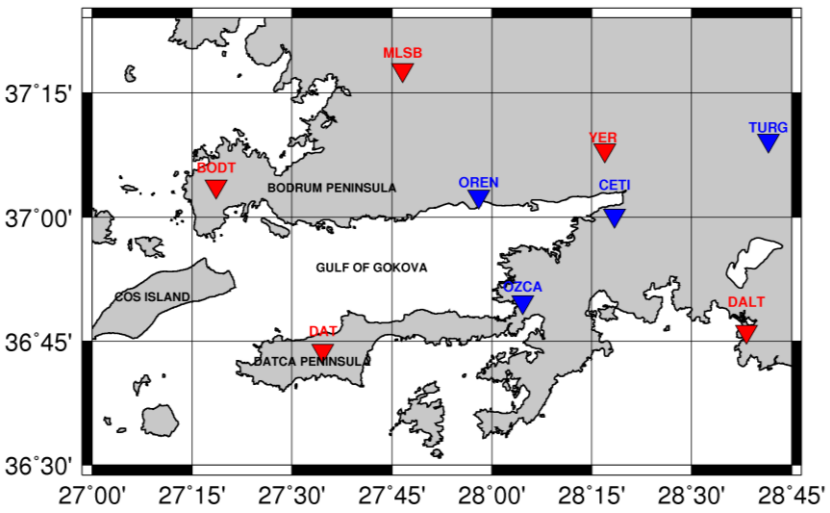

Figure 4.1. Seismic stations around Gökova Bay. The blue triangles represent the temporary stations while the permanent stations are illustrated by red triangles.

During the observation period between 2006 and 2009, 1156 earthquakes were recorded at twelve seismic stations described above. The phases of the earthquakes were picked by using PQL (Passcal Quick Look Package) and the output of the program is converted to HYPO71 format by using shell programs. 972 of these earthquakes can be located with HYPO71 as shown in Figure 4.2. The location output is expressed in Nordic format (i.e. hyp.out file in SEISAN package) and constitutes the primary catalog to be used as input in HYPODD. The magnitude range of these earthquakes is between 1.5 and 4.5 in local magnitude and they localize in the first 25 km depth of the crust (Figure 4.3).

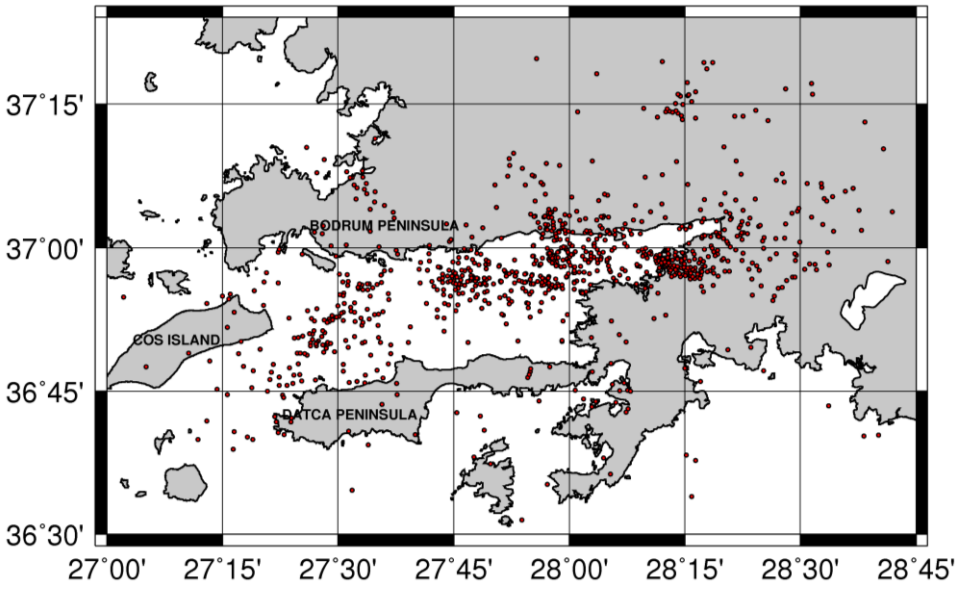

Figure 4.2. The output of HYPO71 (972 earthquakes between 2006-2009).

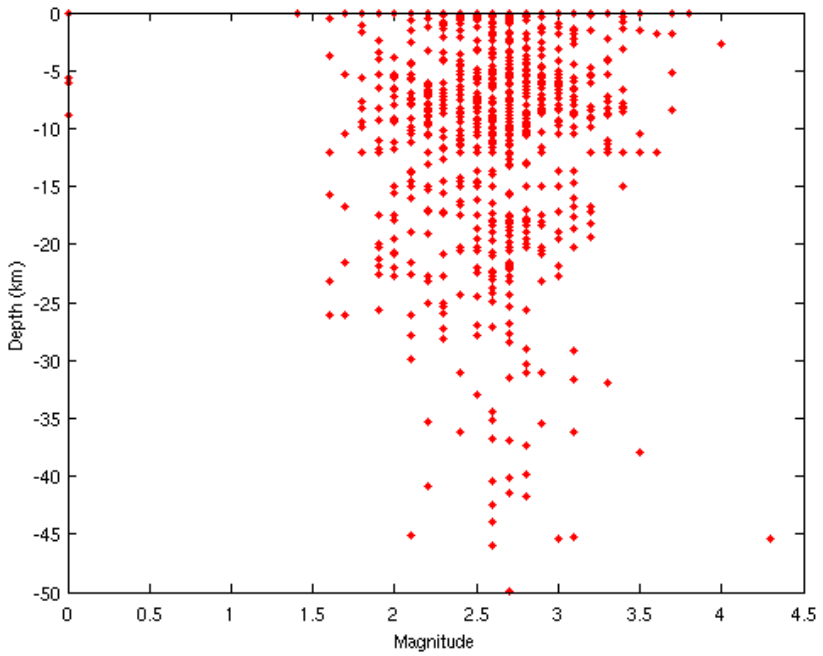

Figure 4.3. The magnitude-depth section.

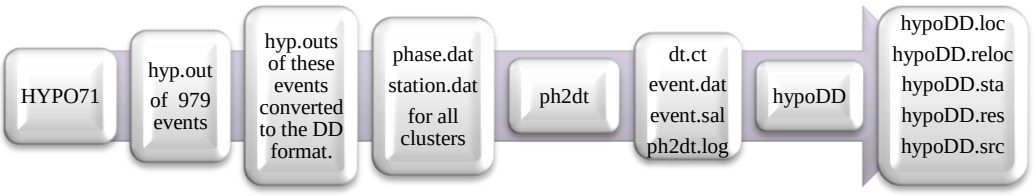

Figure 4.4. Diagram of the Double Difference Relocation Procedure in this study.

Figure 4.4 illustrates the process flow of our study. The output of HYPO71 is not compatible to HYPODD format so it was transformed to DD format by using a subprogram of SEISAN package, namely Nor2dd. This step creates the input data file for hypoDD (i.e. phase.dat) in addition to other auxiliary files such as one which include the station list (i.e. station.dat). The relationship between the hypocenter parameters (epicenter coordinates and the origin time) and the observed parameters (arrival times) is non-linear. Furthermore, in the double difference algorithm the earthquakes are located by creating

event pairs, therefore the dimensions of the hypocenter and observed parameter matrix are also too large. Our complete data contains the 972 earthquakes which is too large to be done in one single block. We separated the data into four clusters according to the earthquake distribution for understanding the HYPODD performance on different data sets and the computer memory restrictions. The clusters are shown in the Figure 4.5. The number of the events, the distance between event and stations and the distance between events are different in each cluster. These features of the clusters are useful for illustrating the performance of the double difference algorithm on different data sets. The phase.dat and station.dat files were created for all individual clusters.

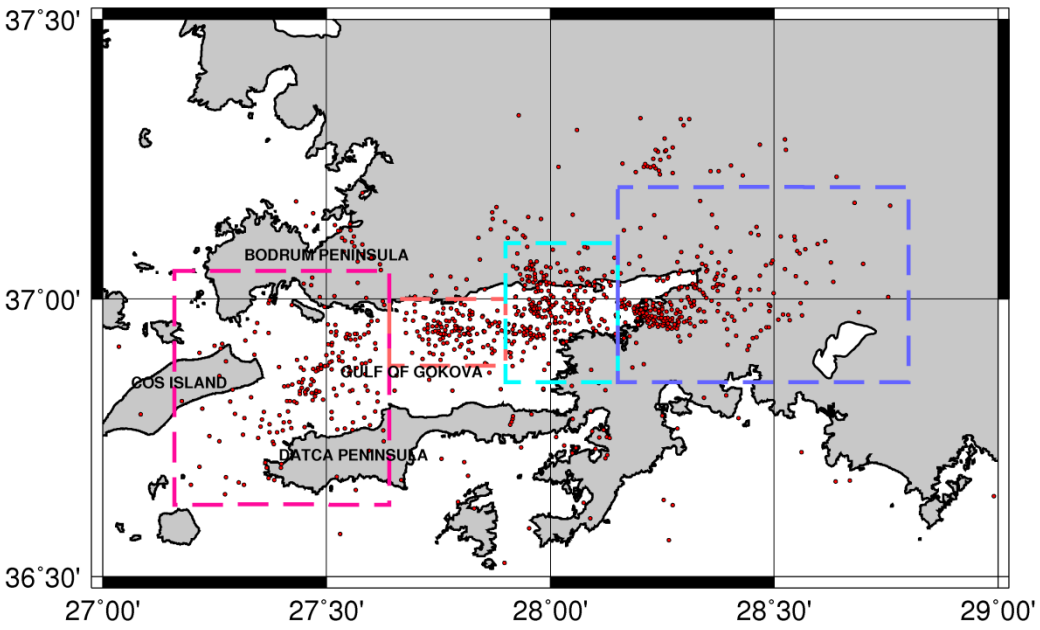

Figure 4.5. Clusters.

In the phase.dat file all earthquakes have an id number and the event pairs are created by using these numbers (Table 4.1). One of the most important things is the weighting of the phases which are not same for all stations and for all earthquakes. The weighting translation is done by Nor2dd. The 0, 1, 2 and 4 weights in hyp.out are expressed by 1.00,

0.75, 0.50 and 0.00 in phase.dat, respectively. The weight for an event pair is found by averaging the weights given in phase.dat and are used by ph2dt for creating dt.ct file.

Table 4.1. Example of phase.dat file format.This file contains the header and travel time informations.

```
#  2006  4  3  3 23 40.0  36.904   27.908  26.7 0.0 0.0 0.0 0.2    1
DAT       6.68 1.00 P
DAT      12.16 1.00 S
YER       7.92 1.00 P
YER      13.56 1.00 S
MLSB     8.06 1.00 P
MLSB    13.92 1.00 S
BODT     9.54 1.00 P
BODT    16.96 1.00 S
#  2006  4  3 12 36 45.1  36.971   27.820  23.1 0.0 0.0 0.0 0.4    2
```

The other output of Nor2dd is station.dat file which contains the latitude and longitudes of the stations in decimal format (Table 4.2).

Table 4.2. Station.dat file contains the latitude and longitude of the stations in decimal format.

DAT	36.7290	27.5778
BODT	37.0622	27.3103
MLSB	37.2953	27.7765
YER	37.1347	28.2828
BLCB	38.3853	27.0420
CETI	37.0032	28.3067
DALT	36.7692	28.6372
FETY	36.6353	29.0835
OREN	37.0417	27.9672
OZCA	36.8292	28.0772
TURG	37.1540	28.6920

In this study we used both catalog and cross-correlation data but before these steps we tried to understand the effects of the ph2dt and hypoDD (inversion process) input parameters to the final performance. These control parameters are directly related to the data set and they should be chosen as much as compatible with the properties of the data.

4.2. Choice of The Input Parameters for Ph2dt

There are mainly two steps in the HYPODD process: the determination of the event pairs and together with their phase differences (ph2dt step), and the inversion process for the relocation (hypoDD step). We have selected the input parameters such that most of the filtering was done in ph2dt phase, where else the filtering at inversion step was kept to a minimum.

Input parameters of the ph2dt program are MINWGHT, MAXDIST, MAXSEP, MAXNGH, MINLNK, MINOBS and MAXOBS. The first parameter MINWGHT represents the minimum pick weight. The unreliable pick weight corresponds to zero in phase.dat file. Increase in the MINWGHT parameter means that the program will use only the reliable phase readings. Numbers of the unreliable phase picks are low in our data and most of these picks represent the distant or malfunctioning stations. Taking into account the relatively low number of stations available, we have decided to include all readings, even the most distant ones, taking however their relative weight into account. We have therefore chosen MINWGHT to be zero for all clusters.

We calculated the distance between the stations and each earthquake by using a matlab code at each cluster. We therefore determine the distribution of the observation distance at each station and choose the MAXDIST parameter accordingly.

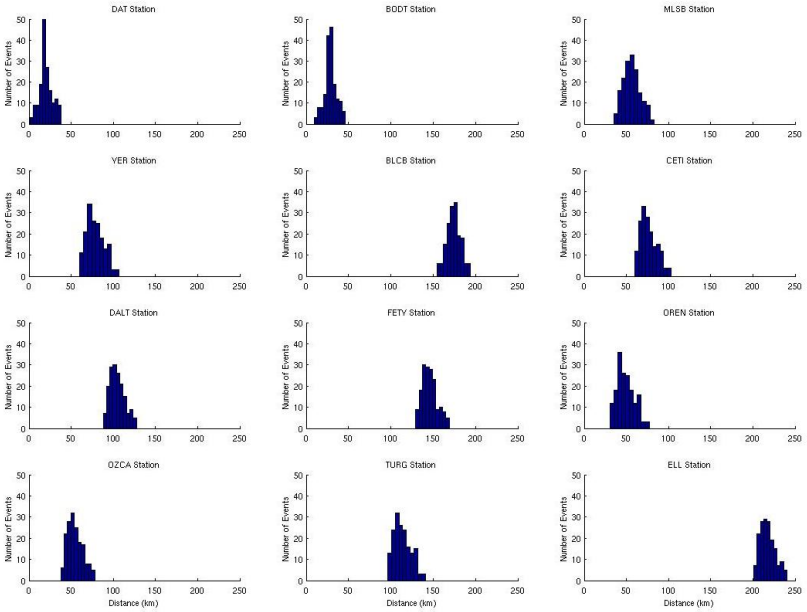

Figure 4.6. Distance between the stations and the earthquakes in Cluster 1. ELL is the most distant station to the earthquakes in Cluster 1 with 217 km averagely. The average of the distance between the nearest station DAT and Cluster 1 is 20 km.

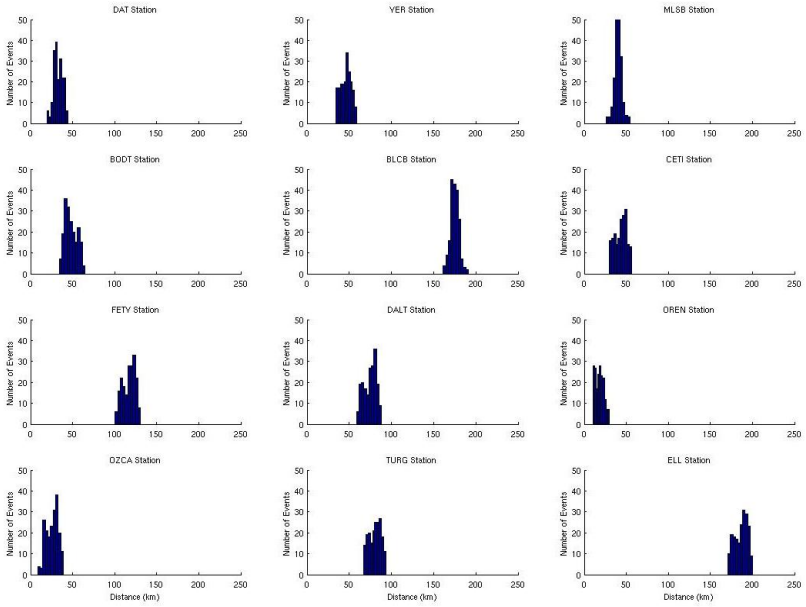

Figure 4.7. Distance between the stations and the earthquakes in Cluster 2. ELL is the most distant station to the earthquakes in Cluster 2 with 186 km averagely. The average of the distance between the nearest station OREN and Cluster 2 is 18 km.

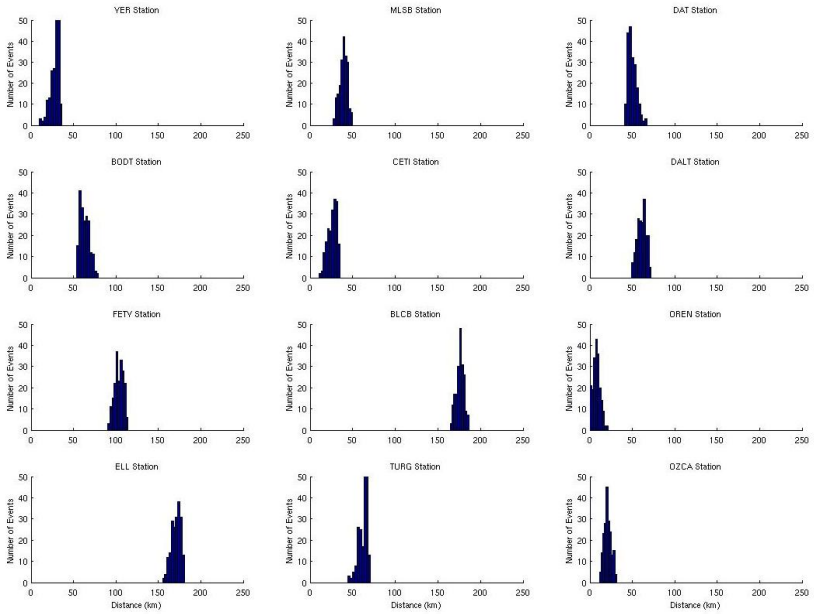

Figure 4.8. Distance between the stations and the earthquakes in Cluster 3. BLCB is the most distant station to the earthquakes in Cluster 3 with 175 km averagely. The average of the distance between the nearest station OREN and Cluster 3 is 8 km.

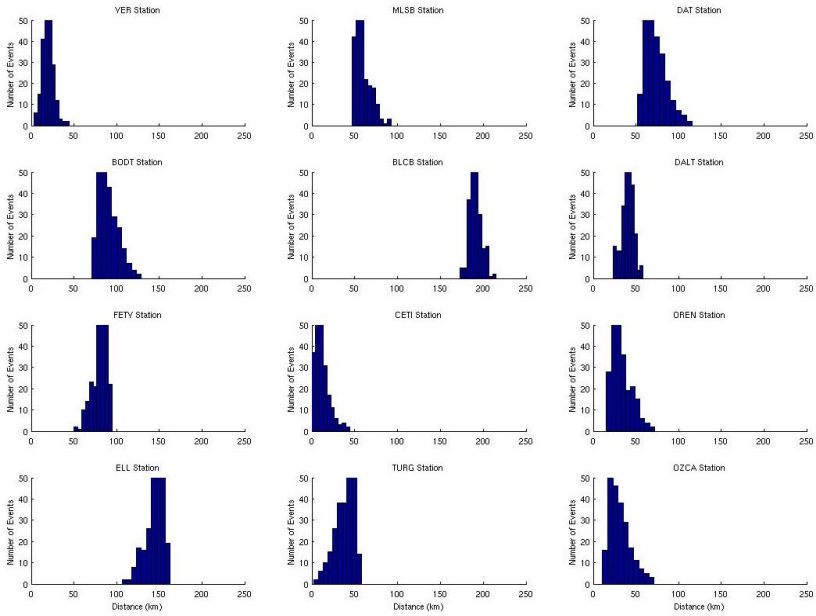

Figure 4.9. Distance between the stations and the earthquakes in Cluster 4. BLCB is the most distant station to the earthquakes in Cluster 4 with 190 km averagely. The average of the distance between the nearest station CETI and Cluster 4 is 11 km.

Some typical examples of the distribution of observation distance are displayed in Figure 4.6 to 4.9. Each figure shows the distance distribution at every station, for each cluster from 1 to 4. According to the results of the distance between the stations and the earthquakes, ELL station is the most distant one at almost all clusters. This station has the largest weights both for P and S phases at almost all earthquakes. Therefore some of the ELL station data may be eliminated from the data set. In this study the MAXDIST parameter of the ph2dt is chosen as 200 km.

The input parameters given above (MINWGHT, MAXDIST) were chosen directly by examining the input HYPO71 data. However, the following input parameters are selected after a number of trial and error experiments are carried out. Ph2dt input parameters should be taken into account together, however for understanding their effects to the outputs, their effect should be considered as individually. For instance MAXSEP parameter is analyzed by changing its values only and fixing the other ones. For understanding the affects of the parameters, dt.ct file are compared to previous ones which are obtained using different set of parameters. At this stage it should noted that ph2dt program calculates the distance by using not only latitude and longitude but also the depth (Figure 4.10). So the 2D sketches are not always enough to understand the real effect of parameters choice.

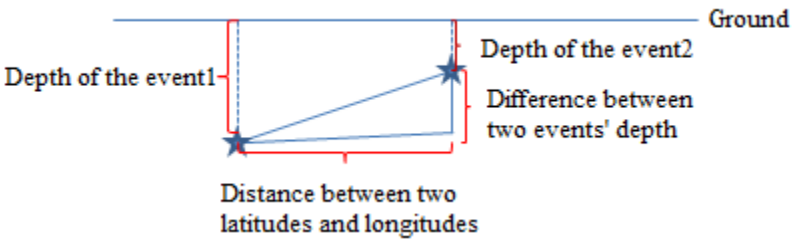

Figure 4.10. Diagram of the distance calculation parameters.

MAXSEP is the distance between two events when creating event pair. Increase in the MAXSEP value creates more event pairs if there is no limitation posed by the other parameters. Formally, MAXSEP should be as small as possible relatively to the distance between the stations and the earthquakes. If MAXSEP is chosen too high, ph2dt create large data set for inversion process (hypoDD) because all available earthquakes in the large search radius will be linked. This may mean that if two linked events are too far from each other, a uniquely defined travel path assumption may not be true anymore. Furthermore too many linked events may also create instability of the inversion. The opposite is also not desired since choosing the number of links too low will fails to make a significant correction in the relocations. For deciding the right MAXSEP value, we selected MAXSEP large enough to allow the majority of link to be taken into account. Figure 4.11 shows the distribution of event pair distances for different cluster. We observe that most of the event pair distances are below 6 km and the number of event pairs is higher in the less scattered clusters (i.e. Cluster 2 in Figure 4.11). Only a small portion is above this threshold value, this mainly due to the fact that we have separated our data into clusters of a certain fixed radius. In the Cluster 1 we also observe that the event pair distances are slightly more evenly scattered between 1 and 8 km. We choose the MAXSEP value as 10 to take into account mostly the scattering in Cluster1. This choice will not modify the final results too much in the other clusters, since in those cases the events are much more squeezed in a single zone. Additionally, we used both MAXSEP = 10 and MAXSEP = 5 options in these three clusters and compared the results.

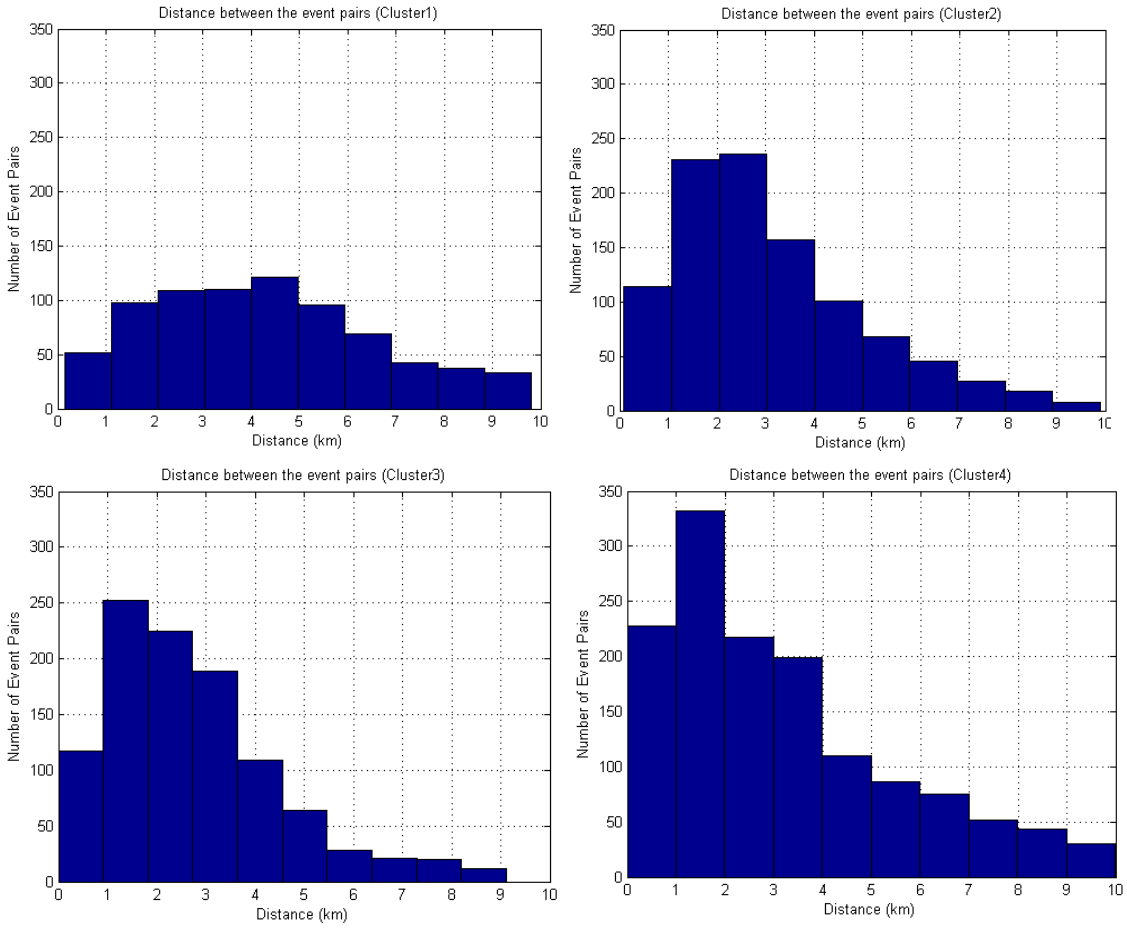

Figure 4.11. Distance between the event pairs for all clusters (MAXSEP =10).

MAXNGH is a parameter which concerns the definition of neighborhood of event. It is defined as the maximum number of the neighbor of an event within the search radius. The search radius is represented by MAXSEP parameter and if we restrict the MAXNGH the ph2dt program eliminates the distant neighbors.

MINLNK is a parameter which concerns an event pair. It is the lower limit of the phase number recorded at common stations. We determined this parameter according to the number of stations and the weakly linked events rate. If the event pairs have more than MINLNK common phases, the event pair is named as strongly linked events. The weakly linked events have less then MINLNK phase pairs and they are selected but not counted as strong neighbor. It is possible that an event is weakly linked with a specific event, but

strongly linked with other events. Strongly located events are always relocated. The weakly linked events are not relocated by hypoDD (inversion process) if they cannot establish the strong links between the other events. The output of the ph2dt shows the weakly linked event percentages. We tried to choose the lowest value possible. The Clusters 1 and 4 have relatively high weakly linked event rate due to the rate of the distant event in these clusters, which are higher than the Cluster 2 and 3. Our number of the station is not large so we accept this parameter as 4 which correspond to one third of the number of the stations.

MINOBS and MAXOBS parameters concerns whether an event pair valid or not, looking at number of common stations. MINOBS puts lower limit to the number of readings which recorded at common station for these two events. Note that if only P-phase readings are available MINOBS is equivalent to MINLNK. The MINOBS is 3 in all clusters because we do not have numerous stations so at least 3 common stations is consistent with our data and the station number. The MAXOBS is the maximum number of common stations and it can be used as large as the number of stations. This parameter can be limited according to the number of distant and near stations. We limited the number of stations and only used six of them in our study but the result of this limitation was mainly same with the unlimited ones. So we did not restrict the MAXOBS and accept the parameter as the number of stations (MAXOBS = 12).

In this study we used both catalog and cross-correlation data inputs for hypoDD but at this stage we mentioned only the creating dt.ct file (the catalog data). We created the cross-correlation data file dt.cc by using the event pairs of the dt.ct. All event pairs are correlated by using a shell program and dt.cc files are created for all clusters separately.

4.3. Choice Input Parameters for The HypoDD

The input parameters for the inversion step, (expressed in hypoDD.inp file) should be selected in accordance with the certain properties of catalog or cross-correlation data.

At the first step we used only the catalog data and organized the hypoDD.inp parameters for this purpose. All P and S phases were used in this step and the distance parameter between the cluster centroid and the stations was chosen to be 200 km.

The WTCCP, WTCCS, WTCTP and WTCTS parameters represent the weights of the P and S phases for cross-correlation and catalog data; respectively. The parameters which are inactive are indicated by -9. For example if catalog and cross-correlation data is used separately, the non-used weights should be selected as -9. There is also an option for using the catalog and cross-correlation data together by setting the parameters accordingly. In each case the phase weighting parameters are determined according to the data set. The weights of the P phases (WTCTP) were chosen to be higher than the S phase weights (WTCTS) at all iterations. The reason of this choice is shown in the Figure 4.12. The most of the number of reliable picks are P phases at all clusters. The S weights were increased gradually at each iteration (<=WTCTS=0.5) while P weights were held fixed (WTCTP=1.0).

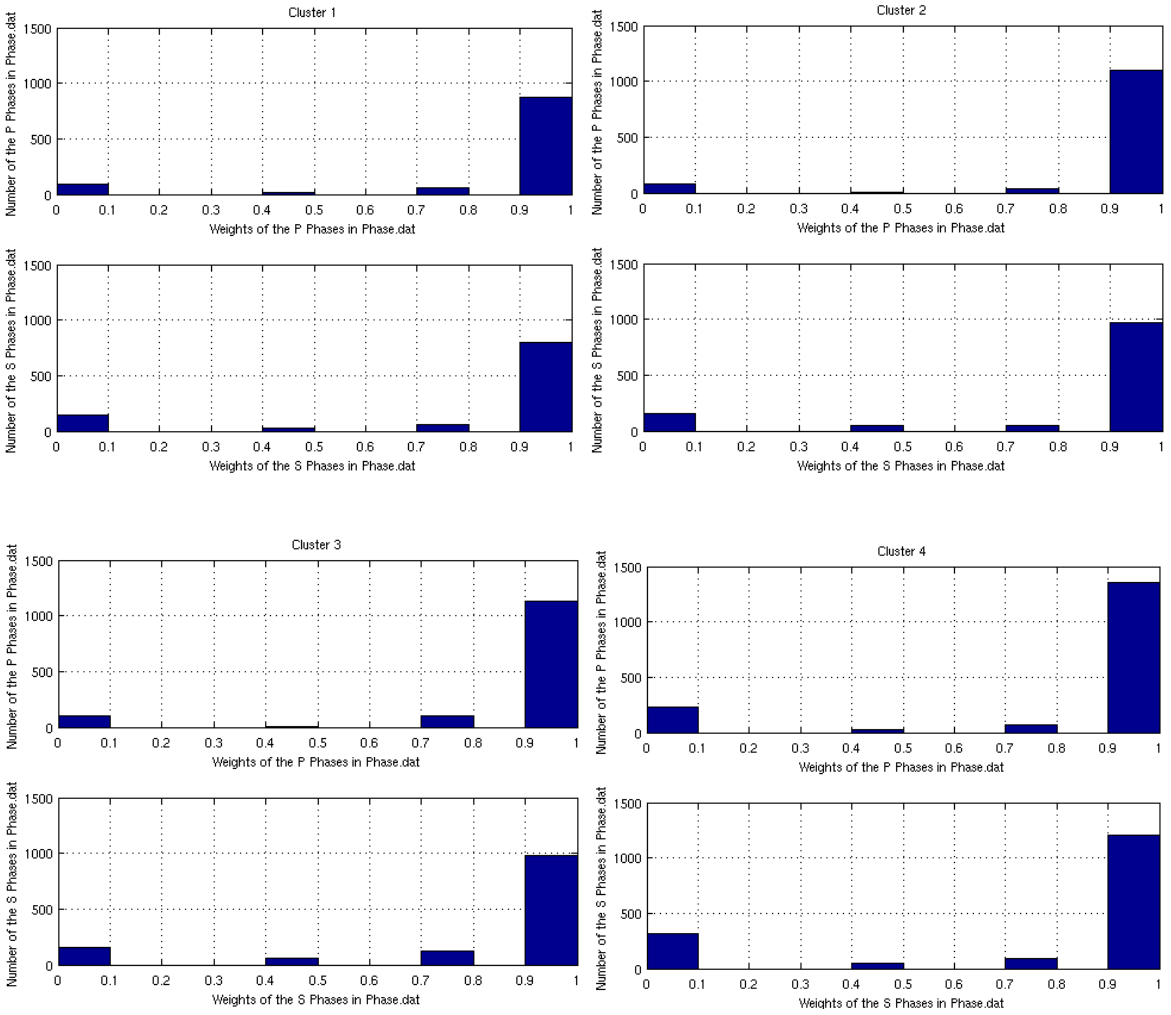

Figure 4.12. The number of the P and S phase weights of each cluster. Number of the P phase weights at all clusters are higher than the number of S phase weights.

The other weighting parameters are WRCC, WRCT, WDCC, WDCT. The maximum distance between the event pairs is restricted by WDCC (cross-correlation) and WDCT (catalog).

The re-weightining parameter WDCT is quite similar to the MAXSEP parameter used in ph2dt step. The main difference between them is that MAXSEP limits the distance between events while WDCT parameter represents the distance between event pairs (km). According to our observation decreasing the WDCC or WDCT parameters only eliminate the distant data. We tested this parameter for different values and according to our observations it is only useful for determining the major trend of the cluster, eliminating the

scattered ones. In practice keeping low values for WDCT makes the cluster cleaner but this may not corresponds to the real situation. In this study WDCT were chosen as 9 or 4, depending on the MAXSEP and to the cluster analyzed. The damping and the weights were determined for each iteration separately according to the residual value of the iteration.

4.4. Choice Input Parameters for Cross-Correlation

An important part of this study is relocating the earthquakes by using cross-correlation for determining phase arrival differences. In this case the arrival differences are now determined by cross-correlating the waveforms instead of taking directly the time difference between phase pickings. From the physical point of view, the catalog data locate the onset of the earthquake rupture while the correlation is expected to locate the centroid.

There is no special tool in HYPODD package for calculating the cross-correlation between waveforms and preparing the input file (dt.cc). This file (ct.cc) was created for each cluster separately by using a combination of shell and FORTRAN programs that were written for the purpose. In this program the event pairs are taken the same as the ones in the dt.ct file. We have selected the parameters for the cross-correlation by considering the magnitude range, the distance range and also applying some tests to the data. Considering the size of the events that are used in the analysis (in general $2<M<3.5$) we have taken the correlation in a time window of 4 second centered around the P-arrival or S-arrivals. We have used the vertical component for the P-phase and horizontal components for the S-phase. For the case of S-phase the component which gave the highest cross-correlation value was chosen as the final time differential. The data were filtered with a 6th order Butterworth bandpass filter between 0.1-12 Hz with two-pass.

We have checked how different the time differentials when estimated from the first readings (i.e. catalog data) and when calculated by cross correlation. Strictly speaking they need not to be the same since they represent different things as explained above. However for small events ($M<4.0$) they are very close to each other. Therefore the results of catalog and correlation approach should be expected to be comparable. We have checked the time

difference between catalog (Δt_{cat}) and cros-corrrelation (Δt_{cor}) for each station components at each cluster. Ideally the plot of Δt_{cat} against Δt_{cor} should give a straight line trough the origin with a slope value of 1. In practice however the two readings are not always the same giving therefore a scaterred line.

Our observations have shown that the catalog-correlation comparison changes according to the study area and the features of the data set. The comparisions of the differential and the correlation times at all stations for both P and S phases (Figure 4.13 and Figure 4.14) have shown that the scattering increases with distance both for P and S-phases. For instance the DAT station is the closest one to the first cluster (20 km) and it is located at the Datça Peninsula. The results of the differential time comparision have shown that the scattering is minimum in that station for P phases (Figure 4.13). On the other hand the comparisions of the differential times at the same station for the fourth cluster which is the furthest one the scettering is high for the same P phase (Figure 4.14). At almost all clusters, the scatering of the differential time comparisions of S phases are higher than the P phases. The high scatering of P phase is observed only when the station is distant to the cluster. The effects of the distance can be also seen by examining the weights of the phases according to the stations. The HYPODD penalize the bad readings by giving a low weight to that phase in the inversion.

In the case when MAXSEP = 10 km, the scatering changes between -0.8 and +0.8 s for the P phase and -1.2 and +1.2 s for the S phases. According to the differential time comparision results the stations away from the sea and the cultural noise have a higher performance like the case for the OZCA station (Figure 4.13 and Figure 4.14).

The maximum value of the differential times should never exceed the maximum arrival difference between the events of a pair. In the case when MAXSEP = 10 km, this is not higher than the 2.0 second. In fact, if we calculate the distance roughly by using the P-wave velocity, the corresponding distance will be almost 2.0x5.0=10.0 km, which is compatible with the MAXSEP parameter.

The Figures 4.15 and 4.16 illustrate the weights distribution at a single station for P and S phases, separately. If we examine the case of DAT station at Cluster 1 and 4, it can be clearly recognized that the high weights correspond to the close distance case and less differential time scattering. Similarly, we observe that high weights assignments correspond also to the smaller scattering in differential time comparision curves.

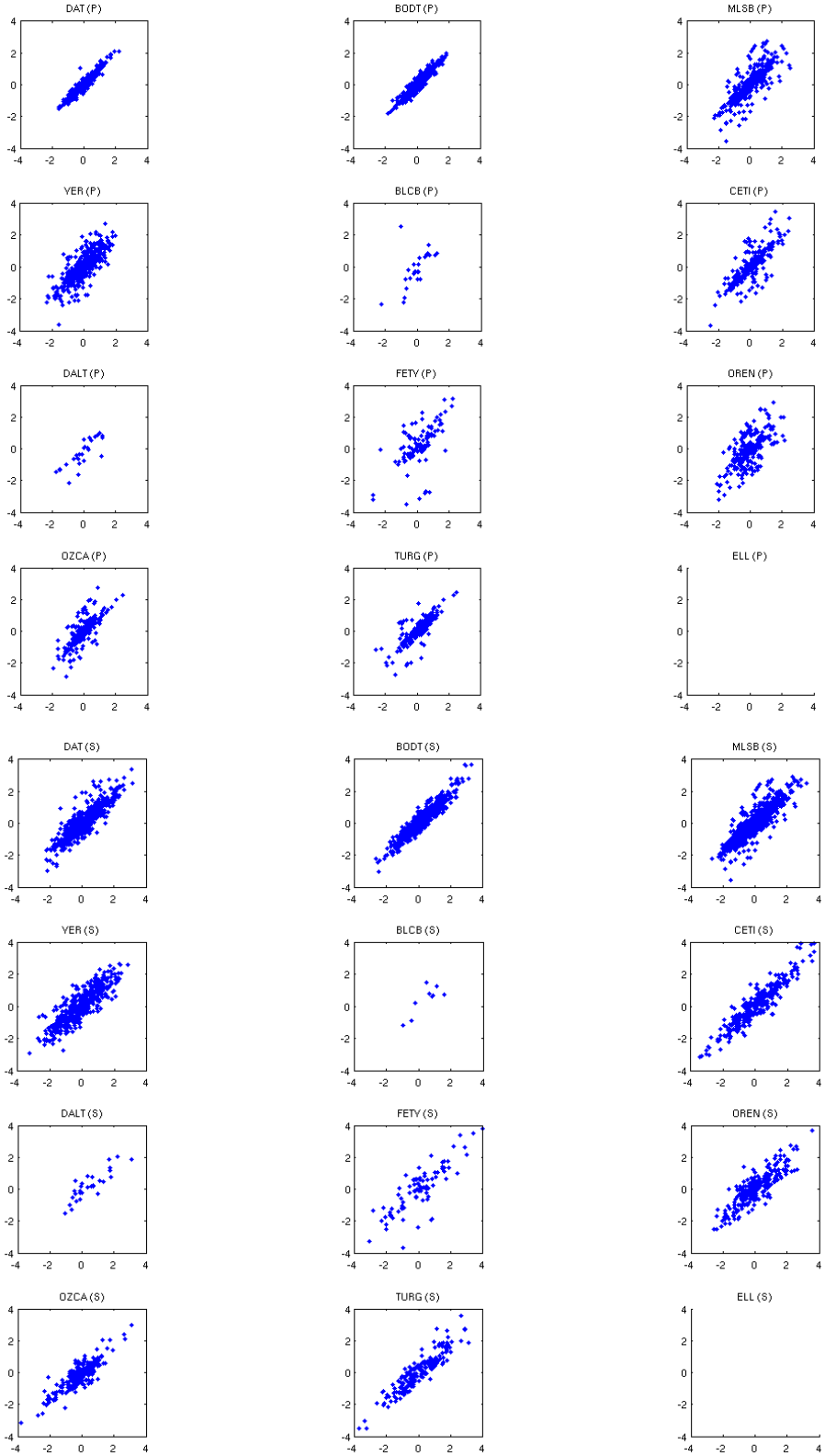

Figure 4.13. Differential times with respect to the correlation time of both phases at all stations (Cluster 1).

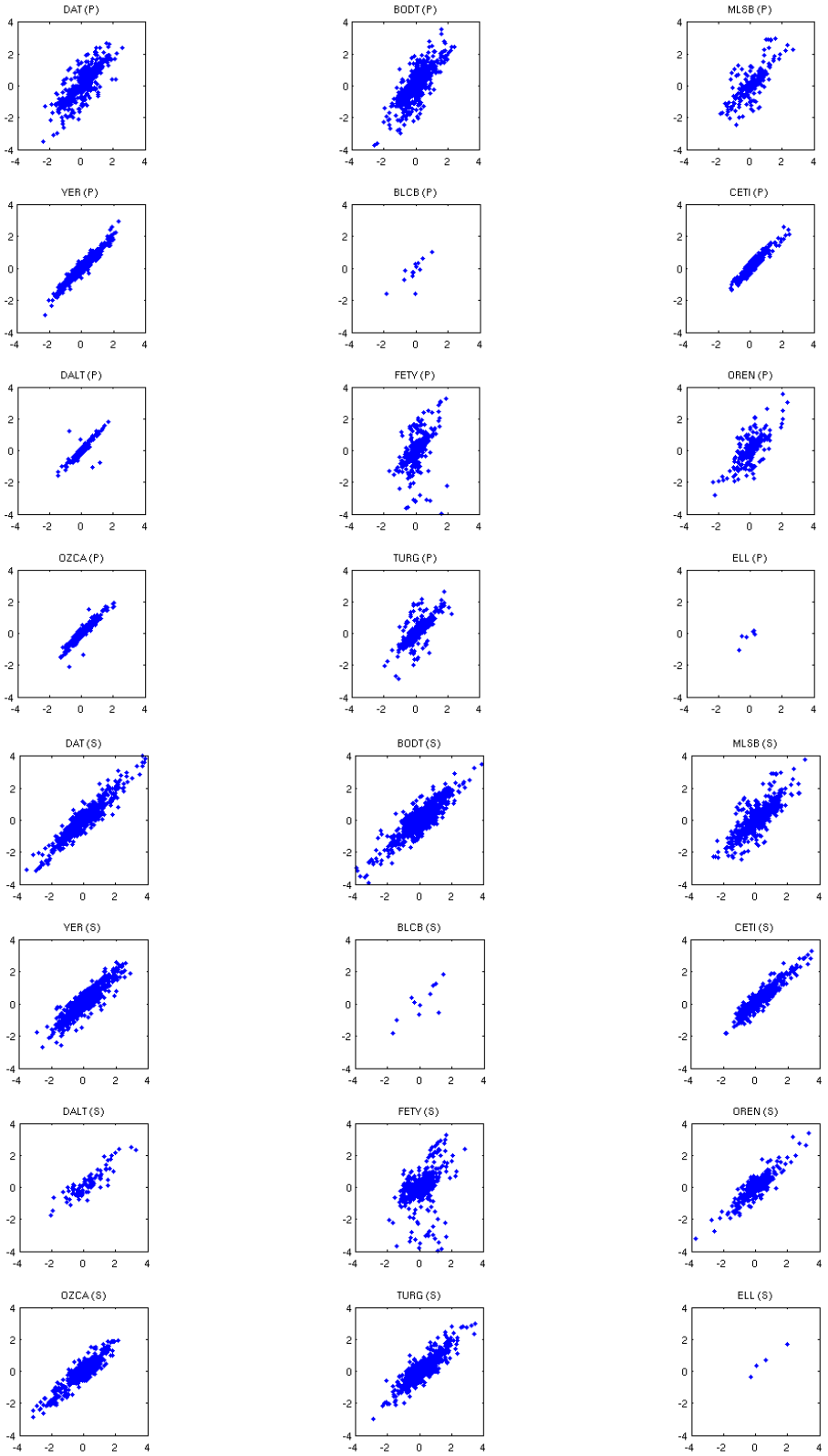

Figure 4.14. Differential times with respect to the correlation time of both phases at all stations (Cluster 4).

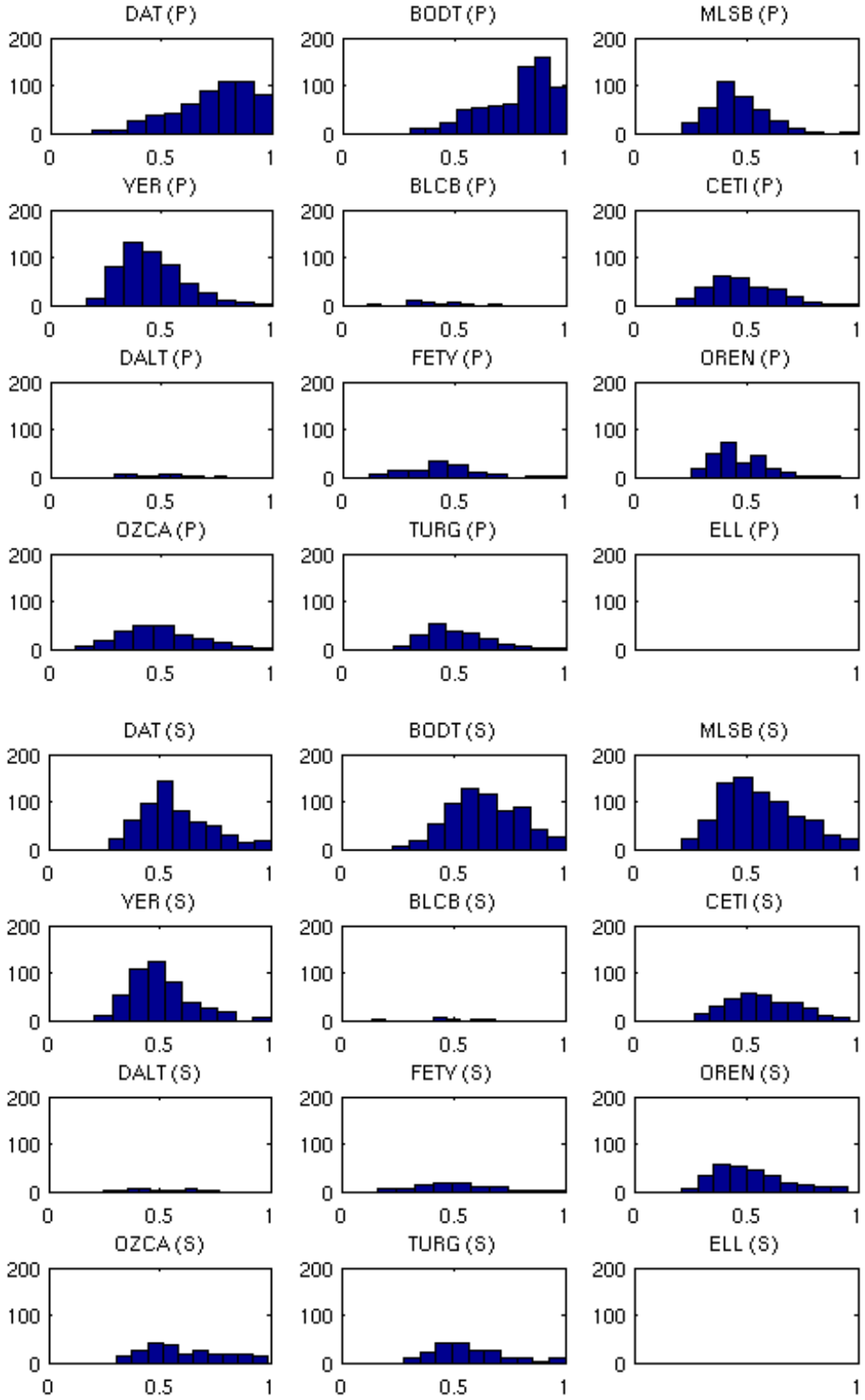

Figure 4.15. Weight distributions of both P and S phases at all stations (Cluster 1).

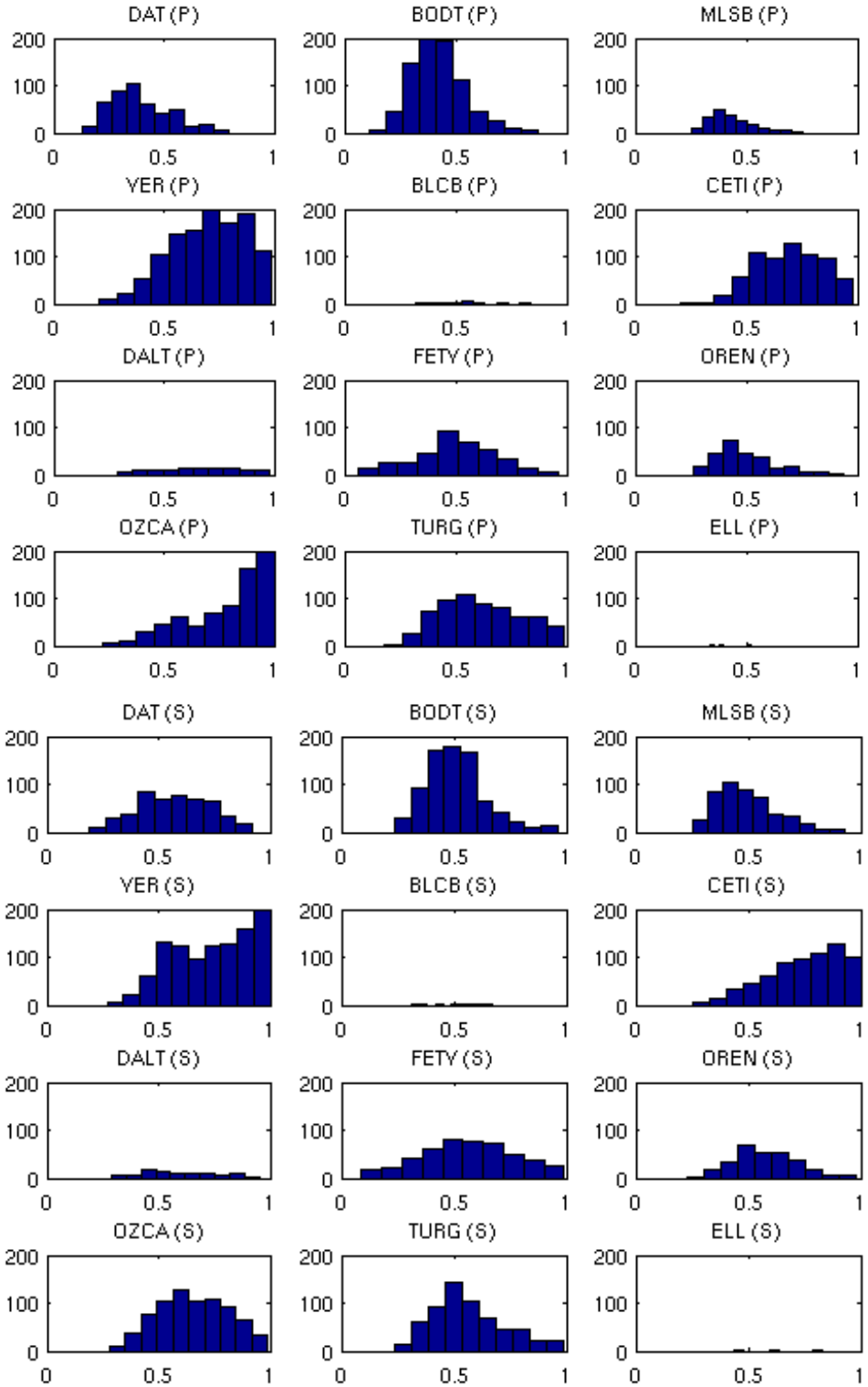

Figure 4.16. Weight distributions of both P and S phases at all stations (Cluster 4).

5. RESULTS AND DISCUSSIONS

In this chapter the results of applying the HYPODD relocation are presented. The method is applied basically with three different options:

- Divide data into four clusters and process each cluster both for catalog and correlation
- Process the total data in one step with a unique set of parameters
- Divide data into four clusters and process each cluster, using joint catalog + correlation. The results of each step are given in Section 5.1, Section 5.2 and Section 5.3.

It is clear that the inversion at the final step which process each cluster individually and which uses both correlation and catalog jointly and optimally should have the best performance. On the other hand, the second step which treats the whole with single set of globally optimal parameters should have the lesser performance. We observe that the differences in all cases are not too large to prefer one approach to the other. However this conclusion is not a general and cannot valid for all data sets.

5.1. The Results of the Clusters for both Catalog and Correlation Process

At the beginning of this section we give the summary of the figures (Table 5.1) which contains both inversion process (catalog and correlation) for two different control parameters (MAXSEP = 5 and MAXSEP = 10).

Table 5.1. Summary of the figures in the following section.

Number of the Figure	Number of the Cluster		Program	Method		
5.1	Cluster 1	Mapview	Hypo71			
5.2	Cluster 1	Mapview	HypoDD	Catalog	Correlation	MAXSEP=10
5.3	Cluster 1	Section	HypoDD	Catalog		MAXSEP=10
5.4	Cluster 1	Section	HypoDD		Correlation	MAXSEP=10
5.5	Cluster 2	Mapview	Hypo71			
5.6	Cluster 2	Mapview	HypoDD	Catalog	Correlation	MAXSEP=10
5.7	Cluster 2	Section	HypoDD	Catalog		MAXSEP=10
5.8	Cluster 2	Section	HypoDD		Correlation	MAXSEP=10
5.9	Cluster 2	Mapview	HypoDD	Catalog	Correlation	MAXSEP=5
5.10	Cluster 2	Section	HypoDD	Catalog		MAXSEP=5
5.11	Cluster 2	Section	HypoDD		Correlation	MAXSEP=5
5.12	Cluster 3	Mapview	Hypo71			
5.13	Ören	Mapview	Hypo71			
5.14	Ören	Section	HypoDD	Catalog	Correlation	MAXSEP=10
5.15	Ören	Waveform				
5.16	Ören	Histogram	Yearly			
5.17	Ören	Histogram	Hourly			
5.18	Cluster 3	Mapview	HypoDD	Catalog	Correlation	MAXSEP=10
5.19	Cluster 3	Section	HypoDD	Catalog		MAXSEP=10
5.20	Cluster 3	Section	HypoDD		Correlation	MAXSEP=10
5.21	Cluster 3	Mapview	HypoDD	Catalog	Correlation	MAXSEP=5
5.22	Cluster 3	Section	HypoDD	Catalog		MAXSEP=5
5.23	Cluster 3	Section	HypoDD		Correlation	MAXSEP=5
5.24	Cluster 4	Mapview	Hypo71			
5.25	Akyaka	Mapview	Hypo71			
5.26	Akyaka	Section	HypoDD	Catalog	Correlation	MAXSEP=10
5.27	Akyaka	Waveform				
5.28	Akyaka	Histogram	Yearly			
5.29	Akyaka	Histogram	Hourly			
5.30	Cluster 4	Mapview	HypoDD	Catalog	Correlation	MAXSEP=10
5.31	Cluster 4	Section	HypoDD	Catalog		MAXSEP=10
5.32	Cluster 4	Section	HypoDD		Correlation	MAXSEP=10
5.33	Cluster 4	Mapview	HypoDD	Catalog	Correlation	MAXSEP=5
5.34	Cluster 4	Section	HypoDD	Catalog		MAXSEP=5
5.35	Cluster 4	Section	HypoDD		Correlation	
5.36	Cluster1+2+3+4	Mapview	HypoDD	Catalog		
5.37	Cluster1+2+3+4	Mapview	HypoDD		Correlation	

5.1.1. Results of HypoDD: Cluster 1

The first cluster is located at the western part of the Gökova Bay near the Cos Island (Figure 5.1). This cluster is the most scattered one as compared to the other three. The Figure 5.2a shows the HYPO71 locations of the earthquakes, which is called as the original data in this study. The black line illustrates the possible fault orientation. This cluster has 169 earthquakes and almost half of them were recorded in 2008. The average distance between the events is 5 km. The histogram of the distance between the events is scattered in a broad sense, and not localized at a specific number, meaning that all kinds of distances were observed (Chapter 4 in Figure 4.10). In this cluster the percentages of the distant earthquakes are higher than the others. If the distant event rate is high in a cluster, it will affect the event pair number therefore the relocated event rate is lower for the case of Cluster 1.

The mapviews in the Figure 5.2 show the displacements of the earthquakes after relocation by using catalog (right column, Figure 5.2b, Figure 5.2d) and cross-correlation (left column, Figure 5.2c, Figure 5.2e) data. The number of events relocated by the catalog and cross-correlation methods was 108 and 113, respectively. The average distance between the located and the relocated events, in other words the horizontal corrections are 2.7 and 2.45 km, respectively for the catalog and the cross-correlation methods.

According to the results of the relocation for both data sets (catalog and cross-correlation) the possible fault orientation is verified by the catalog data. The results of the cross-correlation have shown that the main trend of this possible fault is dispersed. This situation can be due to the insufficient number of events and also the large azimutal gap. The stations do not cover the Cluster1 from the eastern and western orientations so that the azimutal gap is almost 150 degree in most cases. Part of the scattering may be due to this situation.

The depth sections of the HYPO71 and the HYPODD (catalog and correlation) are illustrated by the Figure 5.3 and the Figure 5.4. These orientations of the depth section were taken in the fault parallel and fault normal directions. The most striking effect of applying HYPODD is to shift down all hypocenters which were located at the surface by

HYPO71. This is true for both catalog and correlation approaches. Another striking observation, which is much clear in correlation results, is the existence of a deep seismicity (15-25 km) below the well known upper crustal seismogenic zone (3-15 km). The upper seismicity zone is sharp and its dip angle is almost zero. The lower structure seems horizontal at 20 km, and extends down to almost 30 km depth. Overall we can conclude that available data are not enough for resolving the fault geometry in full detail.

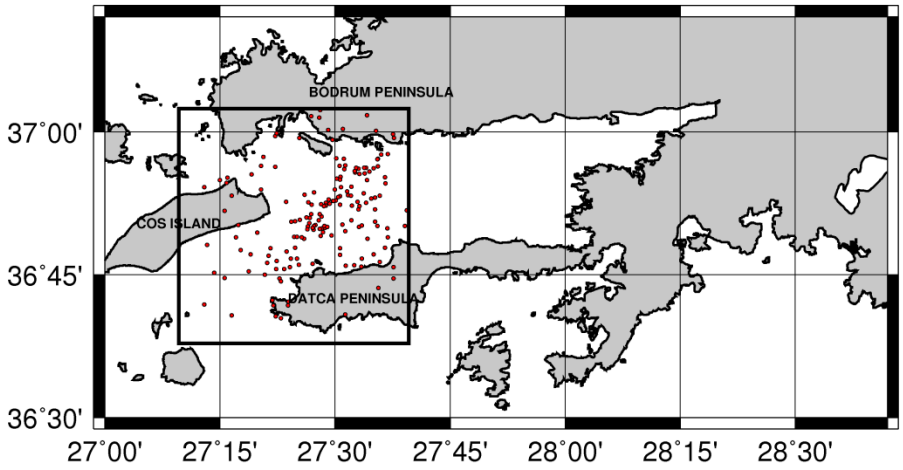

Figure 5.1. Cluster 1.

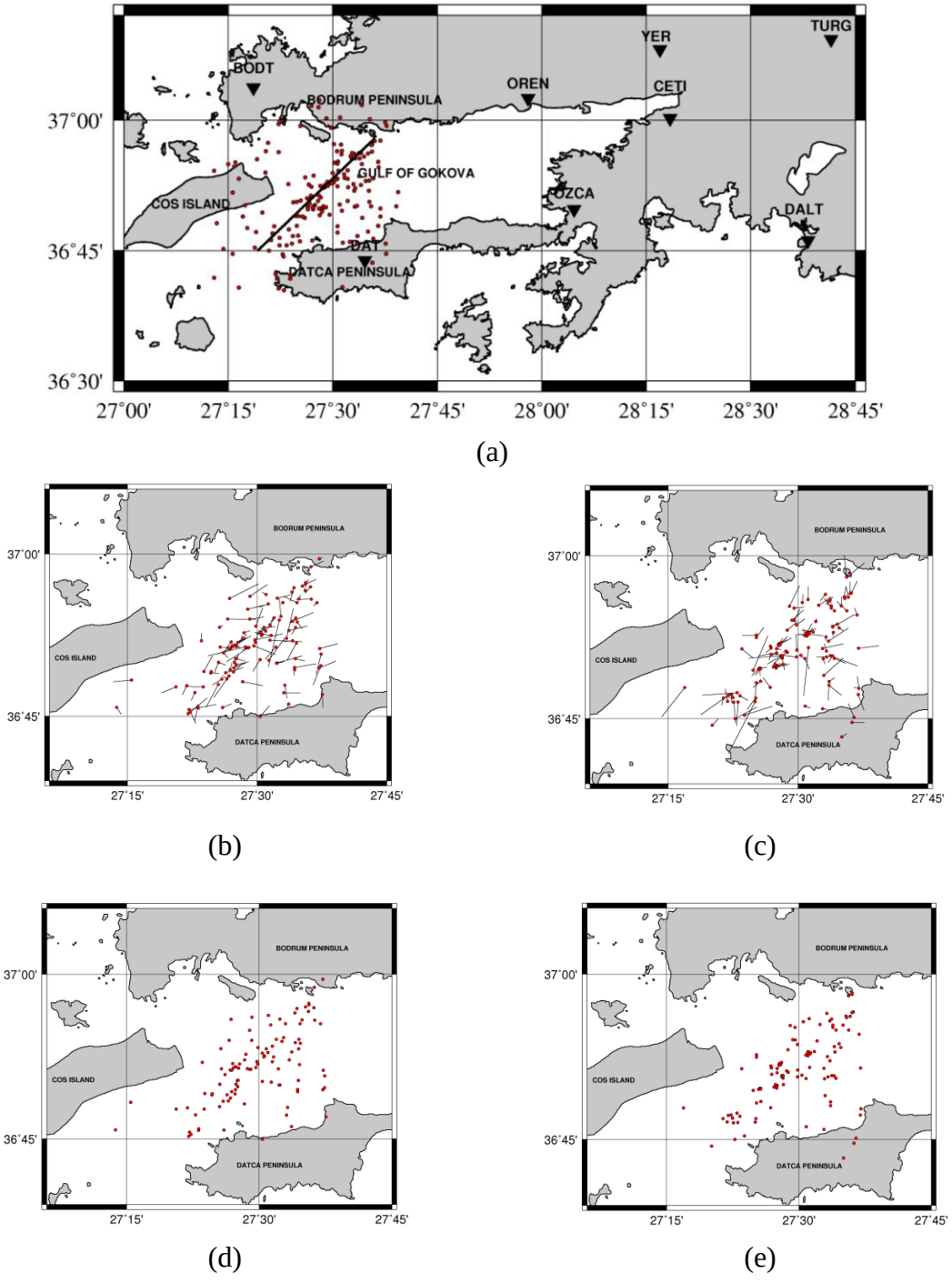

Figure 5.2. (a) Original Locations of the Earthquakes in Cluster 1 (HYPO71); (b) The corrections between the original and HYPODD locations (Catalog Data) (MAXSEP =10); (c) The corrections between the original and HYPODD locations (Cross-Correlation Data); (d) Relocated earthquakes in Cluster 1 (by using Catalog Data); (e) Relocated Earthquakes in Cluster 1 (by using Cross-Correlation Data).

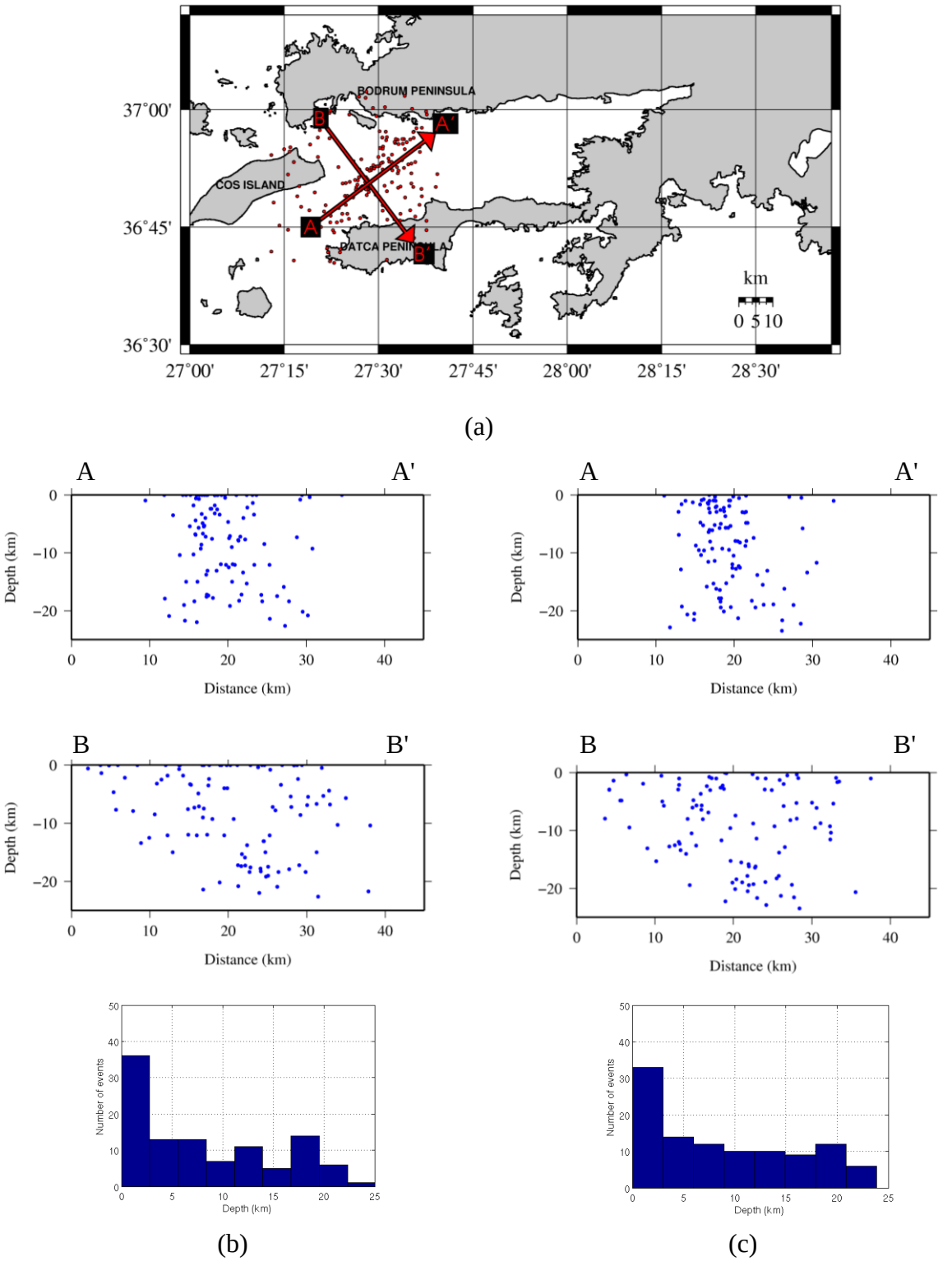

Figure 5.3. (a) Original locations of the earthquakes (Cluster 1) and profiles; (b) Cross sections view in the strike (Az = 53^0N) and normal to the strike direction (Az = 143^0N) (Original Data); (c) Cross sections view in the strike (Az = 53^0N) and normal to the strike direction (Az = 143^0N) (Catalog Data) (MAXSEP = 10).

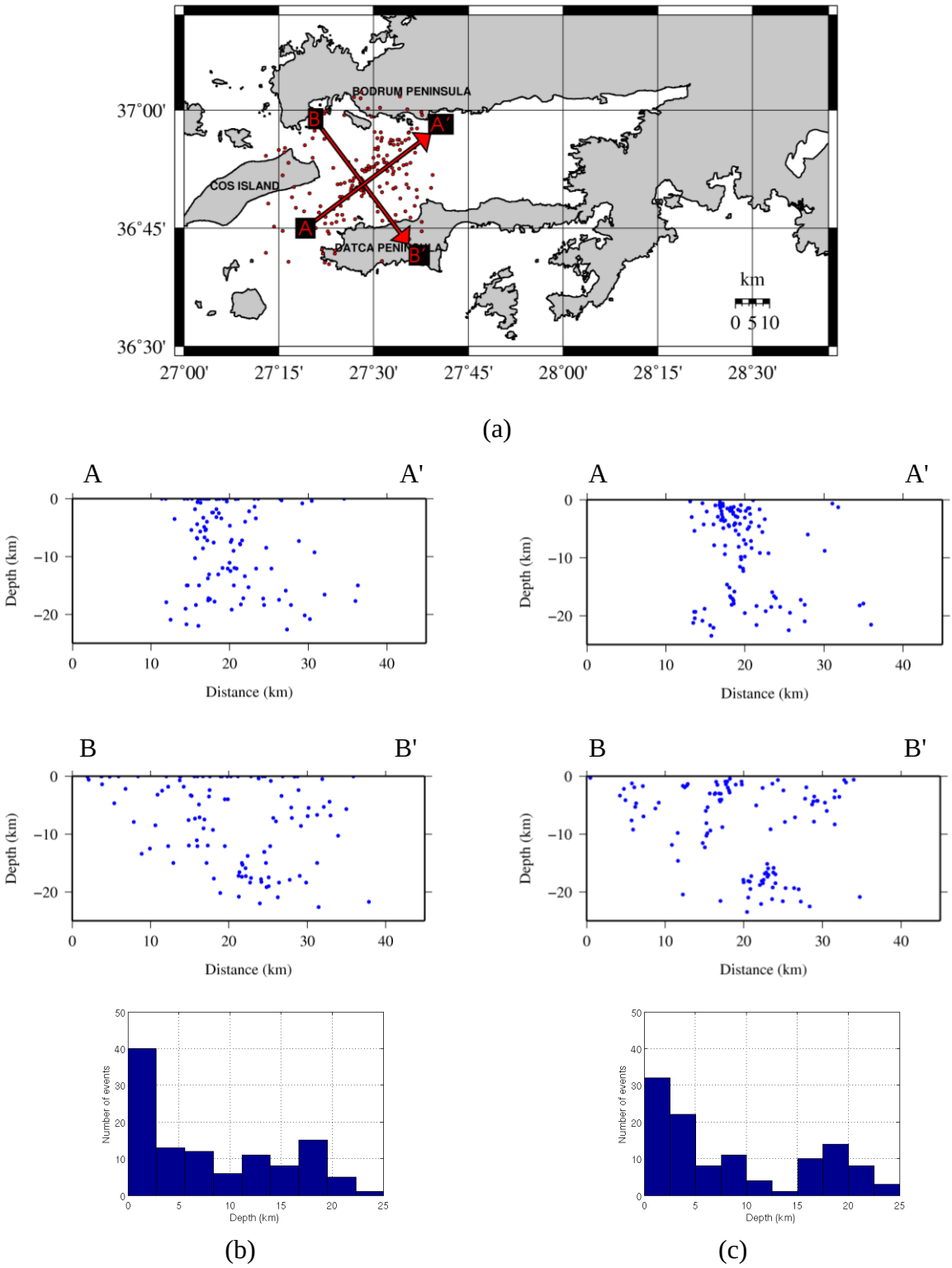

Figure 5.4. (a) Original locations of the earthquakes (Cluster 1) and profiles; (b) Cross sections view in the strike (Az = 53^0N) and normal to the strike direction (Az = 143^0N) (Original Data); (c) Cross sections view in the strike and normal to the strike direction (Az = 143^0N) (Cross-Correlation Data) (MAXSEP = 10).

5.1.2. Results of HypoDD: Cluster 2

The second cluster is located at the center of the Gökova Bay (Figure 5.5). The Figure 5.6a shows the original locations of earthquakes which are much closer to each other as compared to Cluster 1. The black line shows the possible fault orientation and this cluster has 195 earthquakes. The distribution of the earthquakes according to the years is almost uniform. The average distance between the events is 3 km and the percentages of the distant earthquakes are relatively low (Chapter 4 in Figure 4.10). Therefore we created two different input data for the inversion by choosing MAXSEP = 10 and MAXSEP = 5. If the distant event rate is low in a cluster, the catalog and also the correlation results will be expected to be better.

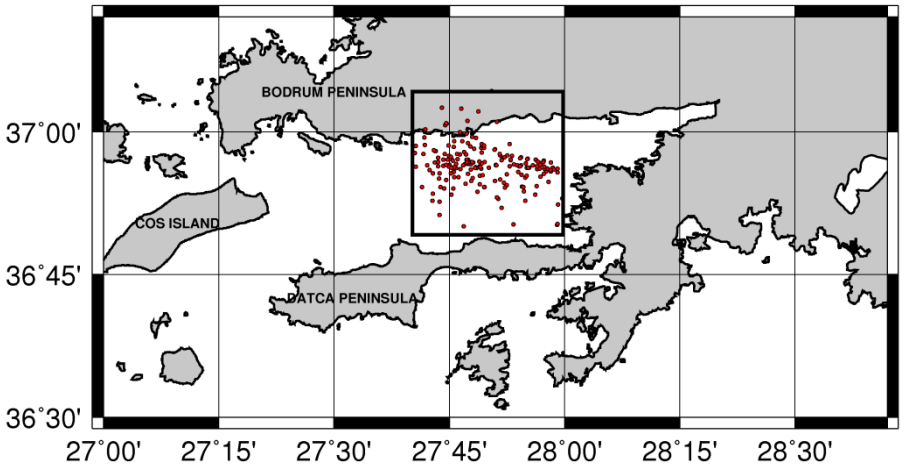

Figure 5.5. Cluster 2.

We first examine the case for MAXSEP = 10. The map views in the Figure 5.6 show the horizontal displacements of the earthquakes after relocation by using the catalog (left column, Figure 5.6b, Figure 5.6d) and the cross-correlation (right column, Figure 5.6c, Figure 5.6e) data. By using the catalog and cross-correlation data 142 and 141 of the events were relocated, respectively. The average distance between the located and the relocated events, in other words the horizontal corrections are 1.49 and 1.85 km, respectively for catalog and cross-correlation methods.

According to the results of the relocation, both data sets (catalog and cross-correlation) give a clear indication for the possible fault orientation. By using the cross-correlation the scattered data rate is decreased significantly. The cross-correlation in this cluster gives a better solution relatively to the case of the first cluster. The increase in performance for this cluster stems from the station coverage, the features of the data set, such as the distance between the events being lower and the stations being closer. As a conclusion, HYPODD results show a clear single offshore fault in the EW direction.

The depth sections of the HYPO71 and the HYPODD (catalog and correlation) are illustrated in the Figure 5.7 and Figure 5.8. Once again as in Cluster 1, the most striking effect of applying HYPODD is to shift down all hypocenters which, in HYPO71case, were located at the surface. This is true for the catalog method and even clearer in the correlation approach. Most of the earthquakes at this cluster are localized the upper 15 km. Both methods affect the depth of earthquakes locations and one of the most striking thing is the seismic activity above and below 20 km depth seems to correspond to two separate structure. Overall the cross-correlation is more effective on the data, and a well defined fault structure is verified.

The case of MAXSEP = 5 is illustrated in Figures 9-11, in a similar fashing to the previous one. We observe that restricting the event distances to 5 km reduces the number pairs to be inverted. The MAXSEP value limits the distance between two events but in this case the distance should not be considered as only horizontally. For instance, the second structure at almost 20 km depth cannot be observed in the case of MAXSEP = 5 because of the drastic decline in the number of events. However, since a smaller distance also means a higher similarity between events in a pair, we expect that the initial assumptions related to doublets are better satisfied in this case. Consequently, the number of earthquakes after the inversion is drastically reduced but we have a much clear and undispersed geometry for the seismic activity.

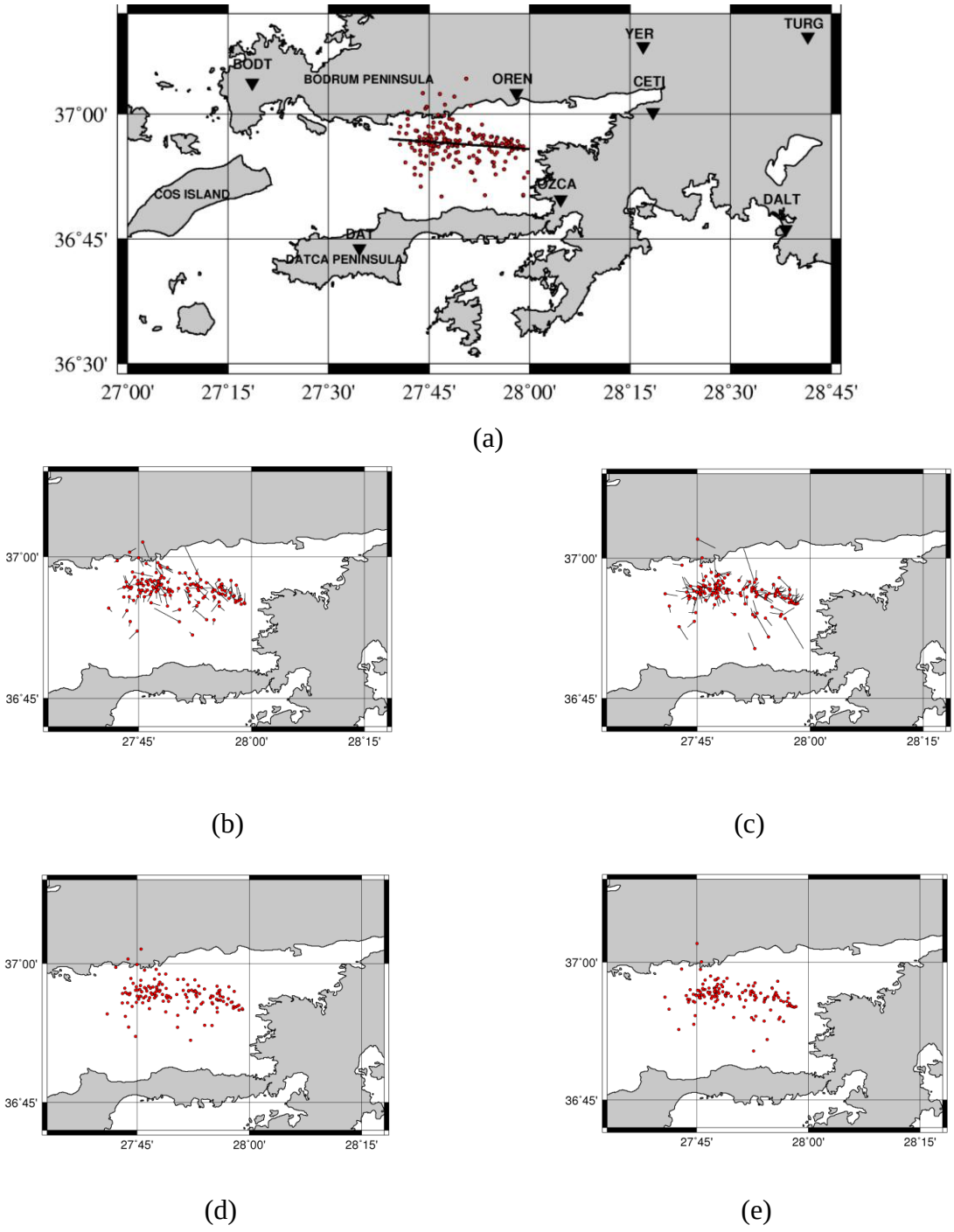

Figure 5.6. (a) Original Locations of the Earthquakes in Cluster 2 (HYPO71); (b) The corrections between the original and HYPODD locations (Catalog Data) (MAXSEP = 10); (c) The corrections between the original and HYPODD locations (Cross-Correlation) (d) Relocated Earthquakes in Cluster 2 (by using Catalog Data); (e) Relocated Earthquakes in Cluster 2 (by using Cross-Correlation Data).

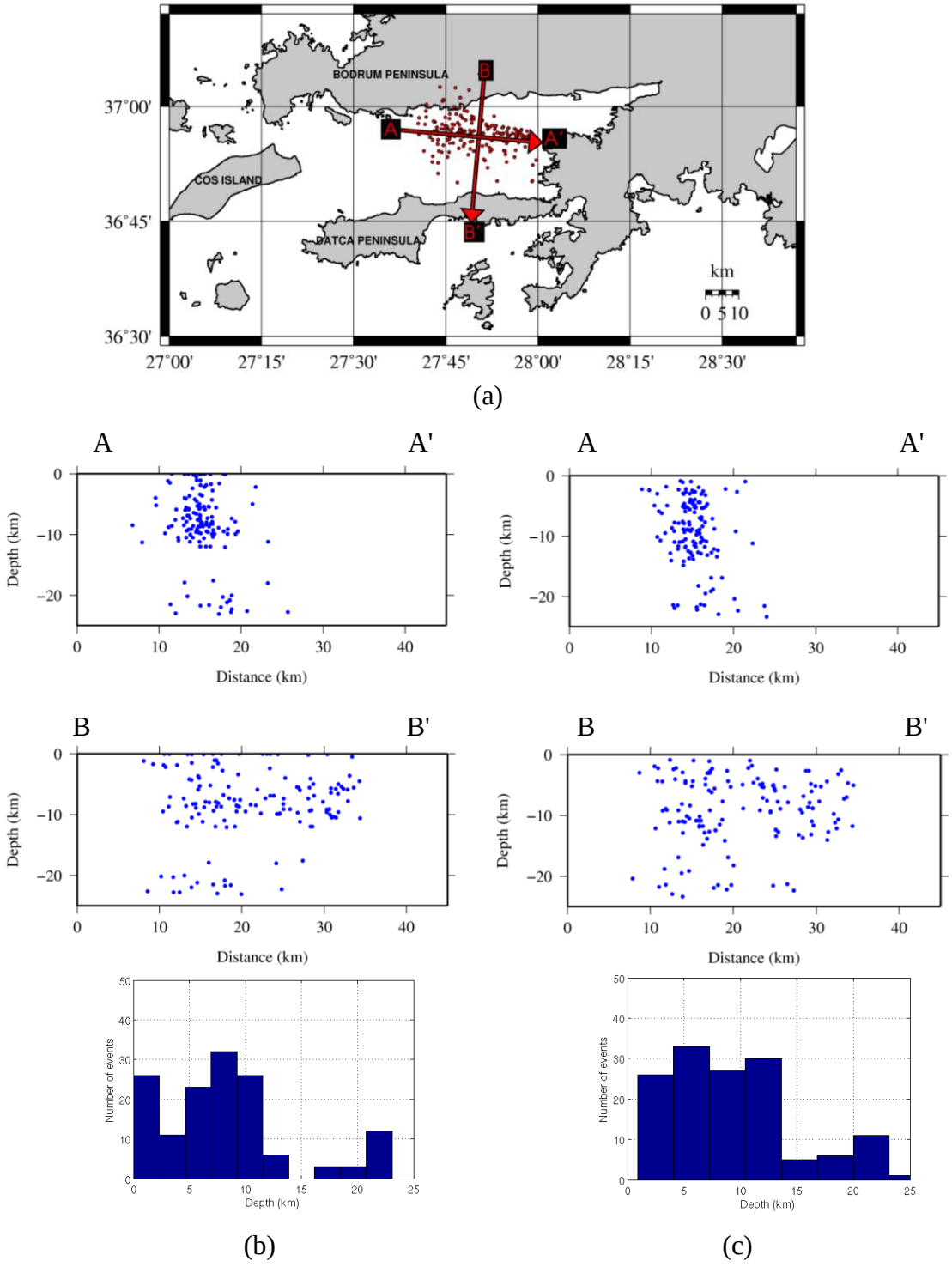

Figure 5.7. (a) Original locations of the earthquakes (Cluster 2) and profiles; (b) Cross sections view in the strike (Az = 95^0N) and normal to the strike direction (Az = 185^0N) (Original Data); (c) Cross sections view in the strike (Az = 95^0N) and normal to the strike direction (Catalog Data) (Az = 185^0N) (MAXSEP = 10).

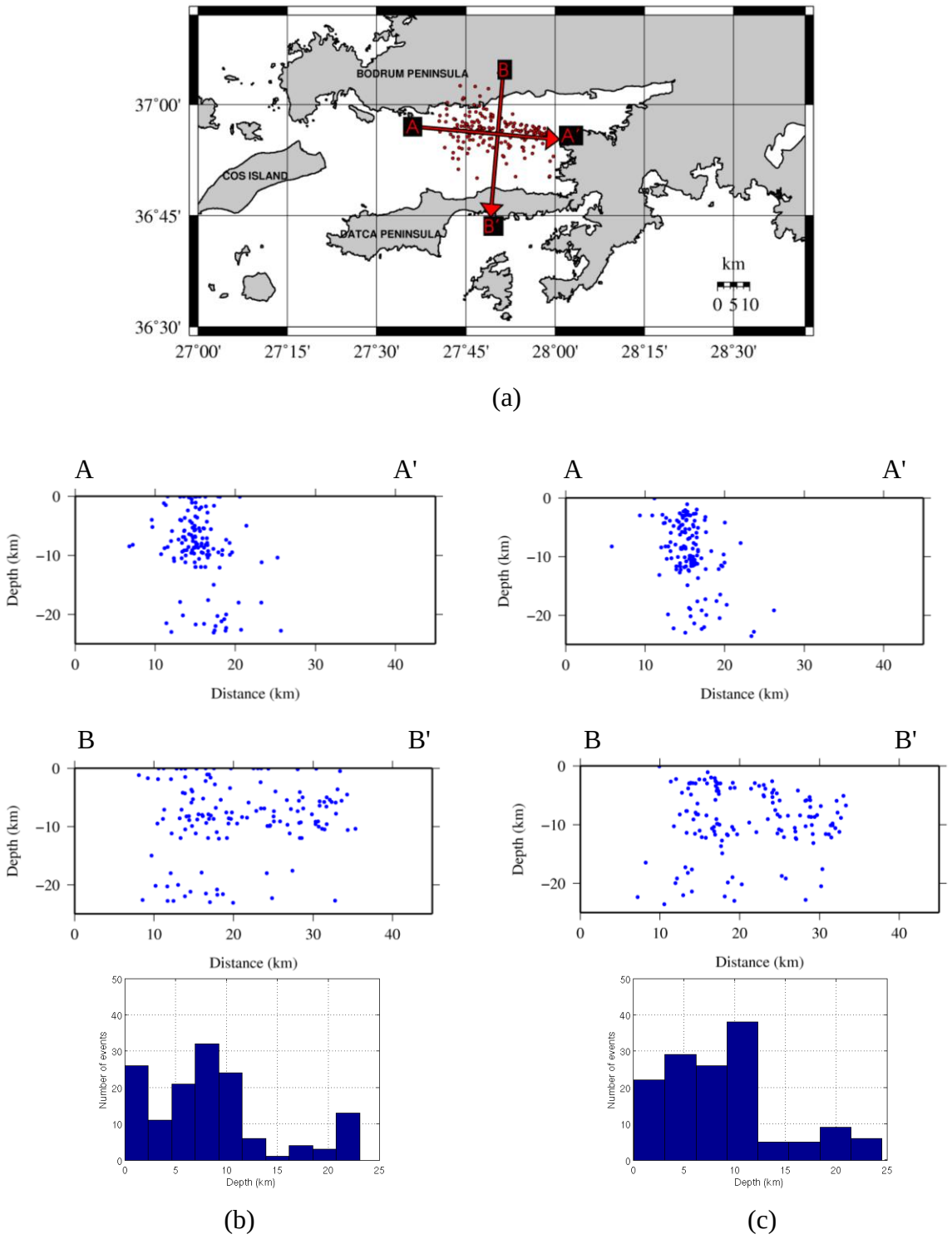

Figure 5.8. (a) Original locations of the earthquakes (Cluster 2) and profiles; (b) Cross sections view in the strike (Az = 95^0N) and normal to the strike direction (Az = 185^0N) (Original Data); (c) Cross sections view in the strike (Az = 95^0N) and normal to the strike direction (Az = 185^0N) (Cross-Correlation Data) (MAXSEP = 10).

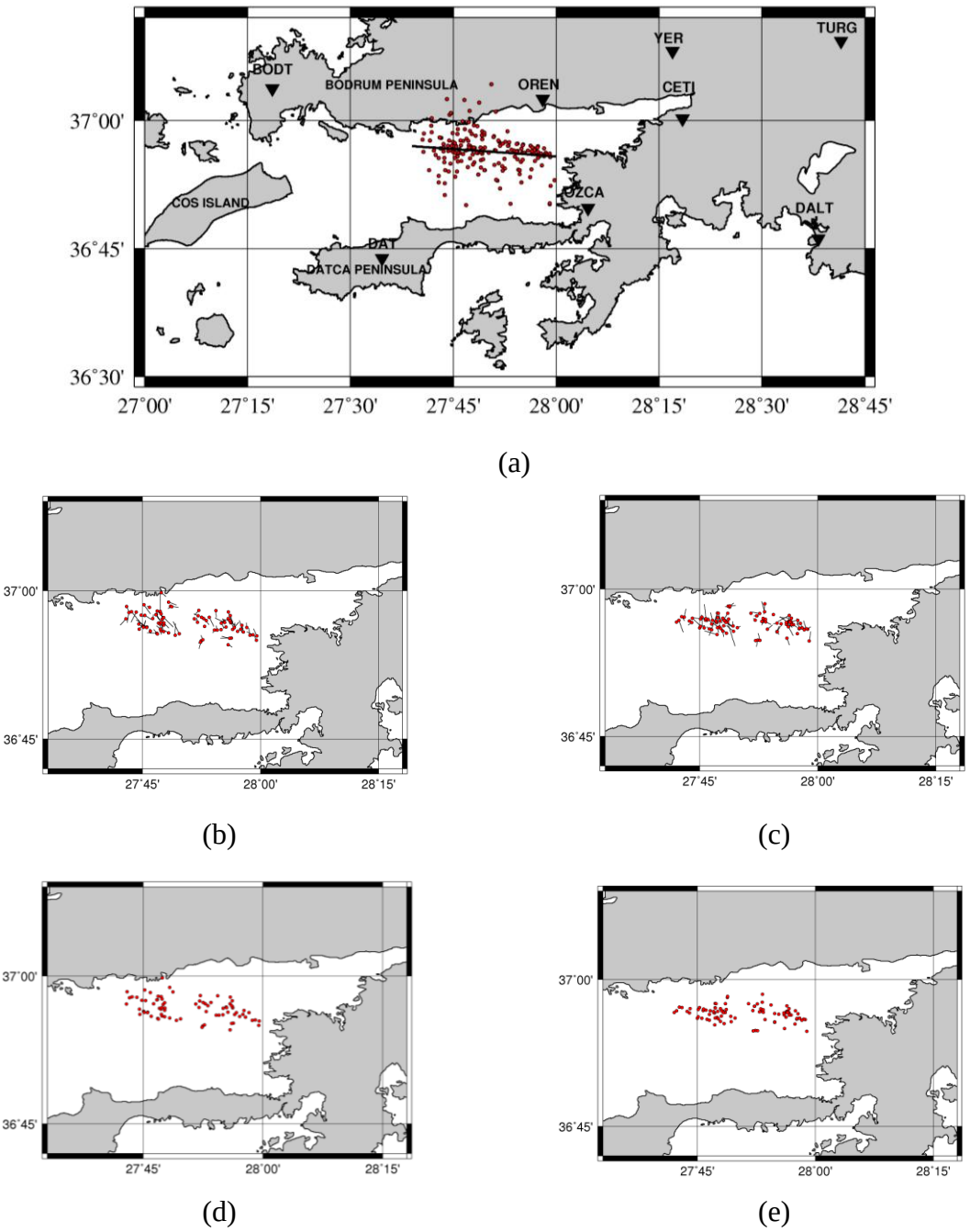

Figure 5.9. (a) Original Locations of the Earthquakes in Cluster 2 (HYPO71); (b) The corrections between the original and HYPODD locations (Catalog Data) (MAXSEP = 5) The average horizontal correction is 1.32 km; (c) The corrections between the original and HYPODD locations (Cross-Correlation). The average horizontal correction is 1.13 km; (d) Relocated Earthquakes in Cluster 2 (by using Catalog Data). The number of relocated earthquakes are 75% of the data (82 earthquakes) were relocated from MAXSEP = 10; (e) Relocated Earthquakes (96 earthquakes) in Cluster 2 (by using Cross-Correlation Data).

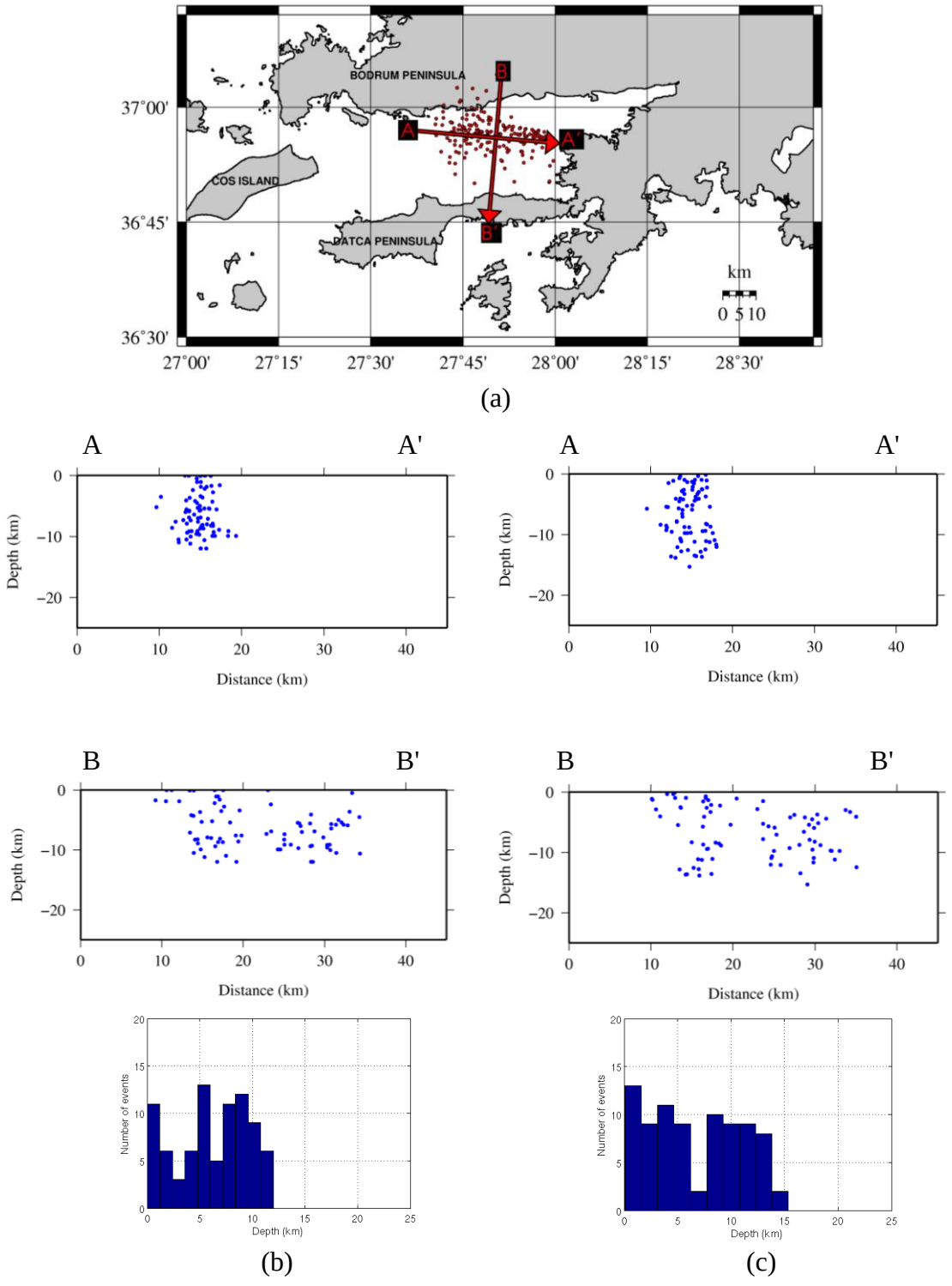

Figure 5.10. (a) Original locations of the earthquakes (Cluster 2) and profiles; (b) Cross sections view in the strike (Az = 95^0N) and normal to the strike direction (Az = 185^0N) (Original Data); (c) Cross sections view in the strike (Az = 95^0N) and normal to the strike direction (Az = 185^0N) (Catalog Data) (MAXSEP = 5).

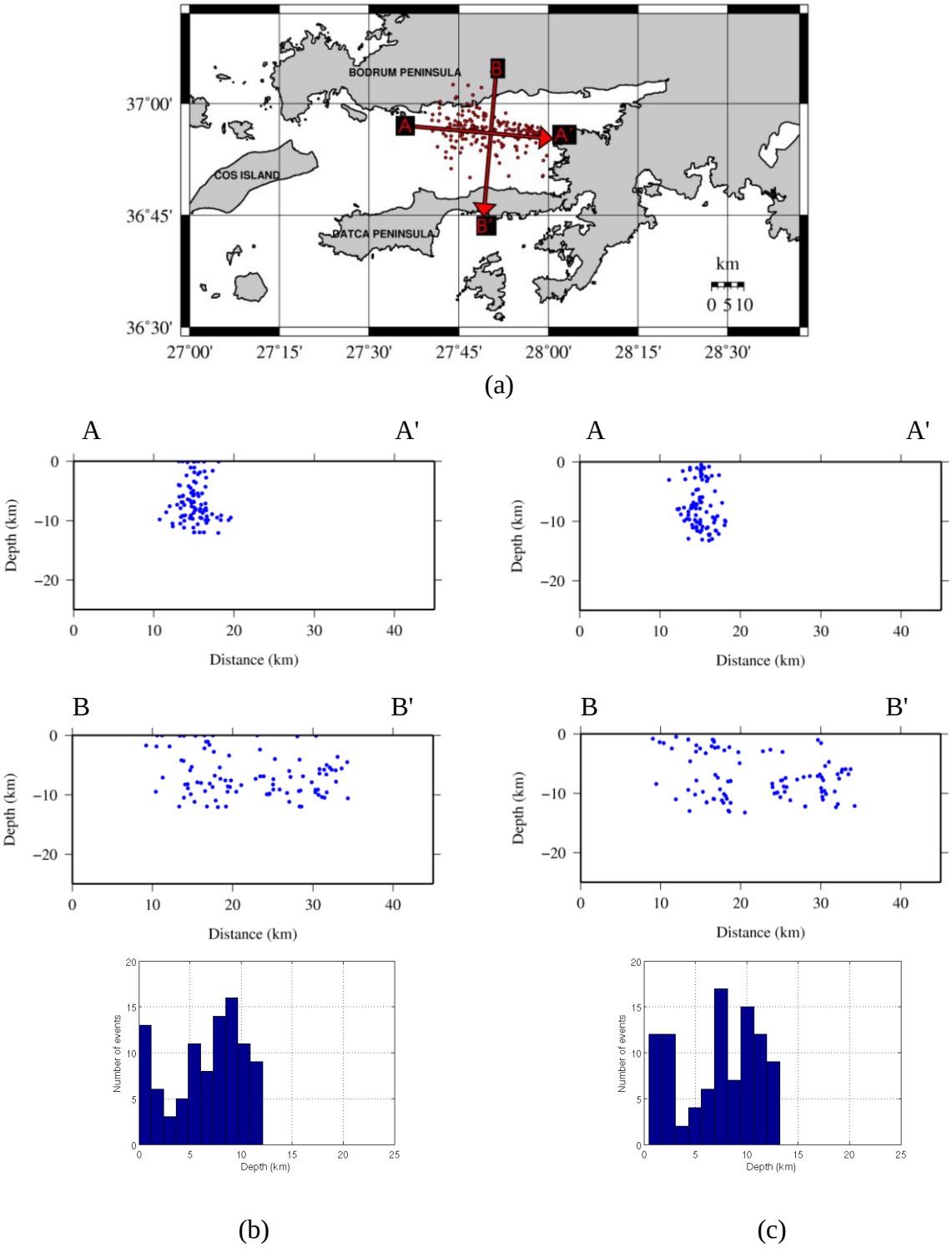

Figure 5.11. (a) Original locations of the earthquakes (Cluster 2) and profiles; (b) Cross sections view in the strike (Az = 95^0N) and normal to the strike direction (Az = 185^0N) (Original Data); (c) Cross sections view in the strike (Az = 95^0N) and normal to the strike direction (Az = 185^0N) (Cross-Correlation Data) (MAXSEP = 5).

5.1.3. Results of HypoDD: Cluster 3

The Cluster 3 is also located at the central part of the Gökova Bay and is closer to the Ören village (Figure 5.12).

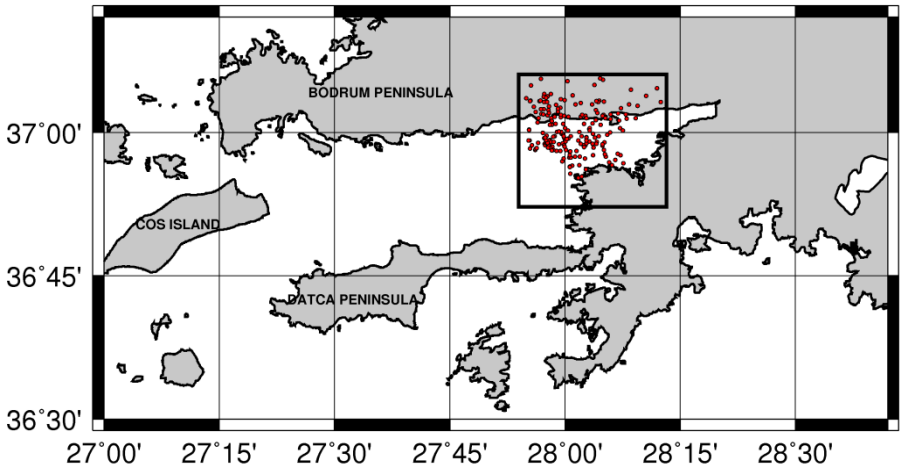

Figure 5.12. Cluster 3.

One of the most striking things of the Cluster 3 is seismic activity on land near Ören village (Figure 5.13). These activities have the possibility to be artificial explosions since there are many quarries on the area. Before relocating all the earthquakes of Cluster 3 we analyzed the inland seismic activity to test for this issue. The Figure 5.13 contains 44 earthquakes. According to the results of both HYPO71 and HYPODD most of these earthquakes localize in the first 10 km of the crust (Figure 5.14). We checked the waveforms and the time of these earthquakes. All of the waveforms have distinct P and S phases which are seldom observed in quarry blasts (Figure 5.15). The highest seismic activity occurred in 2006 which also reduces the likelihood of a quarry activity but this situation cannot be exact evidence (Figure 5.16). Because of this situation we analyzed the distribution of the event according to the time of the day. The earthquakes did not localize at a specific time of the day (Figure 5.17) which again reduces the option of explosive origin. So the preliminary observations show that most of these activities are not quarry explosions although an exact determination will need more complex studies. We have also

checked the polarity of first arrivals of some events and both compressive and dilatational cases were observed. It may be possible that only a certain part of the seismicity on land corresponds to quarry blast, however their number is expected to be quite low. Therefore we assumed that all the events recorded on land are natural seismic events.

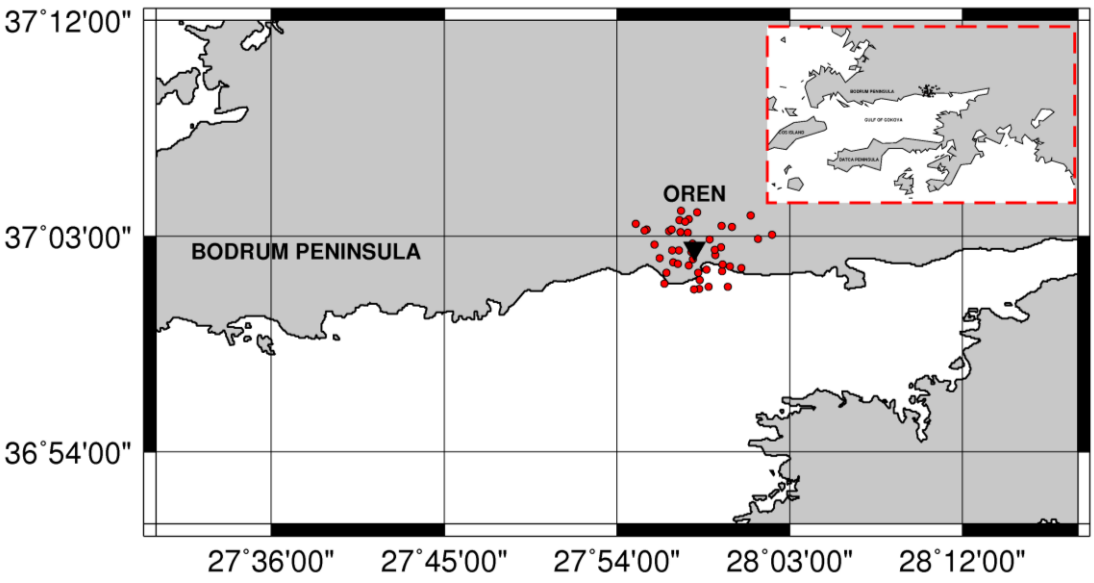

Figure 5.13. Seismic activity on land at Cluster 3 (Black triangle represents the OREN seismic station).

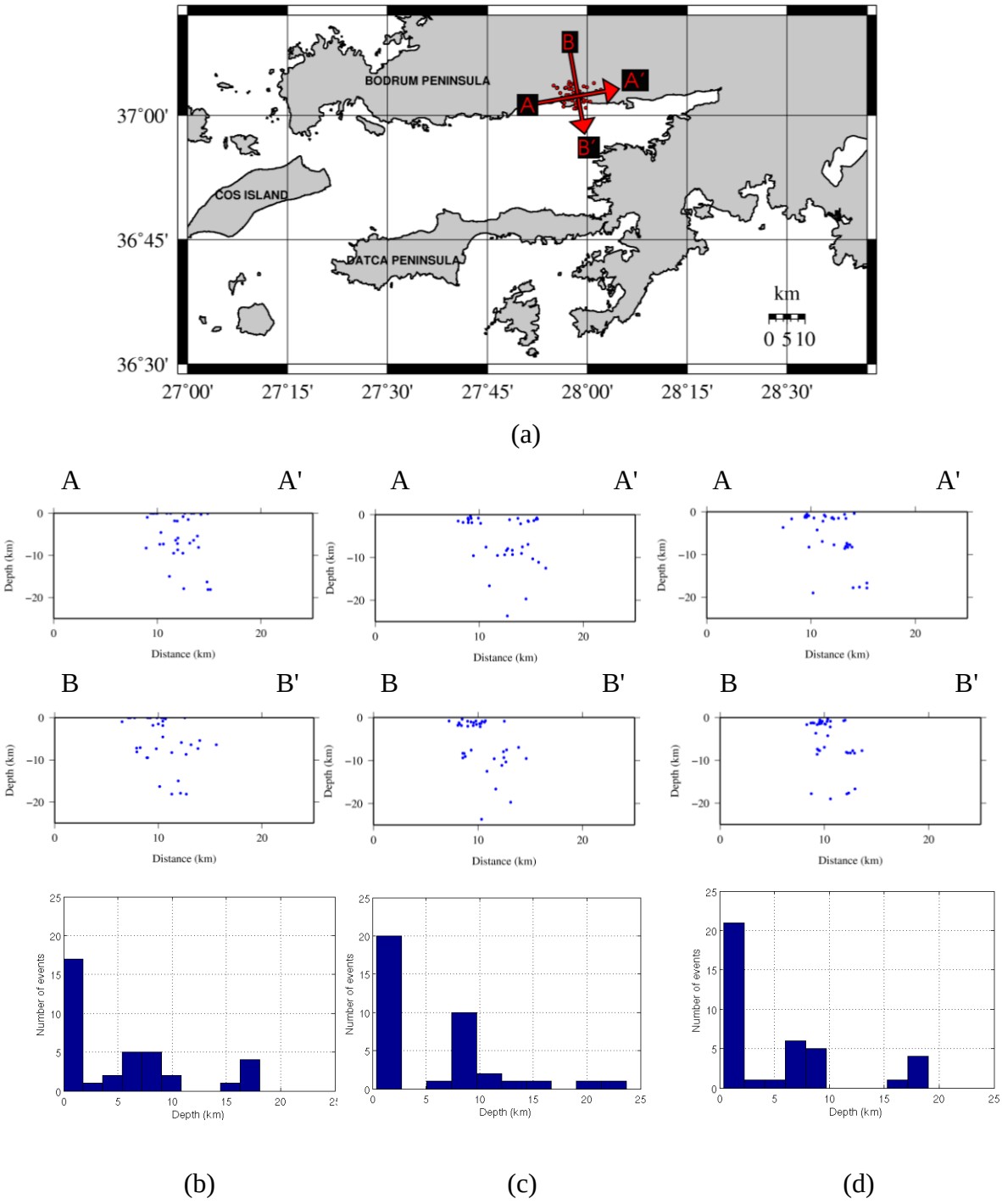

Figure 5.14. (a) Profiles; (b) Cross sections view in the strike (Az = 80^0N) and normal to the strike directions (Az = 170^0N) (Original Data); (c) Cross sections view in the strike (Az = 80^0N) and normal to the strike directions (Az = 170^0N) (Catalog); (d) Cross sections view in the strike (Az = 80^0N) and normal to the strike directions (Az = 170^0N) (Correlation).

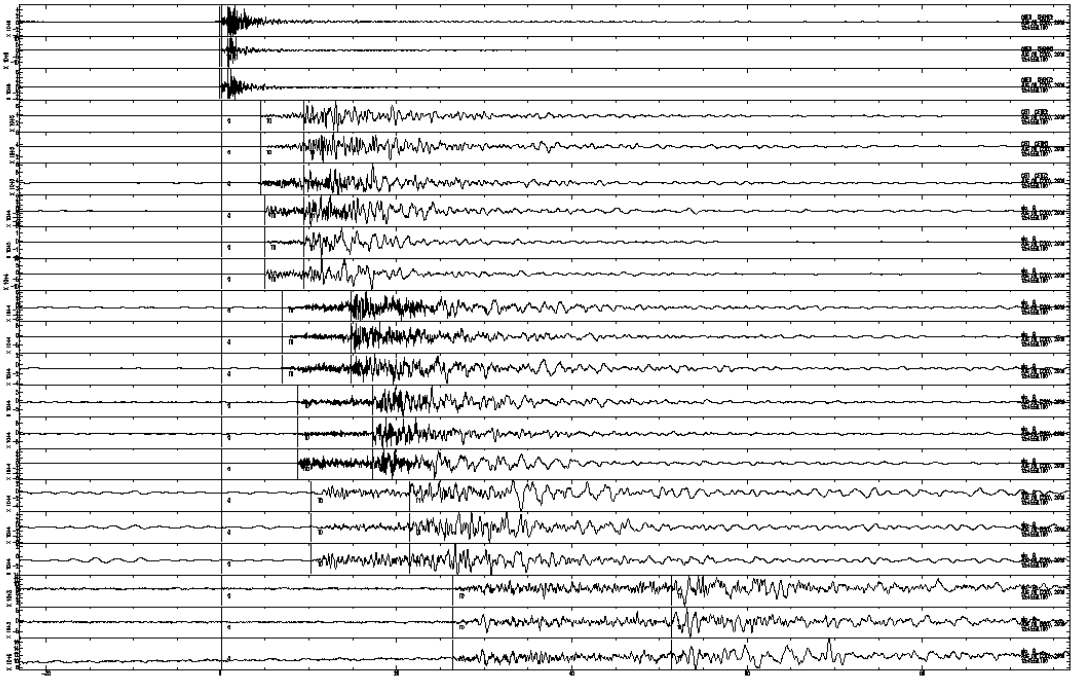

Figure 5.15. Waveforms of the 08/08/2006 18:45:50 earthquake (The order of the station OREN, CETI, YER, DAT, BODT, DALT, BLCB). The depth of this earthquake is 1.5 km.

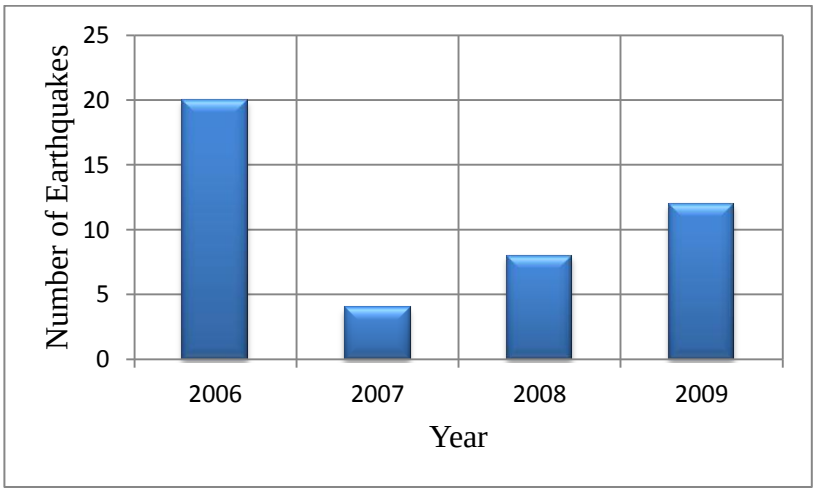

Figure 5.16. The histogram of the number of earthquakes and their occurrence years.

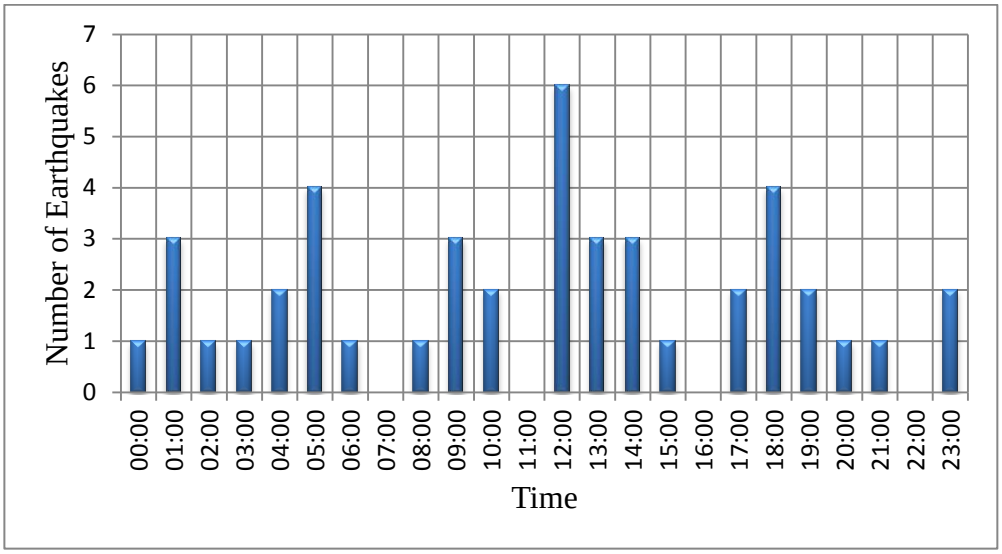

Figure 5.17. The histogram of the number of earthquakes and their occurrence times.

At the center of the bay the earthquakes are much closer to each other relatively and the Cluster 3 is the one located at the eastern part of the central bay. The top map of Figure 5.18 shows the original locations of the events. The black line shows the possible fault orientation. This cluster has 200 earthquakes and over half of the data were recorded in 2006. The average distance between the events is 2.76 km and the percentages of the distant earthquakes are relatively low (Chapter 4 in Figure 4.10).

We first observe the results of hypoDD using MAXSEP = 10. The mapviews in the Figure 5.18 show the horizontal displacements of the earthquakes after relocation by using catalog (left column, Figure 5.18b, Figure 5.18d) and cross-correlation (right column, Figure 5.18c, Figure 5.18e) data. By using the catalog and cross-correlation data 160 and 166 of the events were relocated, respectively. The reason of the small change between the catalog and cross-correlation relocated event number is the small distance between the events. The event pair occurrence being high in this cluster, the hypoDD (inversion process) relocate nearly all available data. The correlation results perform better because of the same reasons as in Cluster 2 and also the relatively close location of the stations to the activity area. The average distance between the located and the relocated events, which are created by using catalog and cross-correlation data, is 1.92 and 1.97 km, respectively.

These displacement values have shown that the catalog and the cross-correlation results are compatible with each others.

The suggested fault orientation is verified by both the results of the both relocation approaches (catalog and cross-correlation). We also observe that the data scattering is decreased when the cross-correlation is used. Therefore the cross-correlation in this cluster gives a better solution just like for the Cluster 2. This improvement stems from the station coverage, the features of the data set such as the distance between the events are relatively low and the stations are relatively closer to this cluster. In particular the positive contribution of OREN station should be taken into account on the results when processing both middle clusters (Cluster 2 and Cluster 3).

The depth sections of the HYPO71 and the HYPODD (catalog and correlation) are illustrated in Figure 5.19 and Figure 5.20. Most of the earthquakes in this cluster are localized in the upper 15 km. The cross-correlation results have shown that the scatter of the depths is decreased (10 km). As a result, we can assume that the cross-correlation is more effective on the data, if the cluster is well covered by the stations and the number of events is large enough.

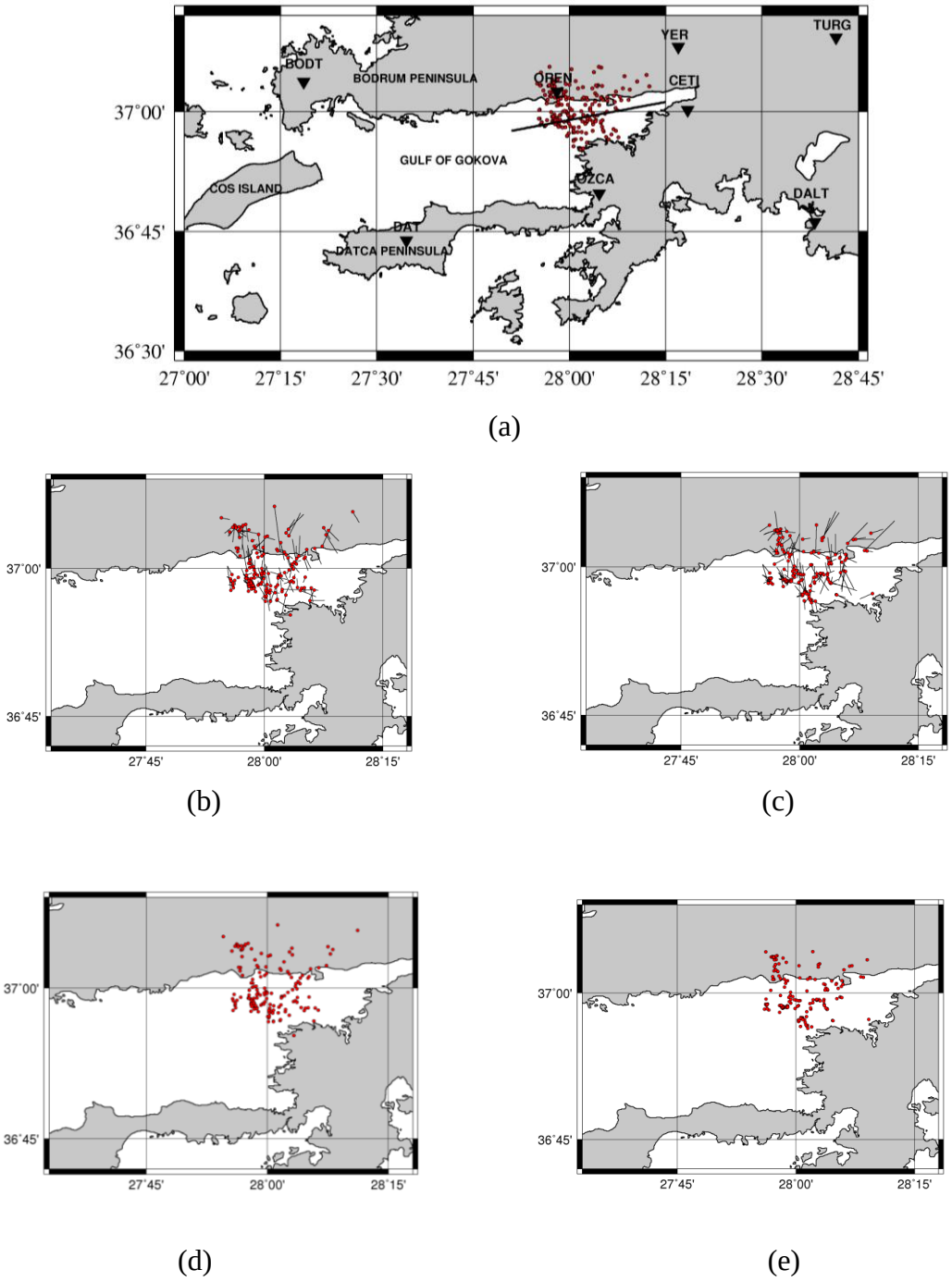

Figure 5.18. (a) Original locations of the earthquakes in Cluster 3 (HYPO71); (b) The corrections between the original and HYPODD locations (Catalog Data) (MAXSEP = 10); (c) The corrections between the original and HYPODD locations (Cross-Correlation); (d) Relocated earthquakes in Cluster 3 (by using Catalog Data); (e) Relocated earthquakes in Cluster 3 (by using Cross-Correlation Data).

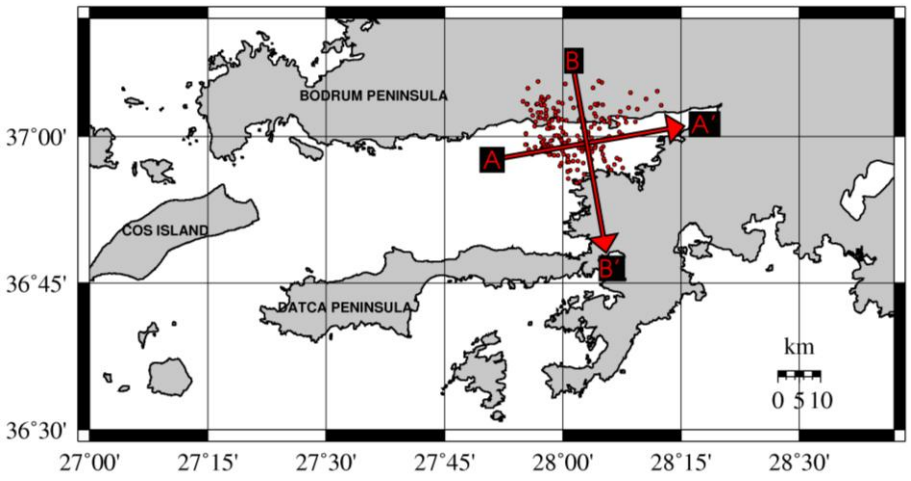

(a)

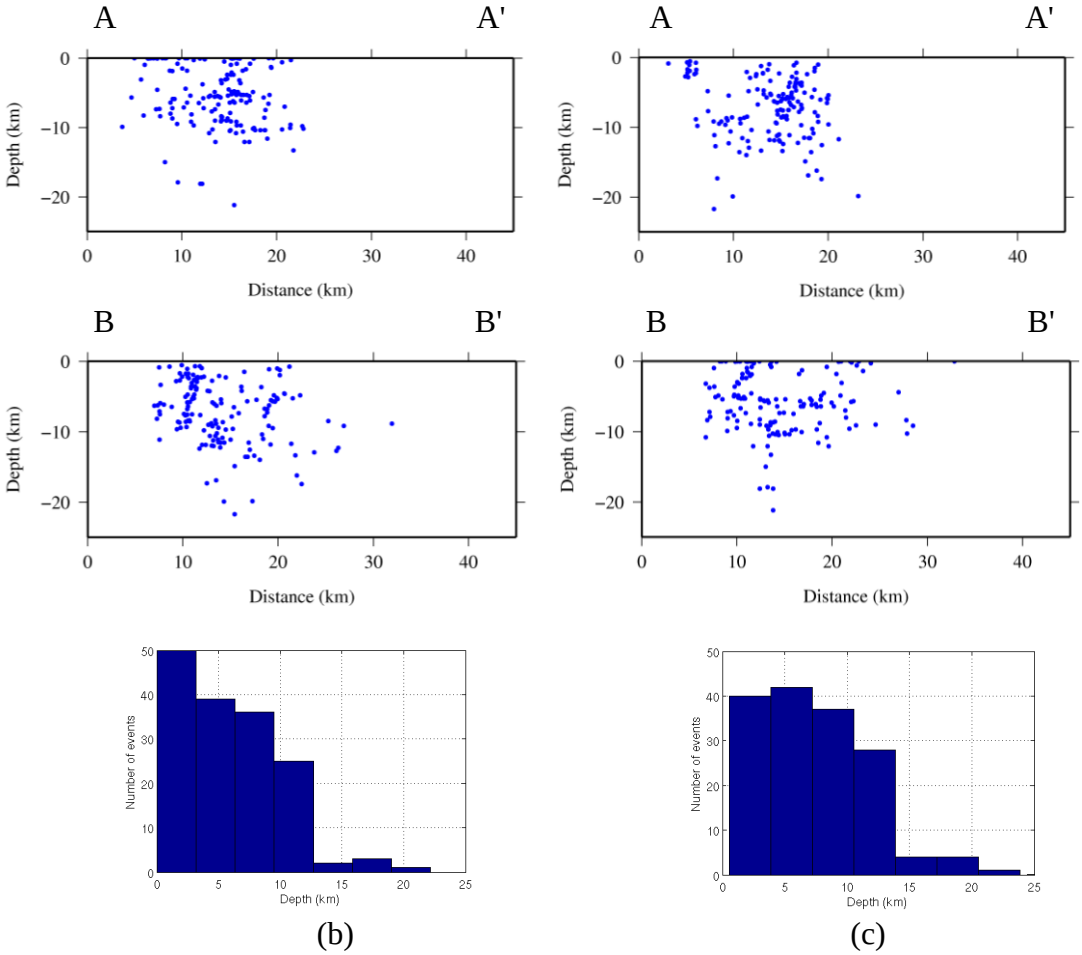

(b) (c)

Figure 5.19. (a) Original locations of the earthquakes (Cluster 3) and profile; (b) Cross sections view in the strike (Az = 80^0N) and normal to the strike directions (Az = 170^0N) (Original Data); (c) Cross sections view in the strike (Az = 80^0N) and normal to the strike directions (Az = 170^0N) (Catalog Data) (MAXSEP = 10).

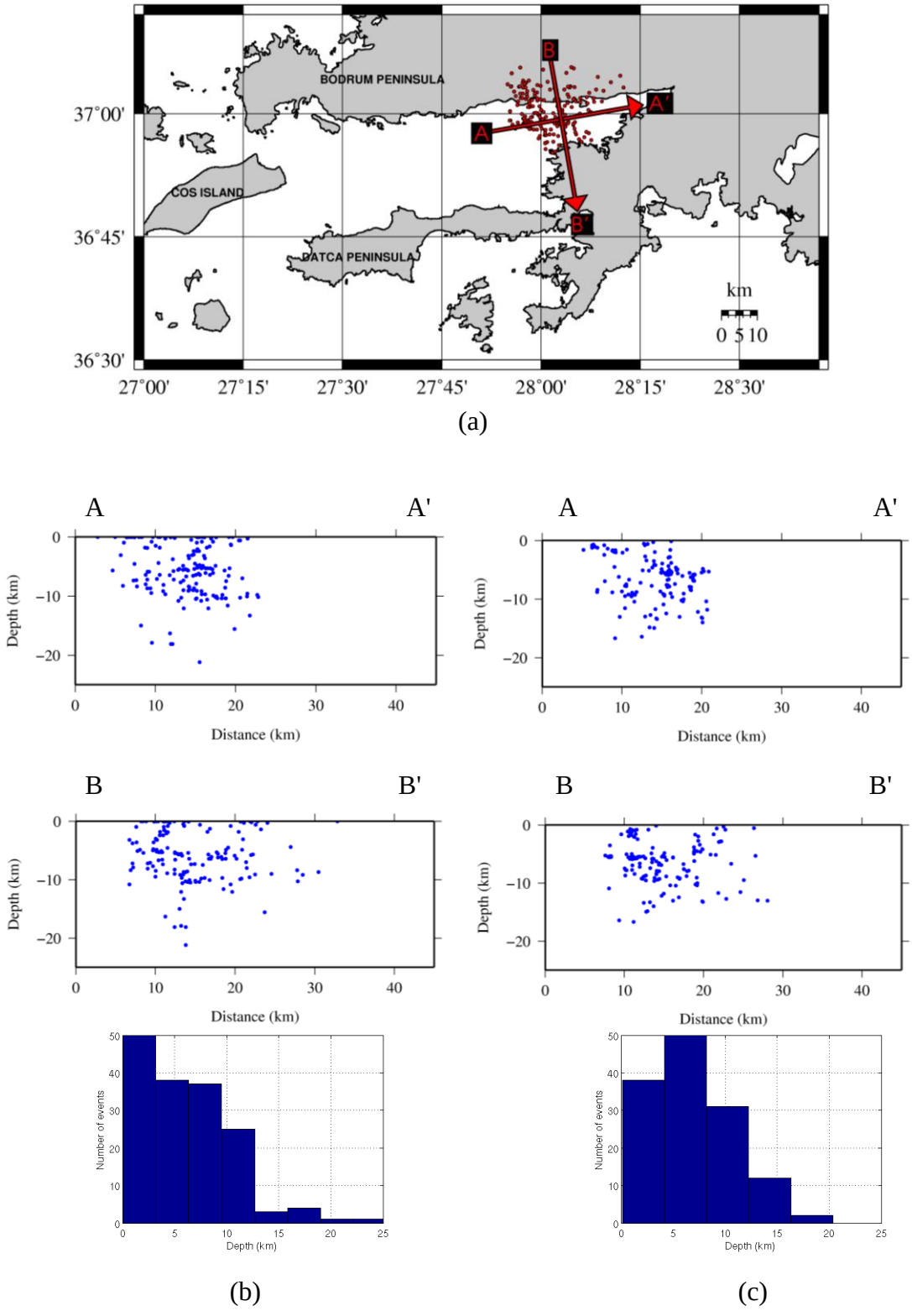

Figure 5.20. (a) Original locations of the earthquakes (Cluster 3); (b) Cross sections view in the strike (Az = 80^0N) and normal to the strike direction (Az = 170^0N) (Original Data); (c) Cross sections view in the strike (Az = 80^0N) and normal to the strike direction (Az = 170^0N) (Cross-Correlation Data) (MAXSEP = 10).

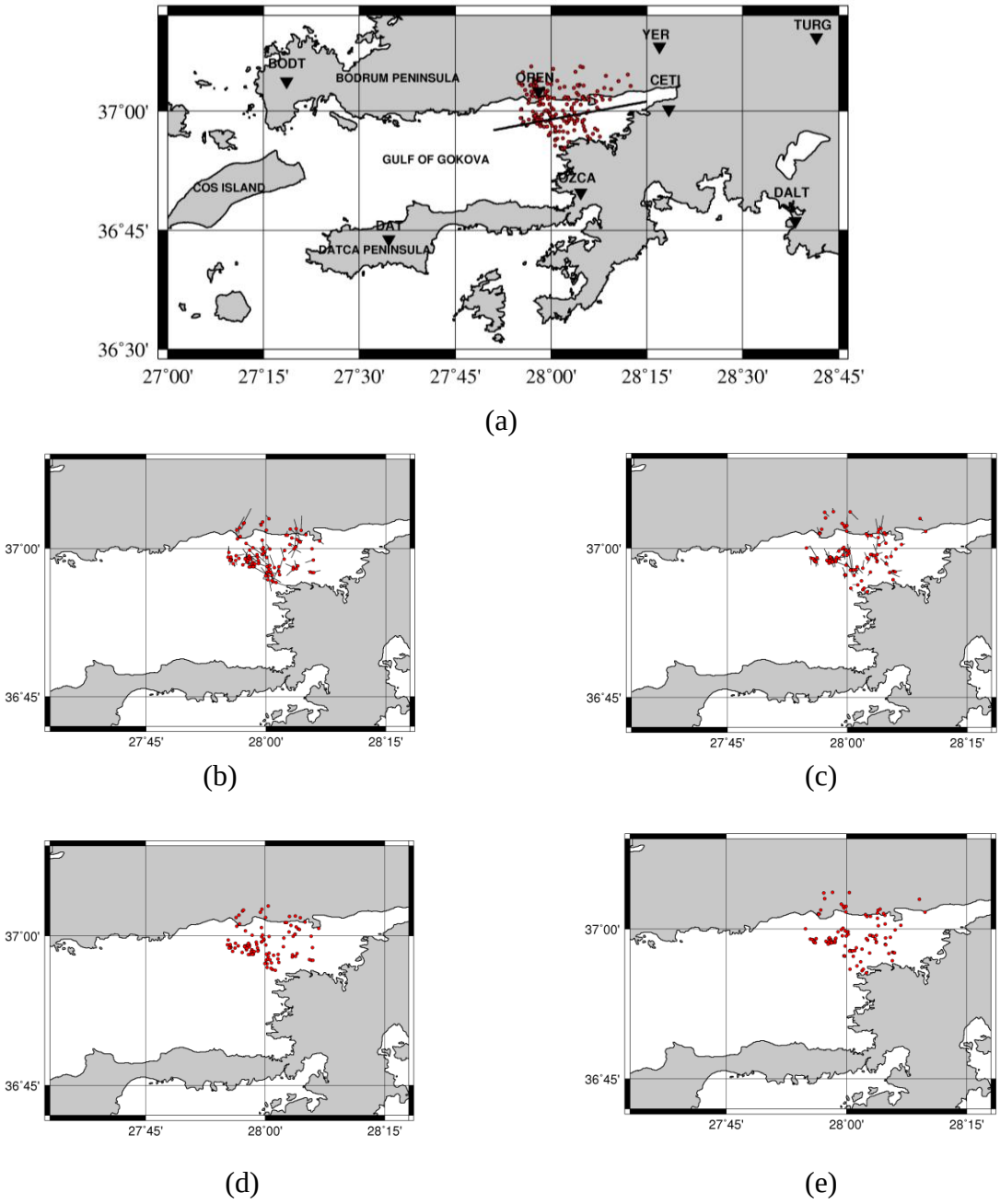

Figure 5.21. (a) Original Locations of the Earthquakes in Cluster 3 (HYPO71); (b) The corrections between the original and HYPODD locations (Catalog Data) (MAXSEP = 5). The average horizontal correction is 1.48 km ; (c) The corrections between the original and HYPODD locations (Cross-Correlation). The average horizontal correction is 1.07 km; (d) Relocated Earthquakes in Cluster 3 (by using Catalog Data). Approximately the half of the events were relocated (104 earthquakes); (e) Relocated Earthquakes (122 earthquakes) in Cluster 3 (by using Cross-Correlation Data).

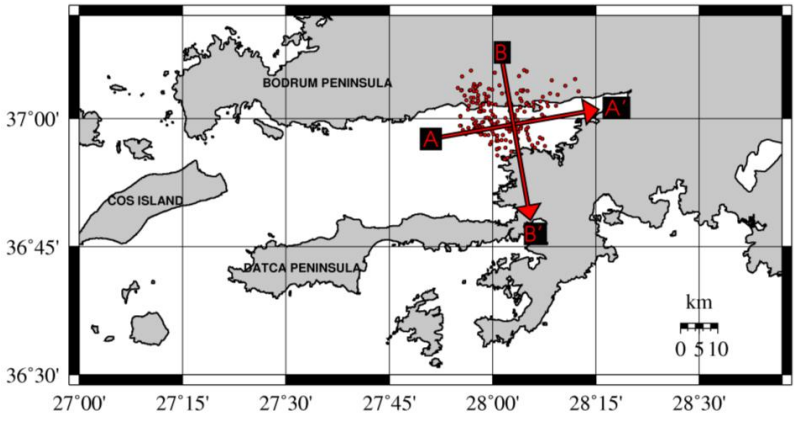

(a)

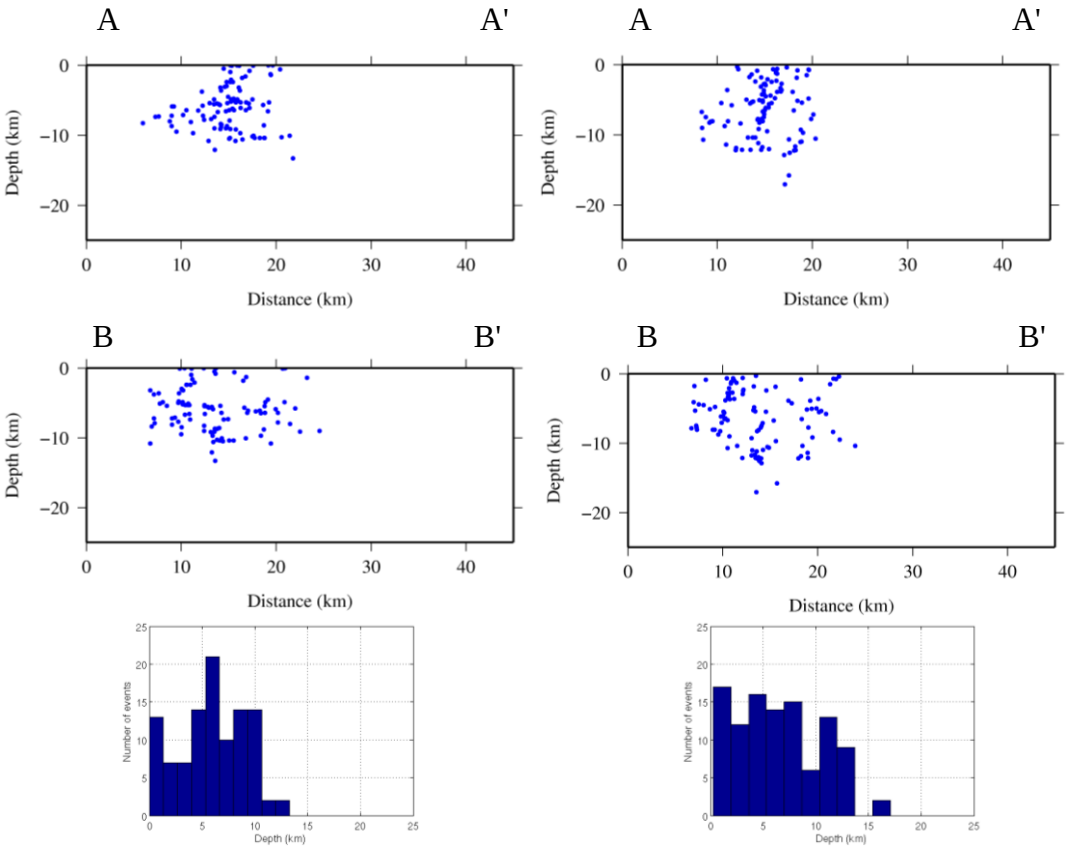

(b) (c)

Figure 5.22. (a) Original locations of the earthquakes (Cluster 3) and profiles; (b) Cross sections view in the strike (Az = 80^0N) and normal to the strike direction (Az = 170^0N) (Original Data); (c) Cross sections view in the strike (Az = 80^0N) and normal to the strike direction (Az = 170^0N) (Catalog Data). The earthquakes localized the upper 15 km. When comparing the depth sections, one has to take into account that the number of data is decreased when MAXSEP = 5.

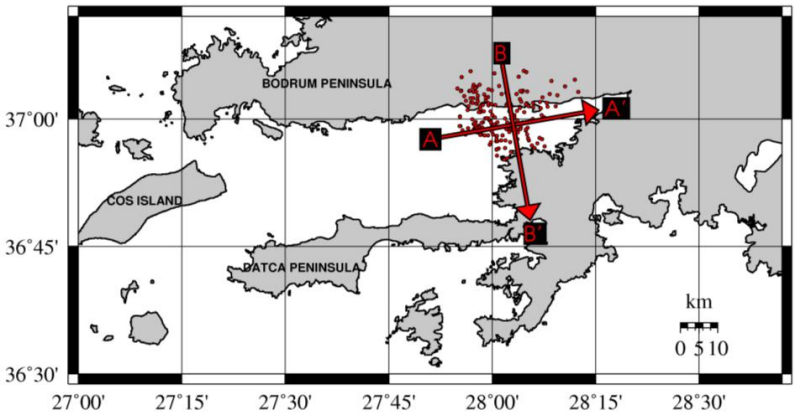

(a)

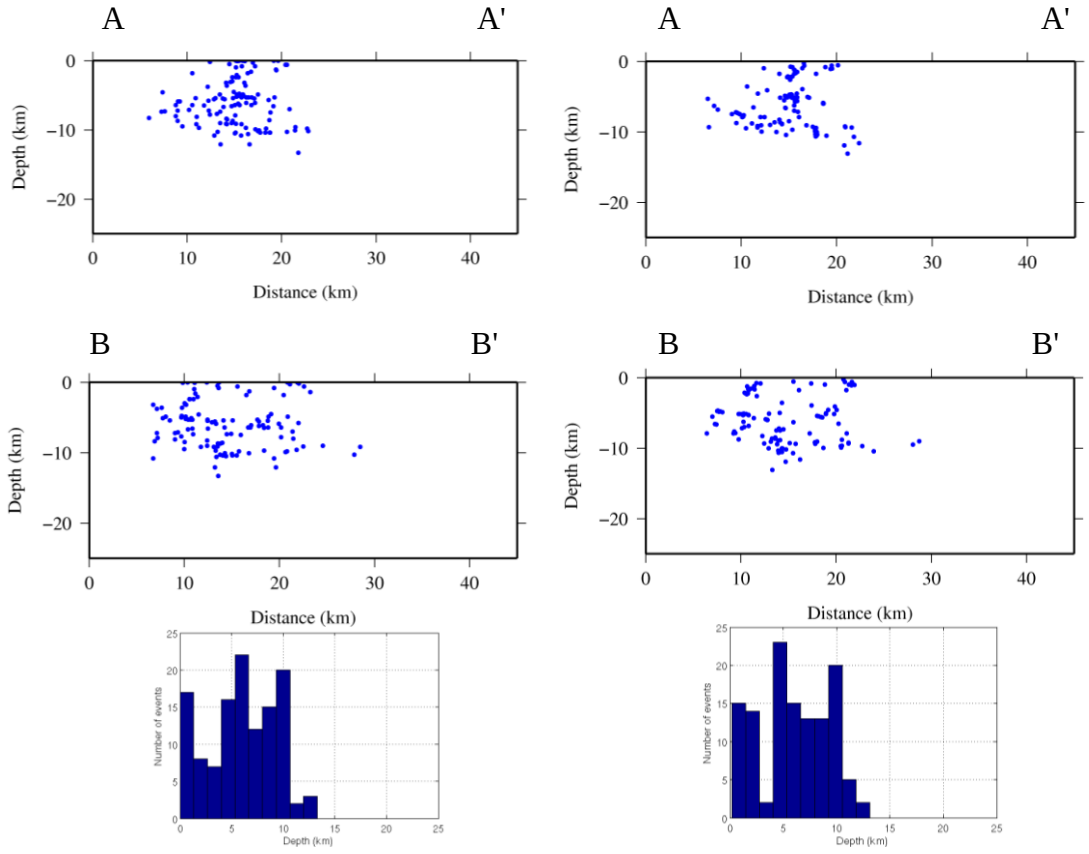

(b) (c)

Figure 5.23. (a) Original locations of the earthquakes (Cluster 3) and profiles; (b) Cross sections view in the strike (Az = 80^0N) and normal to the strike direction (Az = 170^0N) (Original Data); (c) Cross sections view in the strike (Az = 80^0N) and normal to the strike direction (Az = 170^0N) (Cross-Correlation Data). Most of the earthquakes localized the upper 10 km.

5.1.4. Results of HypoDD: Cluster 4

The last Cluster 4 is located at the eastern part of the Gökova Bay (Figure 5.24). The event scatter in this cluster is higher than the middle clusters.

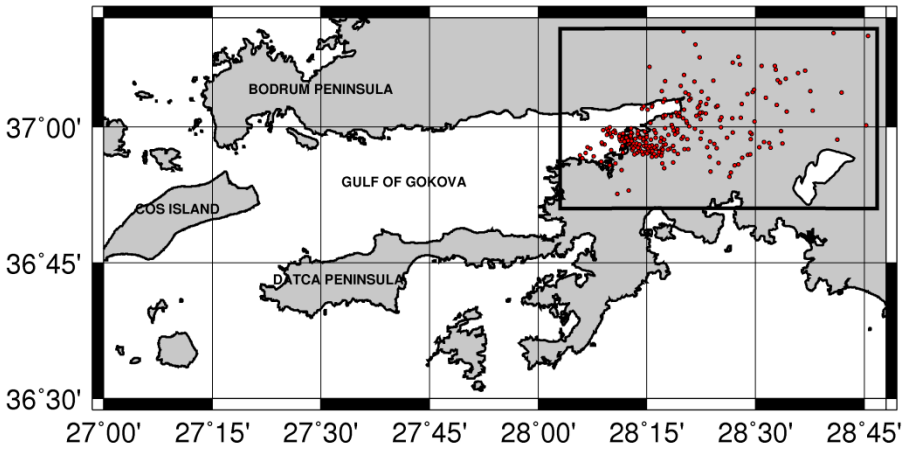

Figure 5.24. Cluster 4.

The seismic activity on land at the Cluster 4 is shown Figure 5.24 which contains 133 earthquakes and according to the results of HYPO71 most of the earthquakes localize in the upper 15 km depth. The results of HYPODD (catalog or cross-correlation data) illustrate two seismic sections at different depths (Figure 5.25). We checked the waveforms and the time of these earthquakes. All of the waveforms have distinct P and S phases as seen in Figure 5.26 and the highest seismic activity occurred in 2009 (Figure 5.27). The earthquakes did not localize a specific time of the day (Figure 5.28) so the first observations show that these activities are not quarry explosions although determining explosions need more complex studies. So we treated all the inland events as natural events.

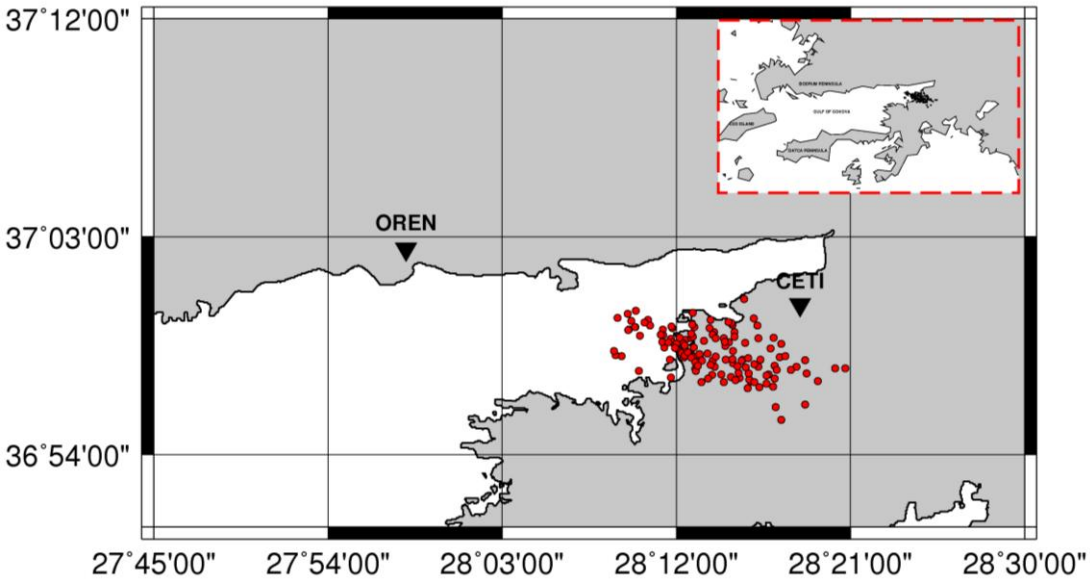

Figure 5.25. Seismic activity on land at Cluster 4 (Black triangles represent the seismic stations OREN and CETI).

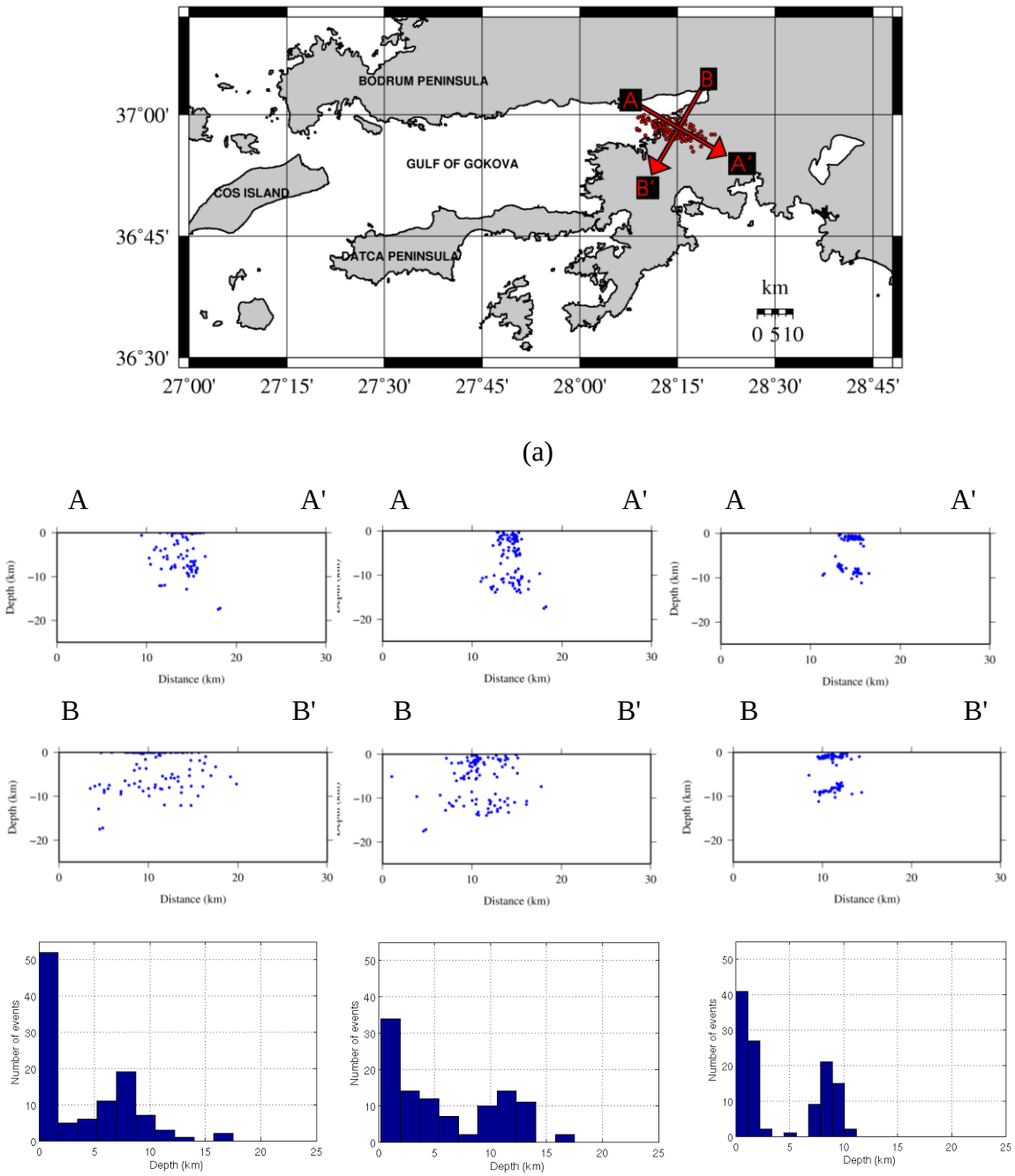

(a)

(b) (c) (d)

Figure 5.26. (a) Profiles; (b) Cross sections view in the strike (Az = 120^0N) and normal to the strike directions (Az = 210^0N) (Original Data); (c) Cross sections view in the strike (Az = 120^0N) and normal to the strike directions (Az = 210^0N) (Catalog); (d) Cross sections view in the strike (Az = 120^0N) and normal to the strike directions (Az = 210^0N) (Correlation).

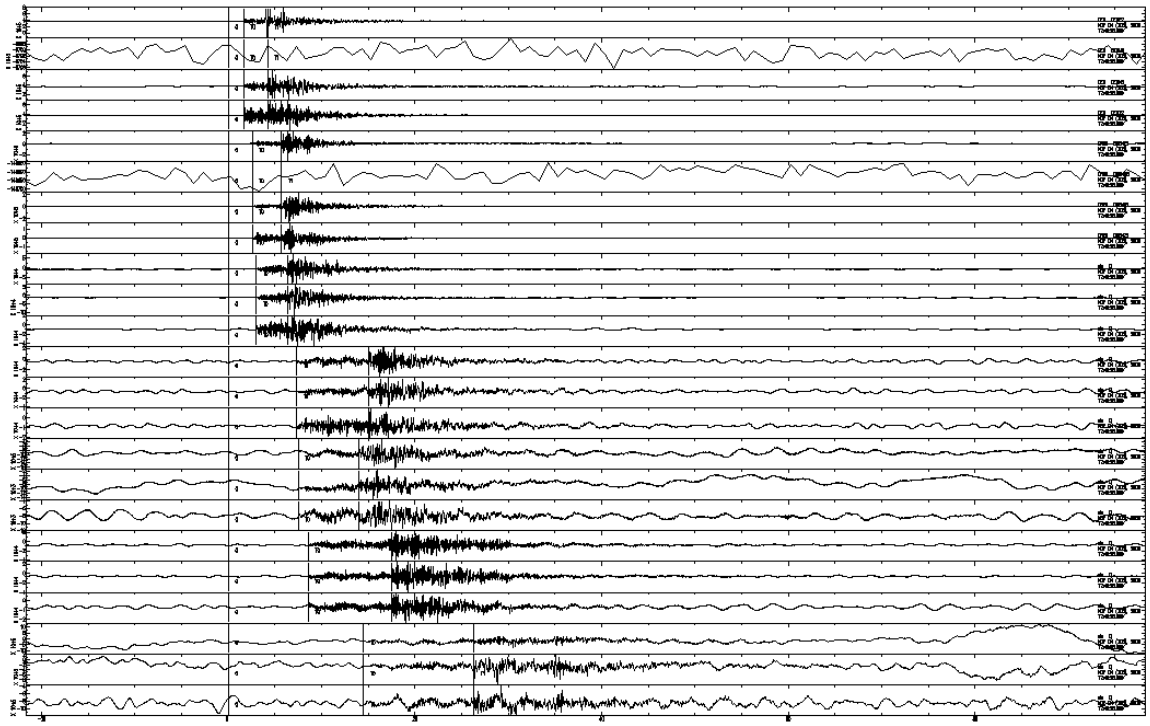

Figure 5.27. Waveforms of the 04/11/2006 17:46:28 earthquake (CETI, OREN, YER, DALT, MLSB, DAT, FETY).The depth of this earthquake is 7.7 km.

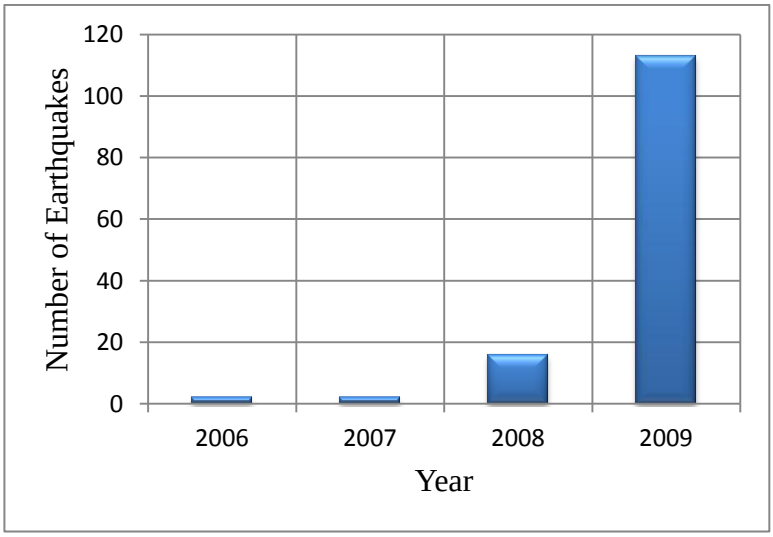

Figure 5.28. The histogram of the number of earthquakes and their occurrence years.

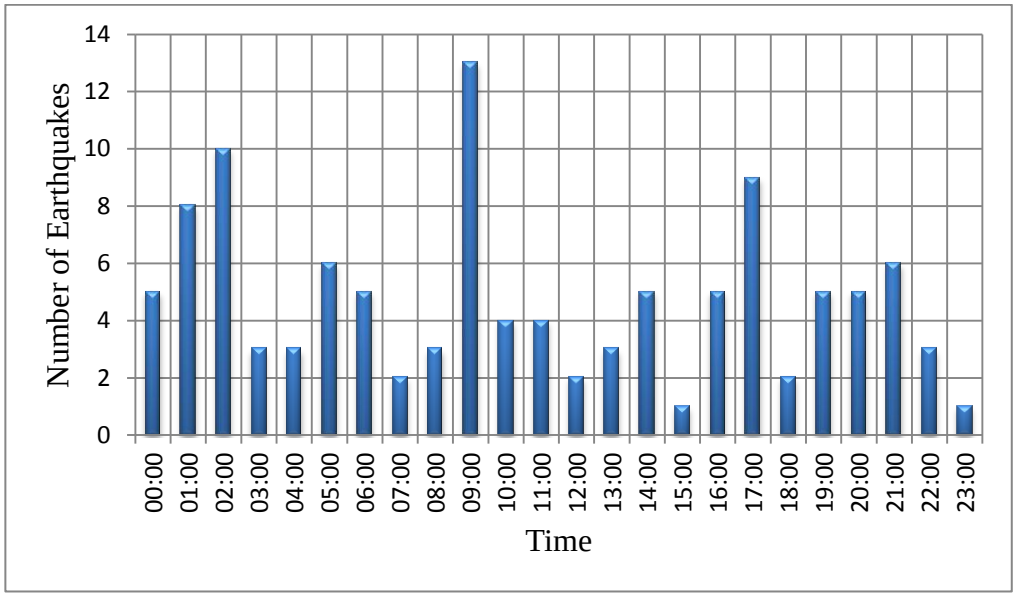

Figure 5.29. The histogram of the number of earthquakes and their occurrence times in 2009.

The Figure 5.30a shows the HYPO71 locations of the earthquakes. The black line illustrates the possible fault orientation (120^0N) based on HYPO71 results. This cluster has 276 earthquakes and over half of them were recorded in 2009. This however is not an aftershock sequence since they do not follow a main event with a higher magnitude. Instead most the events have similar magnitudes and part of this cluster can be considered as a swarm activity. The other part is suspected to be artificial explosive sources as will be more clear with HypoDD analysis. The average distance between the events is 3.17 km but the percentage of the distant events is not low as compared to the Cluster 2 and 3 (Chapter 4 in Figure 4.10). If the distant event rate is high in a cluster, it will affect the event pair number therefore the relocated event rate is lower as in the case of Cluster 1. We observe that most of distant events are eliminated after the application of HYPODD with MAXSEP = 5.

The mapviews in the Figure 5.30 show the displacements of the earthquakes after the relocation by using catalog (right column, Figure 5.30b, Figure 5.30d) and cross-

correlation (left column, Figure 5.30c, Figure 5.30e) data for MAXSEP = 10. The catalog and cross-correlation cases relocated 161 and 192 events, respectively. The average distance between the located and the relocated events, which are created by using catalog and cross-correlation data, is 2.44 and 3.73 km, respectively. The 5.33 shows the same figures as 5.30, this time for MAXSEP = 5.

The depth sections of the HYPO71 and the HYPODD (catalog and correlation) are illustrated by the Figure 5.31 and Figure 5.32 for MAXSEP = 10, Figure 5.34 and Figure 5.35 for MAXSEP = 5. After the application of HypoDD the seismicity trends change significantly. First it becomes clear that most of the shallow seismicity is likely to correspond to quarry blasts. However the deeper ones are earthquakes. Choosing MAXSEP = 5 eliminates most this deep seated seismicity and no clear trend is observed. However when MAXSEP = 10, and the correlation approach is used, a rough figure of a south dipping fault is observed in the depth sections (Figure 5.32c). The strike direction of this dipping fault is about 120^0N. Note that the surface trace of this inferred fault should be much to the north of where we observe the cluster from the mapviews.

A final mapview of the relocated seismicity is given in Figure 5.36 for the catalog data and in Figure 5.37 for the correlation data.

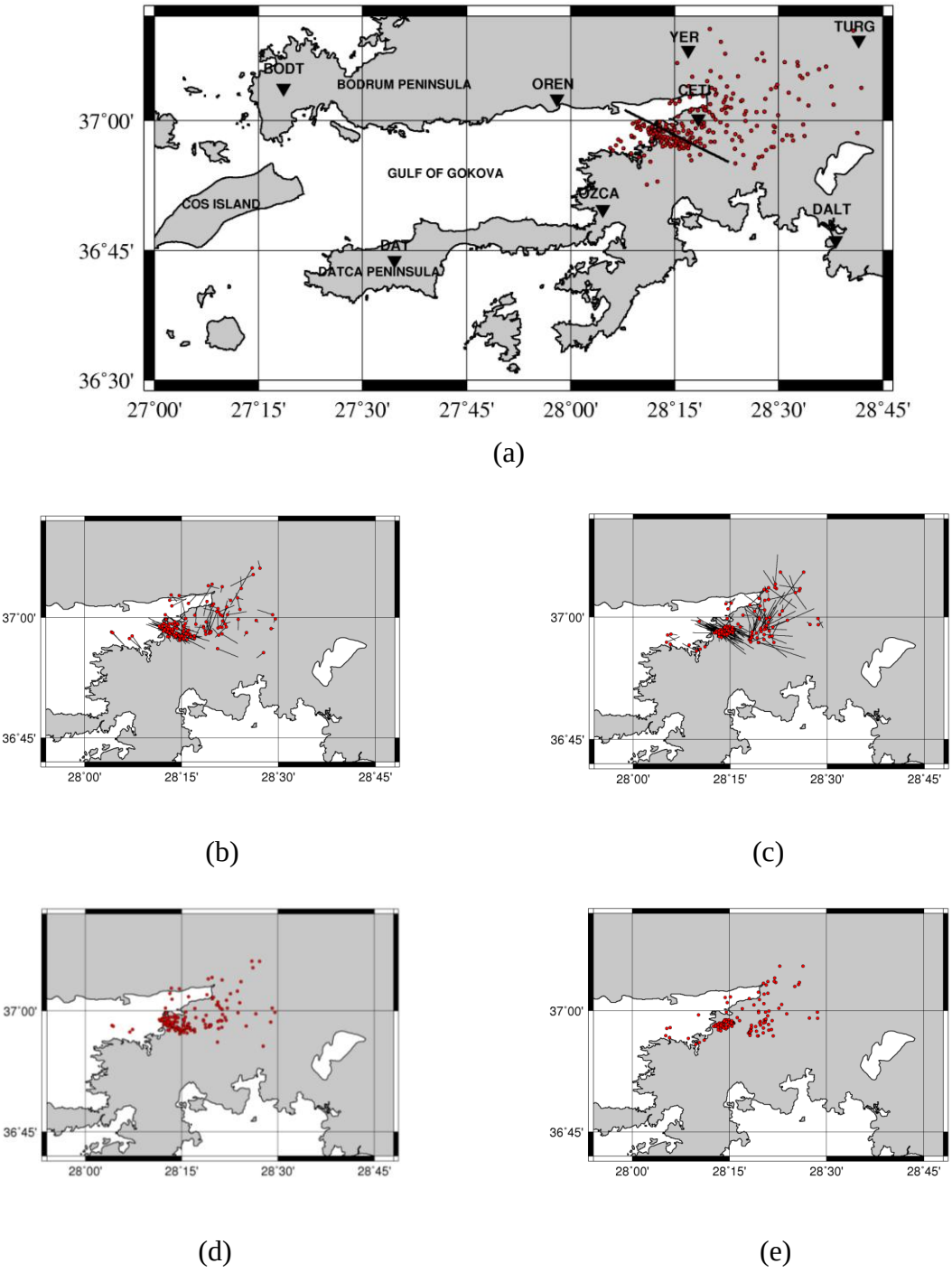

Figure 5.30. (a) Original locations of the earthquakes in Cluster 4 (HYPO71); (b) The corrections between the original and HYPODD locations (Catalog Data) (MAXSEP = 10); (c) The corrections between the original and HYPODD locations (Cross-Correlation); (d) Relocated earthquakes in Cluster 4 (by using Catalog Data); (e) Relocated earthquakes in Cluster 4 (by using Cross-Correlation Data).

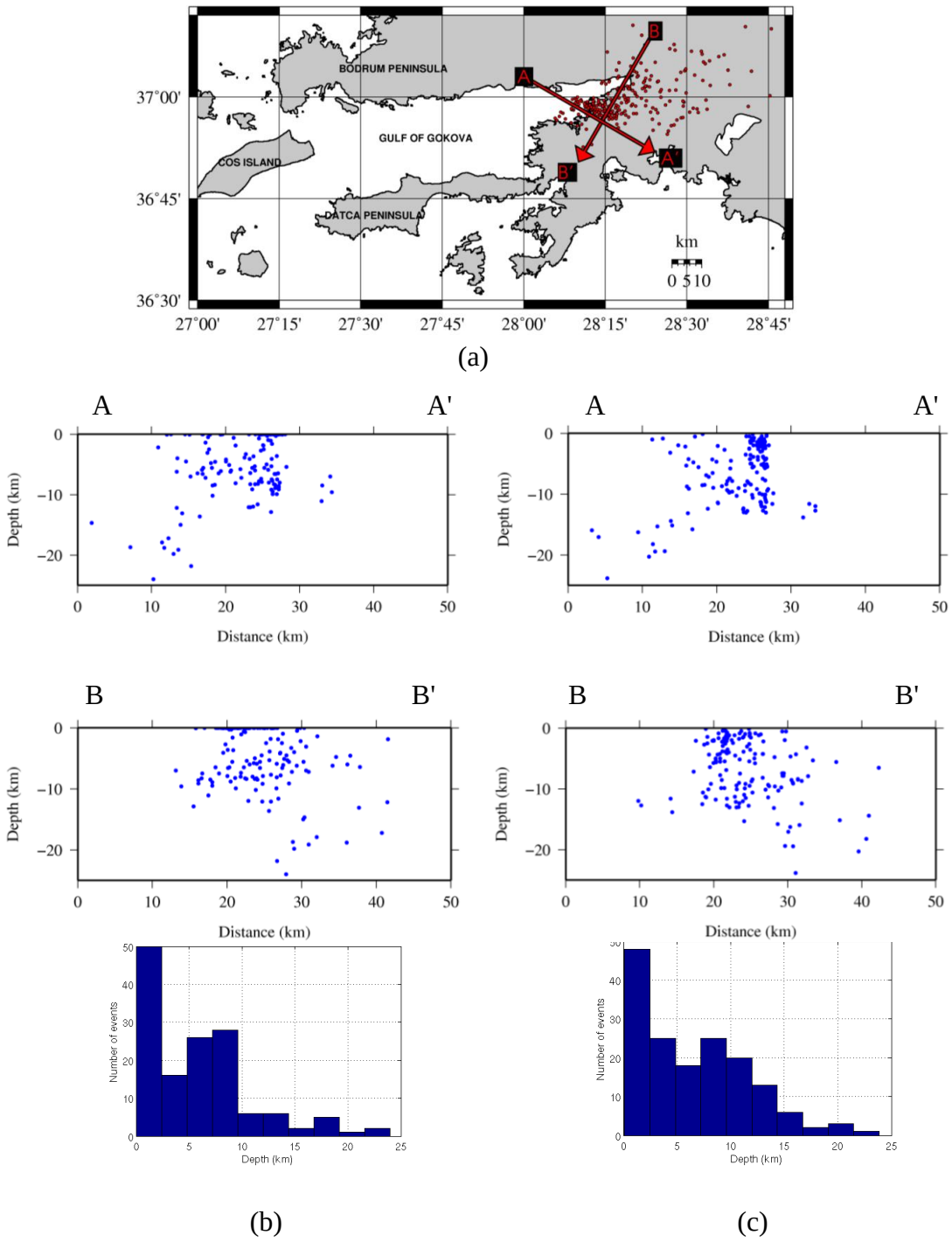

Figure 5.31. (a) Original locations of the earthquakes (Cluster 4) and profiles; (b) Cross sections view in the strike (Az = 120^0N) and normal to the strike direction (Az = 210^0N) (Original Data); (c) Cross sections view in the strike (Az = 120^0N) and normal to the strike direction (Az = 210^0N) (Catalog Data) (MAXSEP = 10).

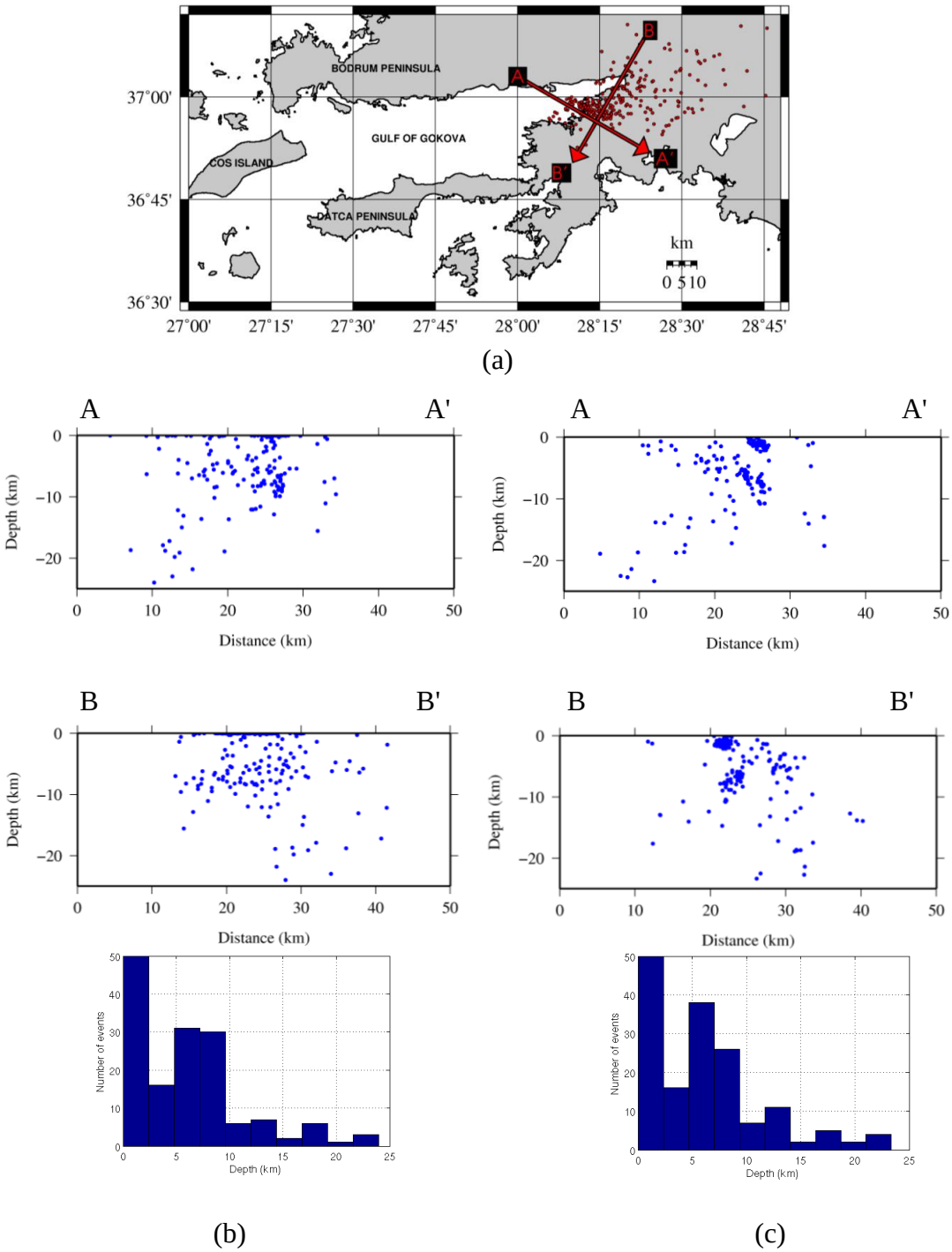

Figure 5.32. (a) Original locations of the earthquakes (Cluster 4) and profiles; (b) Cross sections view in the strike (Az = 120^0N) and normal to the strike direction (Az = 210^0N) (Original Data); (c) Cross sections view in the strike (Az = 120^0N) and normal to the strike direction (Az = 210^0N) (Cross-Correlation Data) (MAXSEP = 10).

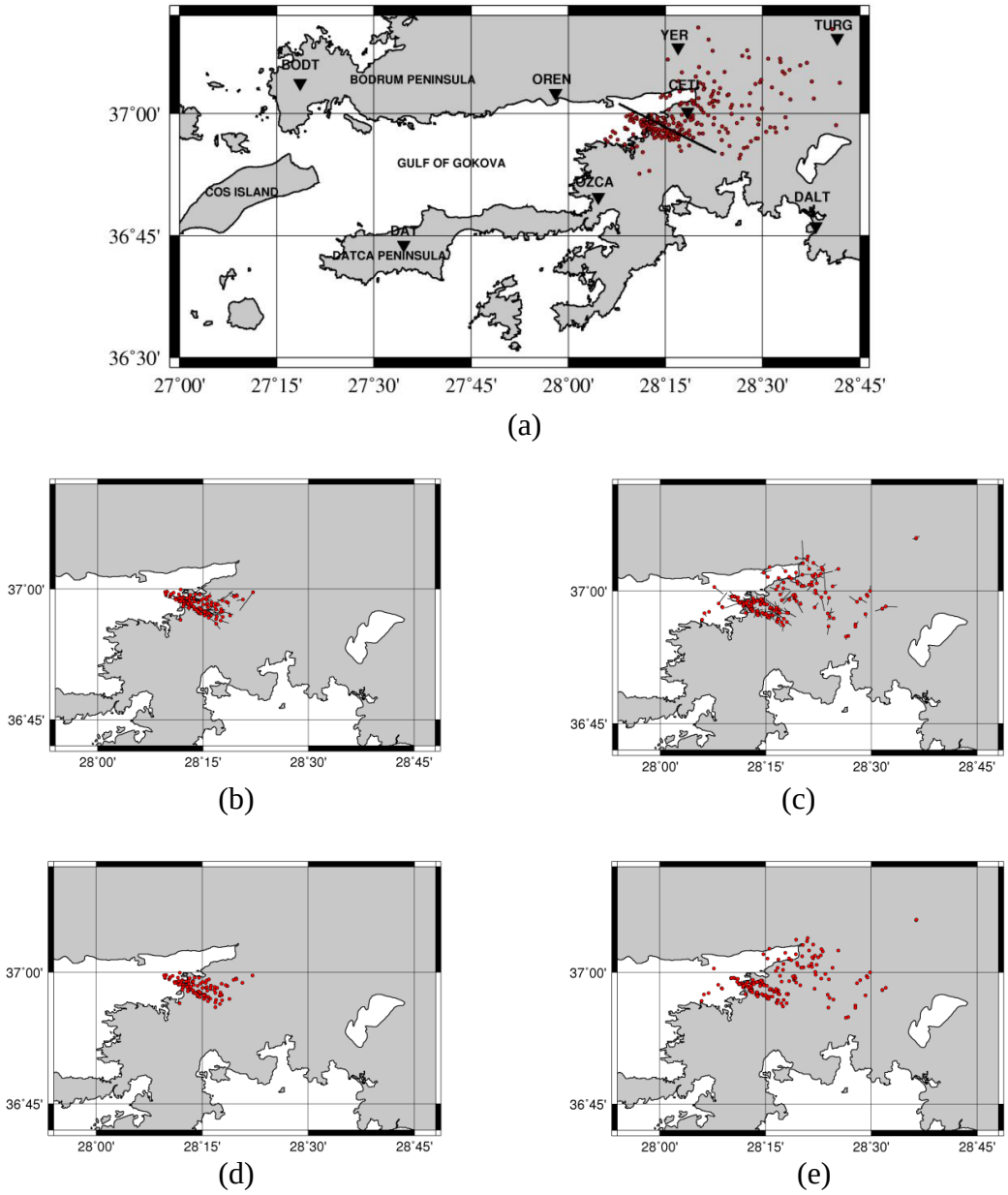

Figure 5.33. (a) Original Locations of the Earthquakes in Cluster 4 (HYPO71); (b) The corrections between the original and HYPODD locations (Catalog Data) (MAXSEP = 5); (c) The corrections between the original and HYPODD locations (Cross-Correlation); (d) Relocated Earthquakes in Cluster 4 (by using Catalog Data). The relocated event number is lower the half of the event number in this cluster (118 earthquakes); (e) Relocated Earthquakes (197 earthquakes) in Cluster 4 (by using Cross-Correlation Data).

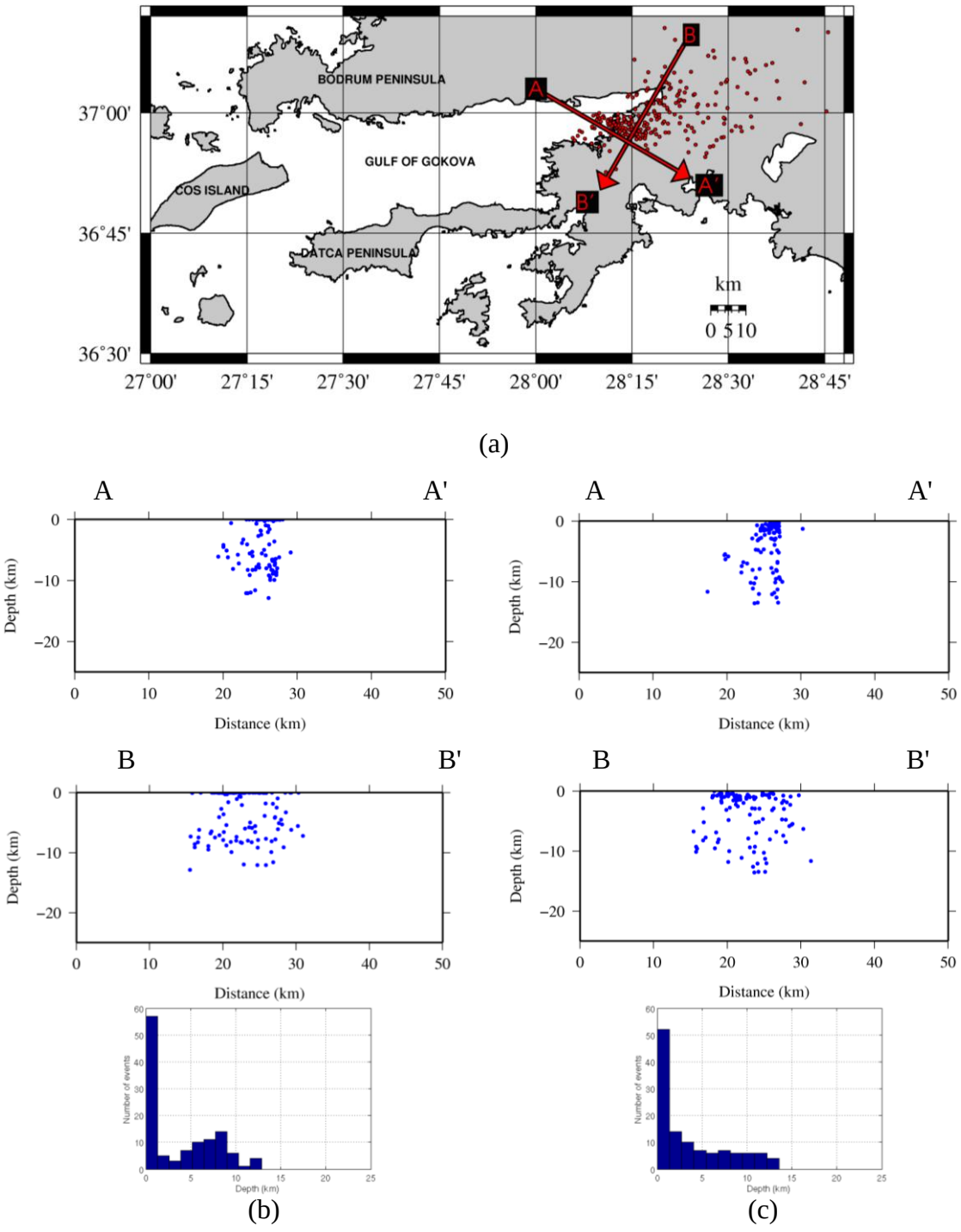

Figure 5.34. (a) Original locations of the earthquakes (Cluster 4) and profiles; (b) Cross sections view in the strike (Az = 120^0N) and normal to the strike direction (Az = 210^0N) (Original Data); (c) Cross sections view in the strike (Az = 120^0N) and normal to the strike direction (Az = 210^0N) (Catalog Data). The earthquakes localized the upper 10 km.

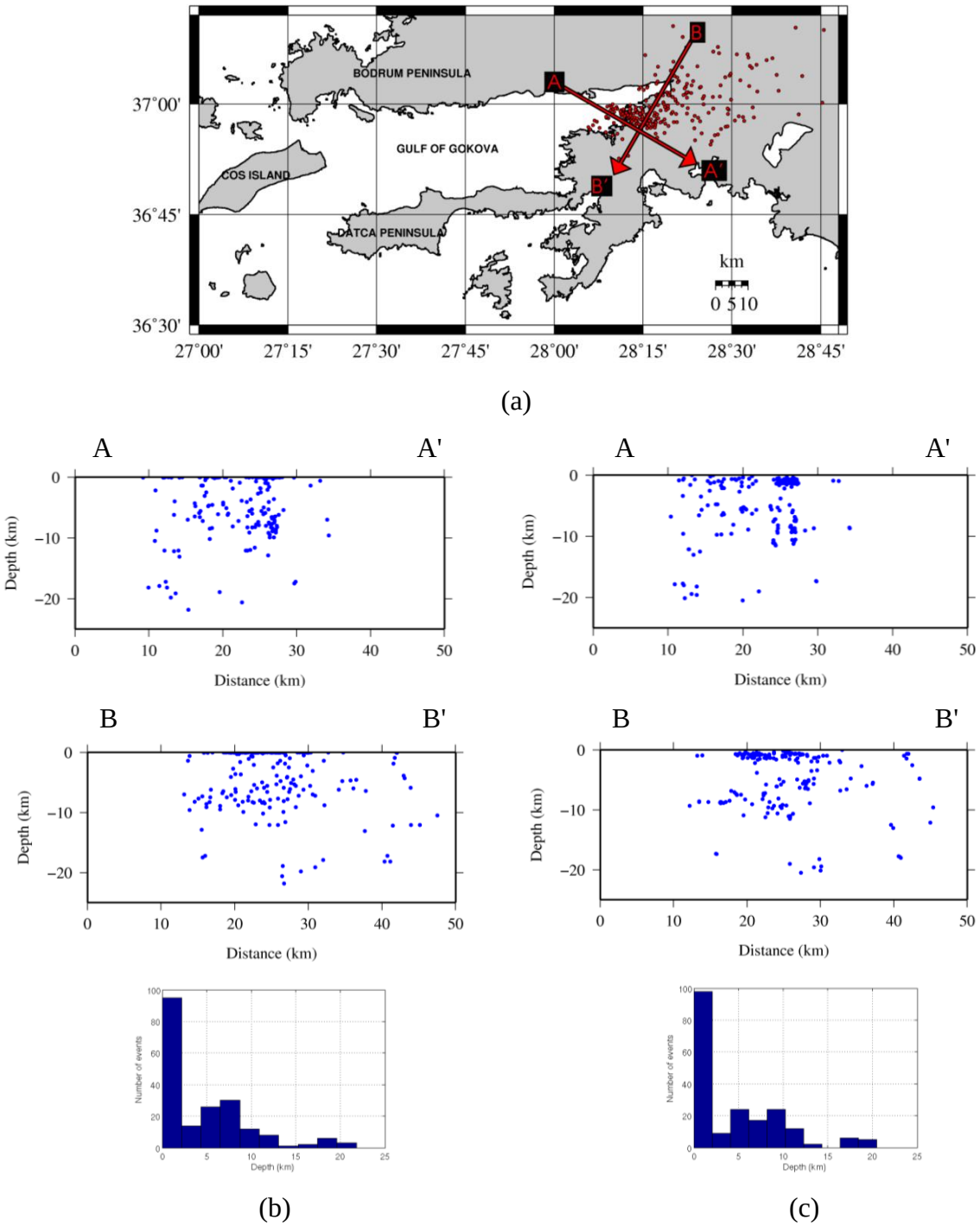

Figure 5.35. (a) Original locations of the earthquakes (Cluster 4) and profiles; (b) Cross sections view in the strike (Az = 120^0N) and normal to the strike direction (Az = 210^0N) (Original Data); (c) Cross sections view in the strike (Az = 120^0N) and normal to the strike direction (Az = 210^0N) (Cross-Correlation Data). The earthquakes localized the upper 10 km which is compatible with the results of cross-correlation and MAXSEP = 10.

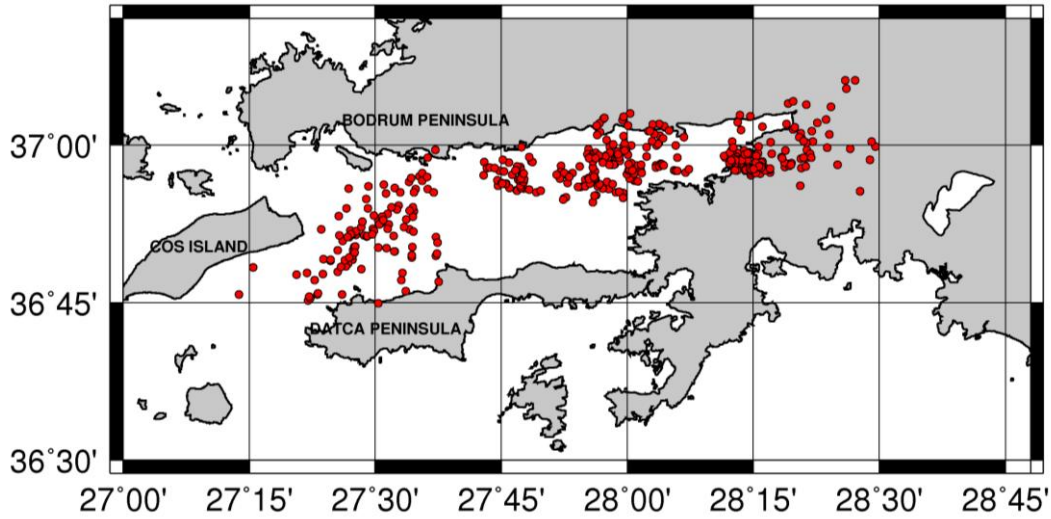

Figure 5.36. Combinations of the clusters (Catalog).

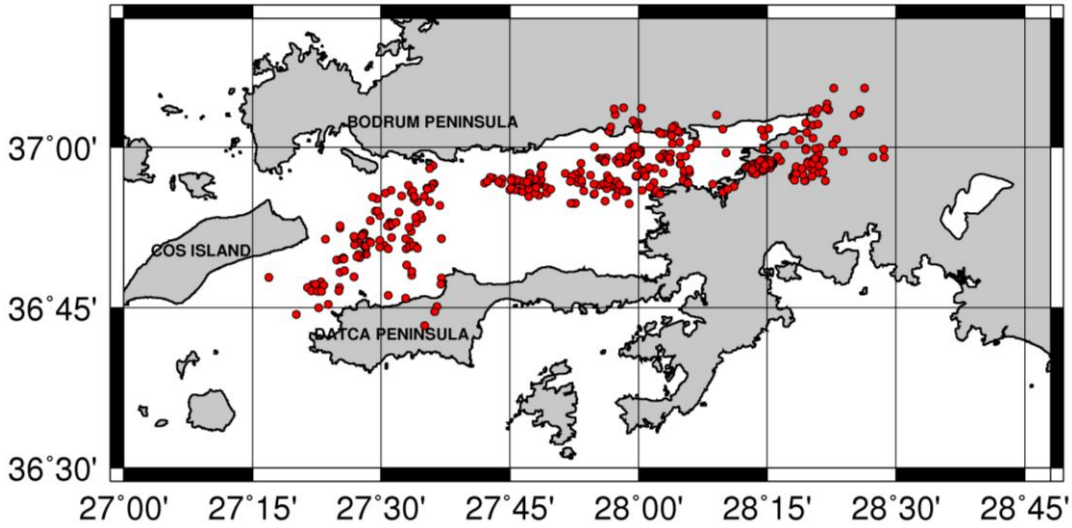

Figure 5.37. Combinations of the clusters (Correlation).

5.2. Joint Inversion of all Clusters

HypoDD can be run on the large data sets if the computer memory is enough for handling large complex inverse matrices. Our complete data contains the 972 earthquakes and we could not run hypoDD on all data set. For comparing the results we start to eliminate the earthquakes starting from the most distant and isolated ones. Finally we have created a large cluster with 864 earthquakes which was just enough to be handled with the computer available for the thesis. These events represent nearly our original data set because the eliminated earthquake number is relatively low and distant, and do not distort the appearance of fault related events.

The advantage of this approach is the simplification in the application of the method. There is no step that will require the separation of data into various clusters. Consequently there is no necessity to find separately the optimal parameters that will be suitable for each cluster. This is expected to be paid off by a reduction in the performance of the inversion because the control parameters are globally optimal, but not necessarily the best choices for each individual clusters.

The original locations of the earthquakes are shown by the Figure 5.38a. The remaining maps are the results of the catalog (right column, Figure 5.38b, Figure 5.38d) and cross-correlation (left column, Figure 5.38c, Figure 5.38e), respectively. By using the catalog and cross-correlation data 557 and 614 of the events were relocated. The average distance between the located and the relocated events, which are created by using catalog and cross-correlation data, is 2.34 and 2.54 km, respectively. The suggested fault orientation is verified by both the results of the both relocation approaches (catalog and cross-correlation) and linearity of the fault is more remarkable at the result of the cross-correlation. We observe that results of the hypoDD are mainly same with the previous studies only for some clusters (1 and 4) and only for the horizontal appearance. Once again we observe that the catalog inversion performs better for Cluster 1 where events are scattered, wherelse correlation is preferable for all the other three clusters. We do not plot depth sections for this case because there is no single azimuth where we can see the faults in profile in a strike direction.

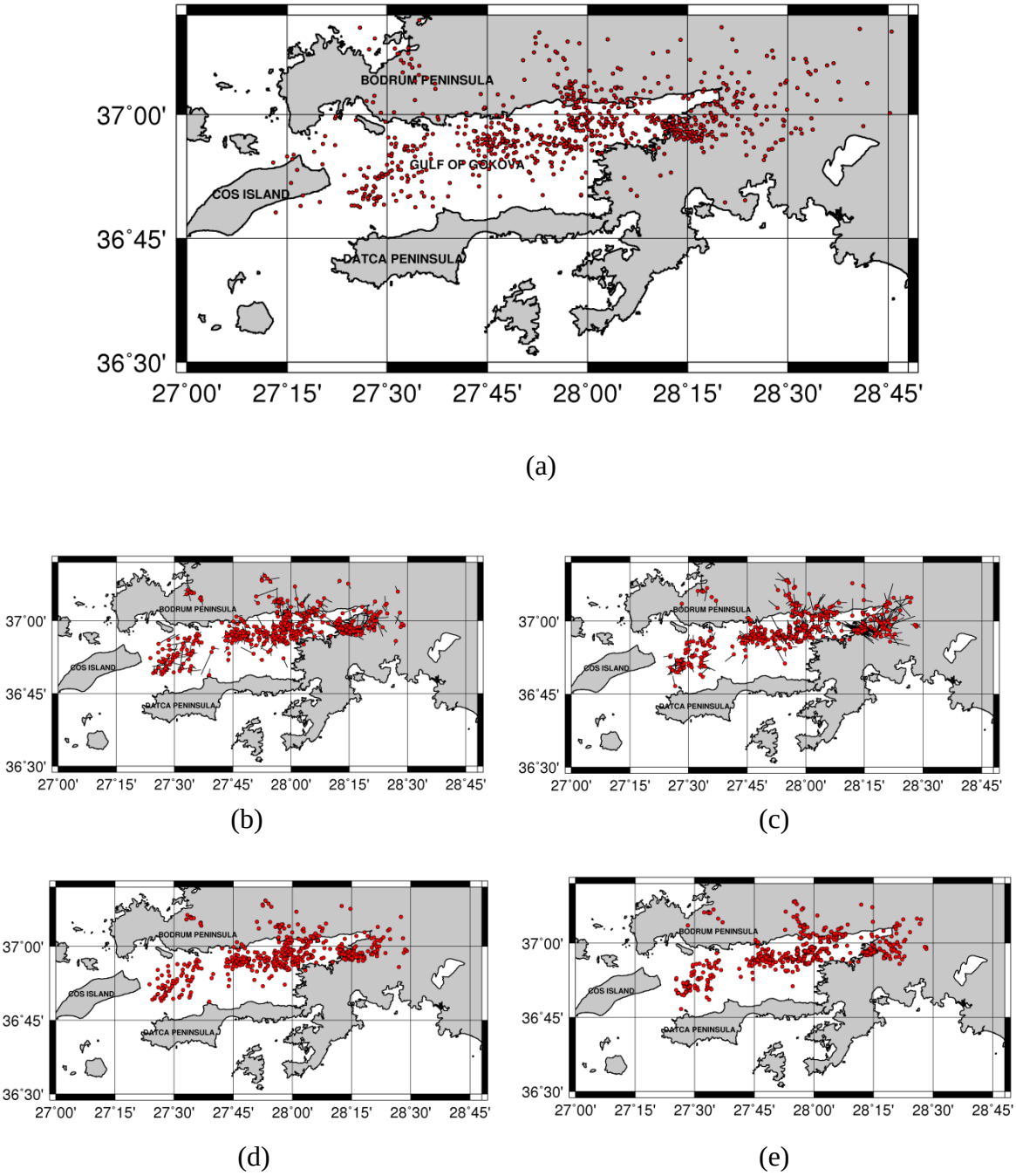

Figure 5.38. (a) Original locations of the earthquakes of all data (HYPO71); (b) The corrections between the original and HYPODD locations (Catalog Data); (c) The corrections between the original and HYPODD locations (Cross-Correlation); (d) Relocated earthquakes (by using Catalog Data); (e) Relocated earthquakes (by using Cross-Correlation Data).

5.3. Results of Combinations of Catalog and Cross-Correlation Data

HypoDD can be run separately on both catalog and cross-correlation data sets as shown in previous sections. There is also the option of combining the data sets and running the hypoDD relocation jointly for catalog and correlation time differentials. In such application the inversion can be adjusted to give a relatively more weight to either the catalog or the correlation data.

This section of the thesis contains the results of both data sets with separated clusters. In practice most of the time, differential error can be expected to be higher in catalog data with respect to the correlation data. However, they can be expected to be consistent with each other, especially for P phases which are clear in the case of close recordings. This is being verified by the comparision of travel time and correlation differences (Chapter 4 in Figure 4.13, Figure 4.14) and the weights of phases at the all seismic stations (Chapter 4 in Figure 4.15, Figure 4.16). So we kept the weights of P phases higher than the S phase weights, similar to the previous tests. The correlation is reliable mostly for close events, so we should prefer them in the double difference relocation solutions. Therefore, the cross-correlation weights are higher only for the close events (<WDCC= 3.0 km) where waveforms are expected to be more similar. According to our observations limiting the distance between event pairs at hypoDD phase is not efficient since it eliminates most of the events. In the previous tests, we did not use low WDCT parameters so that we avoid reducing the data coverage. However, in this section the WDCT parameters were chosen as six at all clusters, because our priority time is to understand the main trend of the seismicity with limited but more consistent data coverage.

In this section we illustrate the results of the joint catalog and cross-correlation inversion for all clusters in Figure 5.39 and Figure 5.40. Note that the clusters where processed individually as the fist approach, and once again different control parameters (such as MAXSEP = 10 for Cluster 1 and MAXSEP = 5 for the rest) were used for each cluster. Our observations show that the results of the joint catalog/cross-correlation inversion did not perform as well as expected. We do not have any clear explanation for

this effect, except that a better choice of inversion parameters may produce improved results.

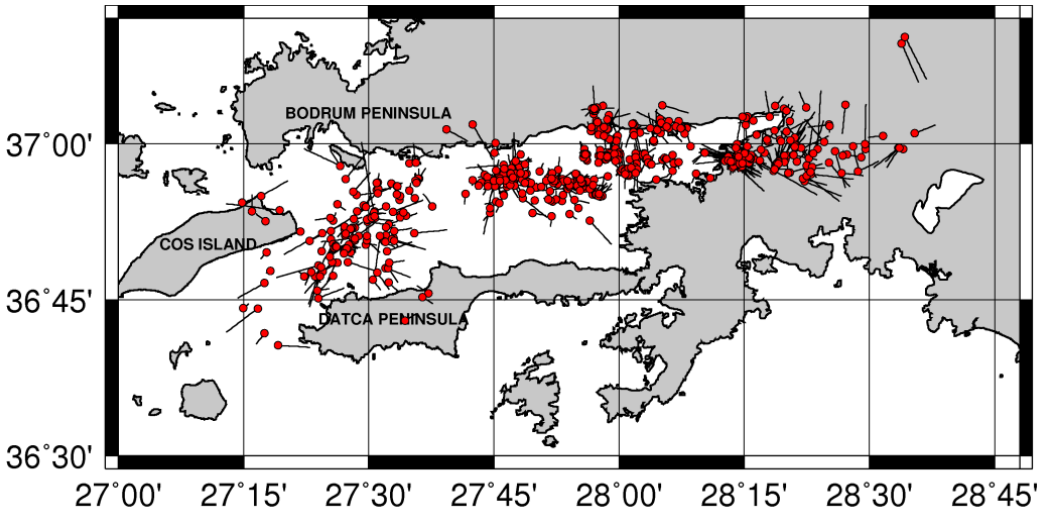

Figure 5.39. The corrections between the original and HYPODD locations (by using combinations of Catalog and Cross-correlation Data).

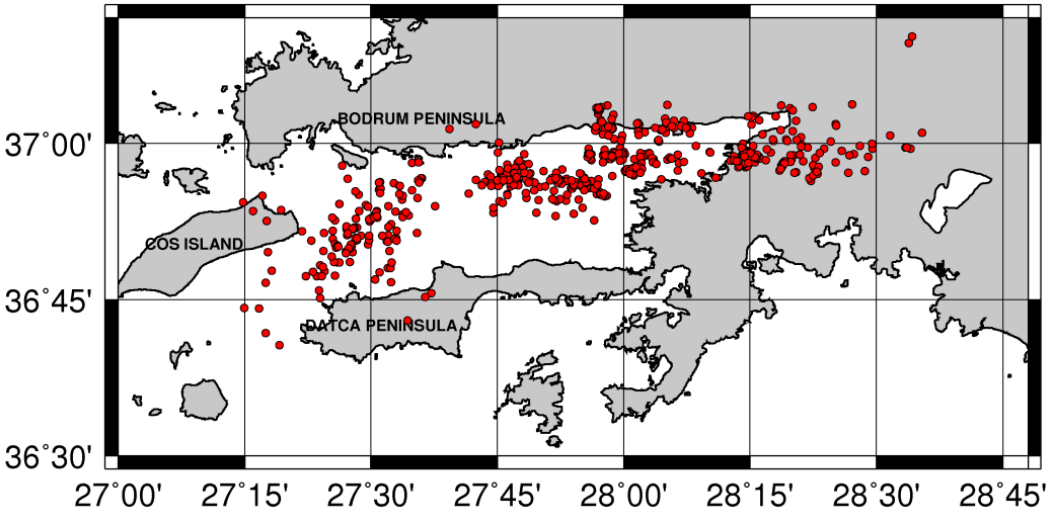

Figure 5.40. Relocated Earthquakes (by using combinations of Catalog and Cross-correlation Data).

6. CONCLUSION

The earthquake location is a complex inverse problem and it is basically affected by the nonlinearity of the inversion, the velocity and measurement errors. Most of the earthquake location programs locate the earthquakes individually by using the first readings. By using HYPODD however, an earthquake is located with respect to the other ones, based on the arrival time differences at each station.

In this study we used four year (April 2006 - December 2009) seismic earthquake recordings. Only 972 of 1156 earthquakes could be picked by using the PQL and then were located by using HYPO71. The magnitudes of the earthquakes changes between 1.5 and 4.5.

At first we separated the data into four clusters with respect to the earthquake distribution. This approach was helpful for understanding the performance of the HYPODD for various seismicity shapes. We have observed that correlation based inversion gives a better picture only if the events in the cluster are close to each other. In the case of a local seismicity where magnitudes are often between 2.0-4.0, the correlation based relocation performs best if interevents separation is less than 3.0 km. In other cases where events are scattered and distant more that 3 km on the average, the catalog based inversion performs better. This is expected since correlation works only when waveforms show strong similarities, which is only true for short interevent distances. The improvement in using hypoDD is mostly apparent when depth sections are analyzed and this is observed in particular when correlation is applied. The other important observation is that the choice parameters and therefore the final performance entirely depend on the distribution of the events and stations. When stations are sufficient in number (>4 stations), and well scattered around the seismic zone at moderate distances (i.e. <60 km), we observe that the performance is high, and do not critically depends on the control parameters. If the number of events is low and they are distant, the HypoDD is hardly effective. We can easily claim that hypoDD is a tool for high number of events, condensed in a small volume, and observed with relatively high number of stations at close distance. It will not perform satisfactorily if one of the above quality factors is not satisfied. The parameters

MAXSEP, MINLNK, MINOBS are very critical parameters because they eventually decide which events will be selected and will be paired with the other ones. Making a conservative selection of these parameters will lead to a drastic reduction of the data set. On the other hand, relaxing these constraints too much will mean an unrealistic neighboring process and will produce erroneous locations.

Separating the data into clusters or not is a matter which entirely depends on the data. If data shows isolated clusters with distinct character each, it would be unrealistic to use a single set of control parameters for all of them, therefore clustering is recommended. On the other extreme, processing each cluster separately is often more time consuming and tends to produce isolated patterns.

We expected that the joint inversion using both catalog and correlation data together, would perform better. However we failed to observe this improvement and presently we have no explanation for this effect. We note that we may have not done enough tests to find the most optimal set of control parameters; therefore a more suitable selection may improve the results.

In term of active fault geometry, it is clear that an offshore fault parallel to the northern boundary is well confirmed. The fault extends from midway between Ören and Çökertme to land close to SE of Akyazı, roughly and single EW trajectory between $27^0$45'W to $28^0$20'W. There may be segments associated with this fault, but the overall strike direction is nearly EW. The depth section of this fault is vertical in the central part, but shows a possible south dipping in the east. At the western end, the fault shows a sudden change in strike direction and turns south with a new strike direction of roughly 36^0N. This fault continues to $36^0$45'N, to the midway between Cos Islands and Datça Peninsula. It possibly continues further SW but we have no data to confirm this. This fault which cuts the Gökova Bay in a transverse way was already mentioned by Uluğ *et al*. (2005) and İşcan *et al*. (2012). But all three, the two proposed earlier and the present one do not exactly have the same location. More investigations are needed to confirm the existence and the detailed geometry of these faults. The mechanisms are not studied in the framework of this thesis, although some suggestions were made by earlier works. Finally, the fault adjacent to the southern shore of the bay which has been mentioned by many

authors (Kurt, Görür, etc.) is not confirmed by our studies. It must be pointed out the active faulting in Gökova Bay is a matter of active debate and more work has to be done in order to provide a reliable picture of the fault geometry and deformation patterns.

REFERENCES

Aktar, M., H. Karabulut, D. Childs, A. Mutlu, M. Ergin, A. Yörük, V. Gecgel, F. Bulut and T. Kaya, 2006, *Active Faults and Present Seismic Activity in Gulf of Gökova*, Tübitak Report, January, No:104Y336.

Allen, S. R. and R. A. F. Cas, 2002, "Transport of Pyroclastic Flows Across the Sea During The Explosive, Ryolitic Eruption of the Kos Plateau Tuff, Greece", *Bulletin of Volcanology*, pp. 441-456.

Ambraseys, N. N. and C. Finkel, 2006, *Türkiye'de ve Komşu Bölgelerde Sismik Etkinlikler, Bir Tarihsel İnceleme 1500-1800*, Tübitak Publisher.

Barka, A., F. Şaroğlu and A. Boray, 1985, *Gökova Termik Santrali' nin Depremler Açısından Değerlendirilmesi*, General Directorate of Mineral Research and Exploration, pp. 82.

Barka, A.,1995, *Gökova ve Saros Çevresindeki Aktif Fayların Deprem Aktivitelerinin Jeolojik, Jeomorfolojik, Paleosismolojik Yöntemlerle Belirlenmesi Alt Projesi*, National Marine Geology and Geophysics Research Project, Turkey, Project No: YDABÇAG-237/G.

Dewey, J. W., 1971, *Seismicity Studies With the Method of Joint Hypocenter Determination*, Ph.D., Dissertation, University of Calfornia, Berkeley, California.

Dewey, J. W., 1972, "Seismicity and Tectonics of Western Venezuela", *Bulletin of the Seismological Society of America*, Vol. 62, pp. 1711-1751.

Dewey , J. F. and A. M. Şengör, 1979, "Aegean and Surrounding Regions: Complex Multiple and Continuum Tectonics in a Convergent Zone", *Bulletin of the Seismological Society of America*, Vol. 90, No. 1, pp.84-92.

Dirik, K., 2007, "Neotectonic Characteristics and Seismicity of the Reşadiye Peninsula and Surrounding Area, Southwest Anatolia", *Geological Bulletin of Turkey*, Vol. 50, Number 3.

Drinia, H., E. Koskeridou, A. Antonarakou and E. Tzortzaki, 2010, "Benthic Foraminifera Associated With The Zooxanthellate Coral Cladocora in the Pleistocene of the Kos Island (Aegean Sea, Greece): Sea Level Changes and Palaeoenvironmental Conditions", *Bulletin of the Geological Society of Grece*, Proceeding of the 12th International Congress, Patras.

Douglas, A., 1967, "Joint Epicenter Determination", *Nature*, Vol. 215, 47-48.

Ecevitoğlu, B., E. Demirbağ, A. Uluğ, E. Özel, M. Duman, M. Avcı, E. Gökaşan and O. Algan, 1996, *Gökova Körfezi'nin Geç Kuvaterner Evrimi, Güneydoğu Ege Denizi: Delta Çökelleri ve Deniz Seviyesi Değişimleri*, National Marine Research Program Workshop V Proceeding Book, pp. 91-97.

Ersoy, Ş., 1991, "Datça (Muğla) Yarımadası'nın Stratigrafisi ve Tektoniği", *Geological Bulletin of Turkey*, Vol. 34, 1-14.

Ercan,T., 1980, "Akdeniz ve Ege Denizindeki Plio-Kuvaterner Ada Yayı Volkanizması", *Bulletin of Geomorphology*, Turkey, Vol. 9, pp. 37-60.

Ercan, T., E. Günay, H. Baş and B. Can, 1984, "Datça Yarımadası'ndaki Kuvaterner Yaşlı Volkanik Kayaların Stratigrafisi ve Yapısı", *Bulletin of the Mineral Research and Exploration*, 97-98, 45-46.

Eyidoğan, H., A. Akıncı, O. Gündoğdu, O. Polat and B. Kaypak, 1996, *Gökova Havzası' nın Güncel Depremselliğinin İncelenmesi*, Project No: YDABÇAG 238-G.

Frechet, J., 1985, *Sismogenese et Doublets Sismiques*, These d'Etat, Universite Scientifique et Medicale de Grenoble, pp. 327.

Gautier, P., J. P. Brun, R. Moriceau, D. Sokoutis, J. Martinod and L. Jolivet, 1999, "Timing, Kinematics and Cause of Aegean Extension: A Scenario Based on a Comparison with Simple Analogue Experiments", *Tectonophysics*, Vol. 315, pp. 31-72.

Georgalas, G.C., 1962, "Catalogue of the Active Volcanoes of the World Including Solfatara Fields: Part XII, Greece", *International Association of Volcanologists*, Roma, pp. 40.

Görür, N., A. M. C. Şengör, M. Sakınç, O. Tüysüz, R. Akkök, E. Yiğitbaş, F. Y. Oktay, A. Barka, N. Sarıca, B. Ecevitoğlu, E. Demirbağ, Ş. Ersoy, O. Algan, C. Güneysu and A. Aykol, 1995, "Rift Formation in the Gökova Region, Southwest Anatolia: Implications for the Opening of the Aegean Sea", *Geological Magazine*, Vol. 132, pp. 637-650.

Gralla, P., 1982, *Das Praneogen der Insel Kos (Dodekanes, Griechenland)*, Ph.D. Thesis, University of Braunschweig, pp. 182.

Gürer, Ö.F. and Y. Yılmaz, 2002, "Geology of the Ören and Surrounding Areas, SW Anatolia", *Turkish Journal of Earth Sciences* (Turkish J. Earth Sci.), Vol. 11, pp. 1-13.

İşcan, Y., H. Tur and E. Gökaşan, 2012, *Morphologic and Seismic Features of the Gulf of Gökova, SW Anatolia: Evidence of Strike-Slip Faulting with Compression in the Aegean Extensional Regime, Geo-Marine Letters*, 33:31-48.

Jacobshagen, V., 1986, *Introduction, Geologie von Griechenland*, Berlin, Gebruder Borntraeger, pp. 1-9.

Jordan, T. H. and K. A. Sverdrup, 1981, "Teleseismic Loction Techniques and Their Application to Earthquake Clusters in the South Central Pacific", *Bulletin of the Seismological Society of America*, Vol. 71, pp.1105-1130.

Keller, J., 1969, "Origin of Rhyolites by Anatectic Melting of Graniteand Crustal Rocks. The Example of Rhyolitic Pumice from the Island of Kos (Aegean Sea)", *Bulletin of Volcanology*, 33:942-959.

Kiratzi, A. and E. Louvari, 2003, "Focal Mechanisms of Shallow Earthquakes in the Aegean Sea and the Surrounding Lands Determined by Waveform Modelling: A New Database", *Journal of Geodynamics*, 36, 251-274.

Kurt, H., E. Demirbağ and İ. Kuşçu, 1999, "Investigation of the Submarine Active Tectonism in The Gulf of Gökova, Southwest Anatolia-Southeast Aegean Sea, by Multi-Channel Seismic Reflection Data", *Tectonophysics*, 305, 477-496.

Le Pichon, X. and J., Angelier, 1979, "The Hellenic Arc and Trench System: A Key to the NeoTectonic Evolution of The Eastern Mediterranean Area", *Tectonophysics*, Vol. 60, pp. 1-41.

McClusky, S., S. Balassanian, A. Barka, C. Demir, S. Ergintav, I. Georgiev, O. Gürkan, M. Hamburger, K. Hurst, H. Kahle, K. Kastens, G. Kekelidze, R. King, V. Kotzev, O. Lenk, S. Mahmoud, A. Mishin, M. Nadariya, A. Ouzounis, D. Paradissis, Y. Peter, M. Prilepin, R. Reilinger, I. Sanli, H. Seeger, A. Tealeb, M. N. Toksöz and G. Veis, 2000, "Global Positioning System Constraints on Plate Kinematics and Dynamics in the Eastern Mediterrenean and Caucasus", *Journal of Geophysical Research*, Vol. 105, No: B3, Pages 5695-5719.

McKenzie, D. P., 1970, "Plate Tectonics of the Mediterranean Region", *Nature*, Vol. 226, p. 239-242.

Nomikou, P. and D. Papanikolaou, 2010, "The Morpho-Tectonic Structure of Kos-Nisyros-Tilos Volcanic Area Based on Onshore and Offshore Data", Scientific Annals, School of Geology, Aristotle Univerity of Thessaloniki, *Proceeding of the XIX CBGA Congress*, Thessaloniki, Greece, Special Vol. 99, 557-564.

Nomikou, P., K. L. C. Bell, D. Papanikolaou, I. Livanos and J. Fero Martin, 2013, "Exploring the Avyssos-Yali-Strogyli Submarine Volcanic Complex at the Eastern Edge of the Aegean Volcanic Arc", *Zeitschrift für Geomorphologie*, Vol. 57, Suppl. 3, 125-137.

Papadopoulos, G., M. Sachpazi, G. Panopolou and G. Stavrakakis, 1998, *The Volcanoseismic Crisis of 1996-97 in Nisyros, SE Aegean Sea, Greece,* Terra Bova, 10, 151-154.

Pavlis, L. G., 1986, "Appraising Earthquake Hypocenter Location Errors: A Complete Practical Approach for Single-Event Locations", *Bulletin of the Seismological Society of America*, Vol. 76, No. 6, pp. 1699-1717.

Reilinger, R., S. McClusky, P. Vernant, S. Lawrence, S. Ergintav, R. Cakmak, H. Ozener, F. Kadirov, I. Guliev, R. Stepanyan, M. Nadariya, G. Hahubia, S. Mahmoud, K. Sakr, A. ArRajehi, D. Paradissis, A. Al-Aydrus, M. Prilepin, T. Guseva, E. Evren, A. Dmitrotsa, S. V. Filikov, F. Gomez, R. Al-Ghazzi and G. Karam, 2006, "GPS Constrains on Continental Deformation in the Africa-Arabia-Eurasia Continental Collision Zone and Implications for the Dynamics of Plate Interractions", *Journal of Geophysical Research*, Vol. 111, B05411, doi: 10.102972006JB004051.

Smith, P. E., D. York, Y. Chen and N. M. Evensen, 1996, *Single Crystal 40 Ar/39Ar Dating of the Late Quaternary Paroxysm on Kos,Greece; Concordance of Terrestrial and Marine Ages, Geophysical Research Letters* 23 (21):3047-3050.

Şaroğlu, F., Ö. Emre and İ. Kuşçu, 1992, *Active Fault Map of Turkey*, Mineral Research Exploration of Turkey Press, Ankara.

Şengör, A. M. and Y. Yılmaz, 1981, "Tethyan Evolution of Turkey: A Plate Tectonic Approach", *Tectonophysics*, Vol. 75, pp.181-241.

Taymaz, T., Y. Yılmaz and Y. Dilek, 2007, "The Geodynamics of the Aegean and Anatolia: Introduction", *Geological Society of London, Special Publications*, Vol.291; p1-16, doi:101144/SP291.1.

Uluğ, A., M. Duman, M. Avcı, E. Özel, B. Ecevitoğlu, E. Demirbağ, O. Algan and E. Gökaşan, 1996, *Gökova Körfezi'nin Geç Kuvaterner Evrimi, Güneydoğu Ege Denizi: Delta Çökelleri ve Deniz Seviyesi Değişimleri*, 11th. Petroleum Congress Proceedings Book, Turkey, pp. 59-72.

Uluğ, A., M. Duman, M. Avcı, E. Özel, B. Ecevitoğlu, E. Demirbağ, O. Algan and E. Gökaşan, 1998, *Gökova Körfezi'nin Geç Kuvaterner Evrimi, Güneydoğu Ege Denizi: Delta Çökelleri ve Deniz Seviyesi Değişimleri*, National Marine Research Program Workshop IV- Proceeding Book, Turkey, pp.71-77.

Uluğ, A., M. Duman, Ş. Ersoy, E. Özel and M. Avcı, 2005, "Late Quaternary Sea-level Change, Sedimentation and Neotectonics of the Gulf of Gökova: Southeastern Aegean Sea", *Marine Geology*, 221, 381-395.

Waldhause, F. and W. L. Ellsworth, 2000, "A Double-Difference Earthquake Location Algorithm: Method and Application to the Northern Hayward Fault, California", *Bulletin of the Seismological Society of America*, 90, 6, pp. 1353-1368.

Waldhauser, F., 2001, *hypoDD -- A Program to Compute Double Difference Hypocenter Locations*, *U.S. Geological Survey*, Open File Report 01-113.

Yılmaz, Y., 2010, "Ege Bölgesi'nde Genç Magmatizmanın Oluşumu ile Lithosferin Evrimi Arasındaki İlişkiler Üzerine Düşünceler", *Turkish Journal of Earth Sciences Geophysics*, 09,10, 107-110.

Yolsal, S. and T. Taymaz , 2010, "Gökova Körfezi Depremlerinin Kaynak Parametreleri ve Rodos-Dalaman Bölgesinde Tsunami Riski", *Bulletin of Istanbul Technical University*, Turkey, p. 53-65, Vol 9.

APPENDIX A

HypoDD results for joint inversion of catalog and correlation data, processing each cluster separately.

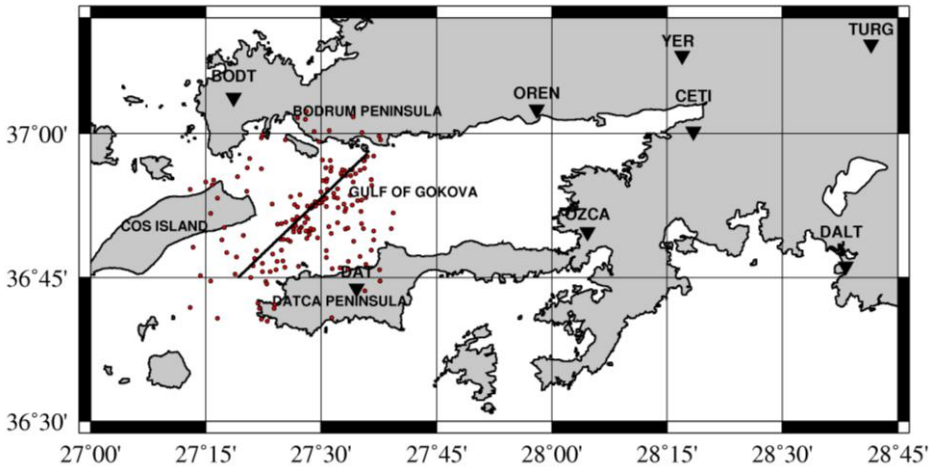

(a)

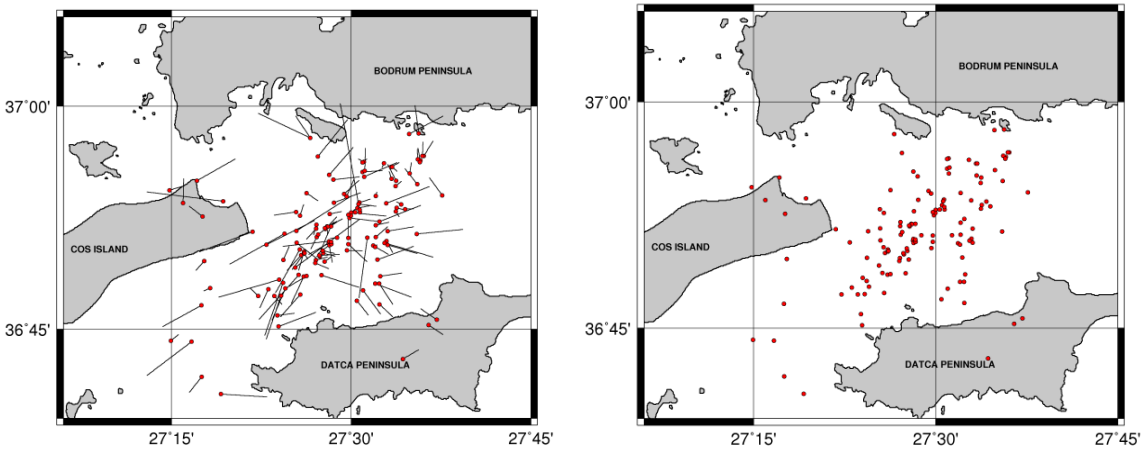

(b) (c)

Figure A.1 (a) Original locations of the earthquakes of Cluster 1 (HYPO71); (b) The corrections between the original and HYPODD locations (by using Catalog and Cross-correlation Data). The average correction is 3.38 km; (c) Relocated earthquakes (100 earthquakes) (by using Catalog and Cross-correlation Data) (MAXSEP = 10).

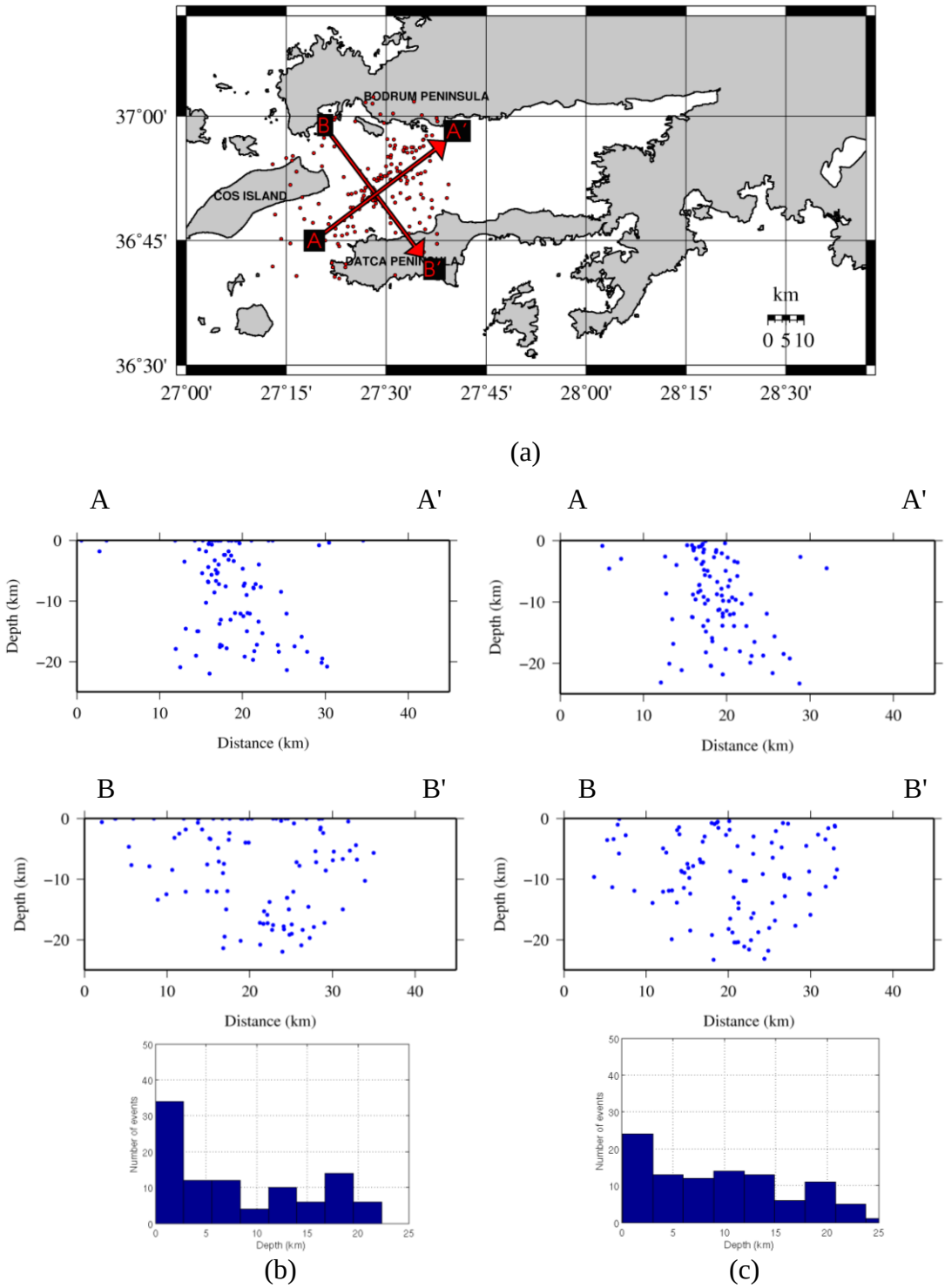

Figure A.2. (a) Original locations of the earthquakes (Cluster 1) and profiles; (b) Cross sections view in the strike (Az = 53^0N) and normal to the strike direction (Az = 143^0N) (Original Data) (Cluster 1); (c) Cross sections view in the strike (Az = 53^0N) and normal to the strike direction (Az = 143^0N) (Catalog and Cross-correlation Data) (MAXSEP = 10).

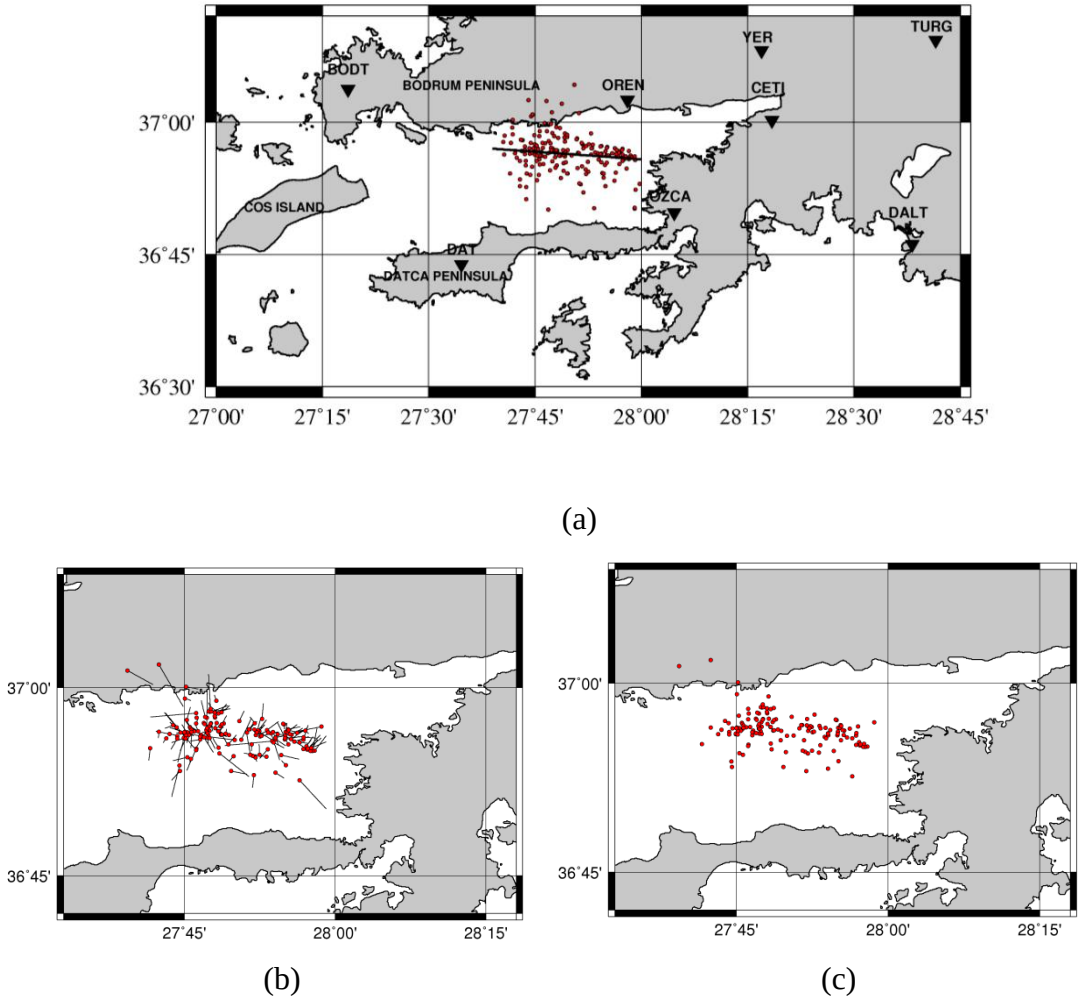

Figure A.3. (a) Original Locations of the Earthquakes of Cluster 2 (HYPO71); (b) The corrections between the original and HYPODD locations (by using Catalog and Cross-correlation Data). The average correction is 2.15 km; (c) Relocated Earthquakes (113 earthquakes) (by using Catalog and Cross-correlation Data) (MAXSEP = 10).

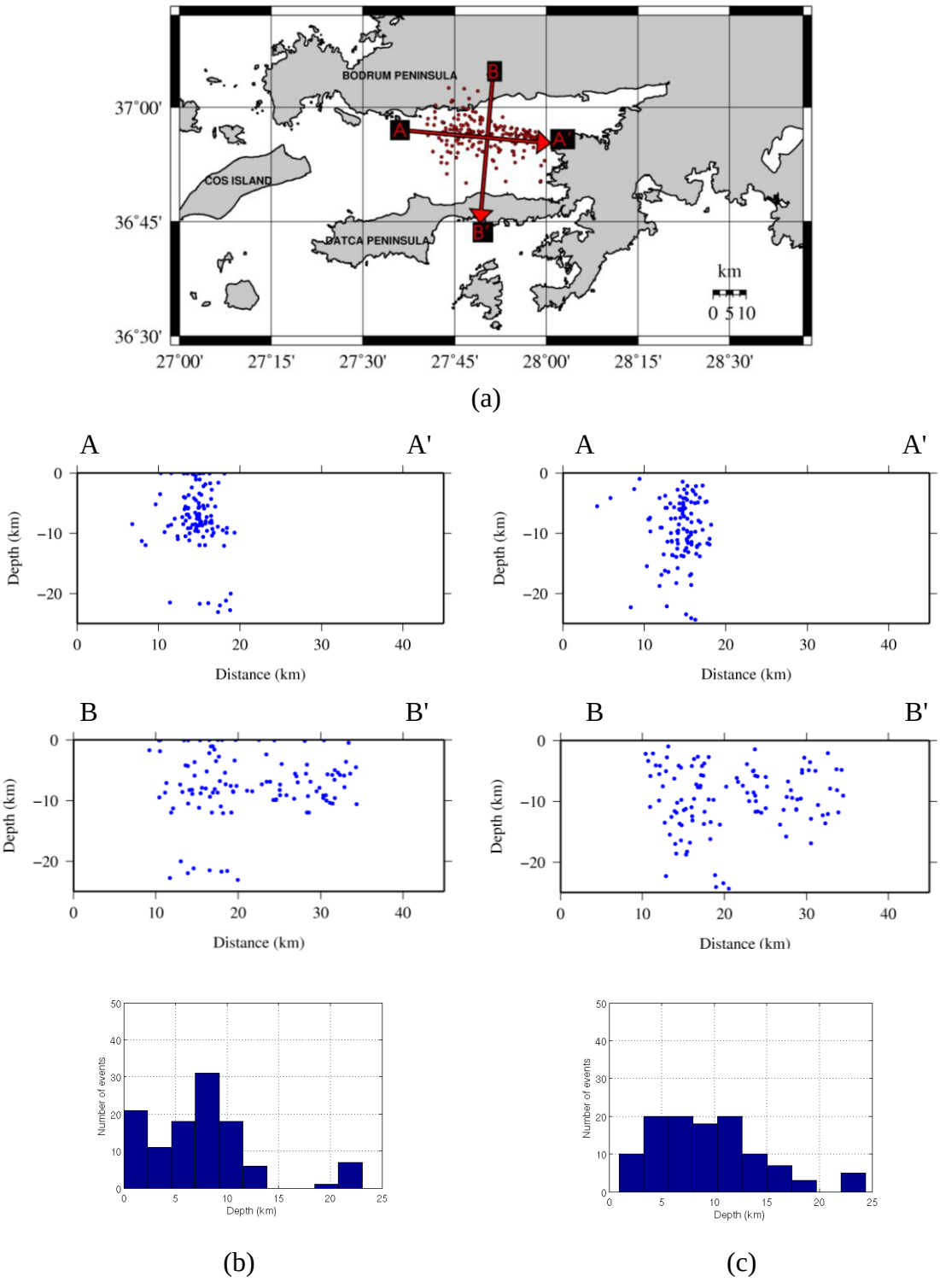

Figure A.4. (a) Original locations of the earthquakes (Cluster 2) and profiles; (b) Cross sections view in the strike (Az = 95^0N) and normal to the strike direction (Az = 185^0N) (Original Data) (Cluster 2); (c) Cross sections view in the strike (Az = 95^0N) and normal to the strike direction (Az = 185^0N) (Catalog and Cross-correlation Data) (MAXSEP = 10).

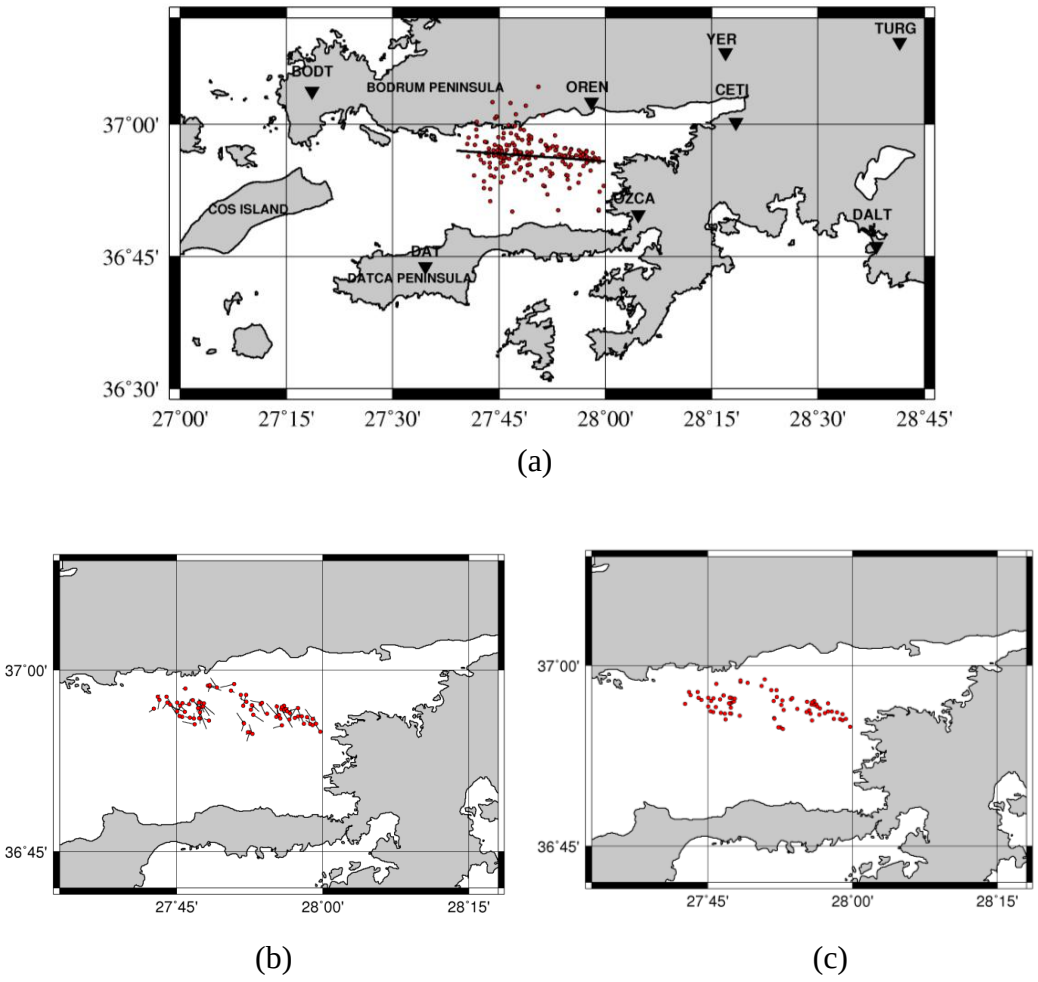

Figure A.5. (a) Original Locations of the Earthquakes of Cluster 2 (HYPO71); (b) The corrections between the original and HYPODD locations (by using Catalog and Cross-correlation Data) The average distance between the located (by using HYPO71) and relocated earthquakes is 1.34 ; (c) Relocated Earthquakes (80 earthqaukes) (by using Catalog and Cross-correlation Data) (MAXSEP = 5).

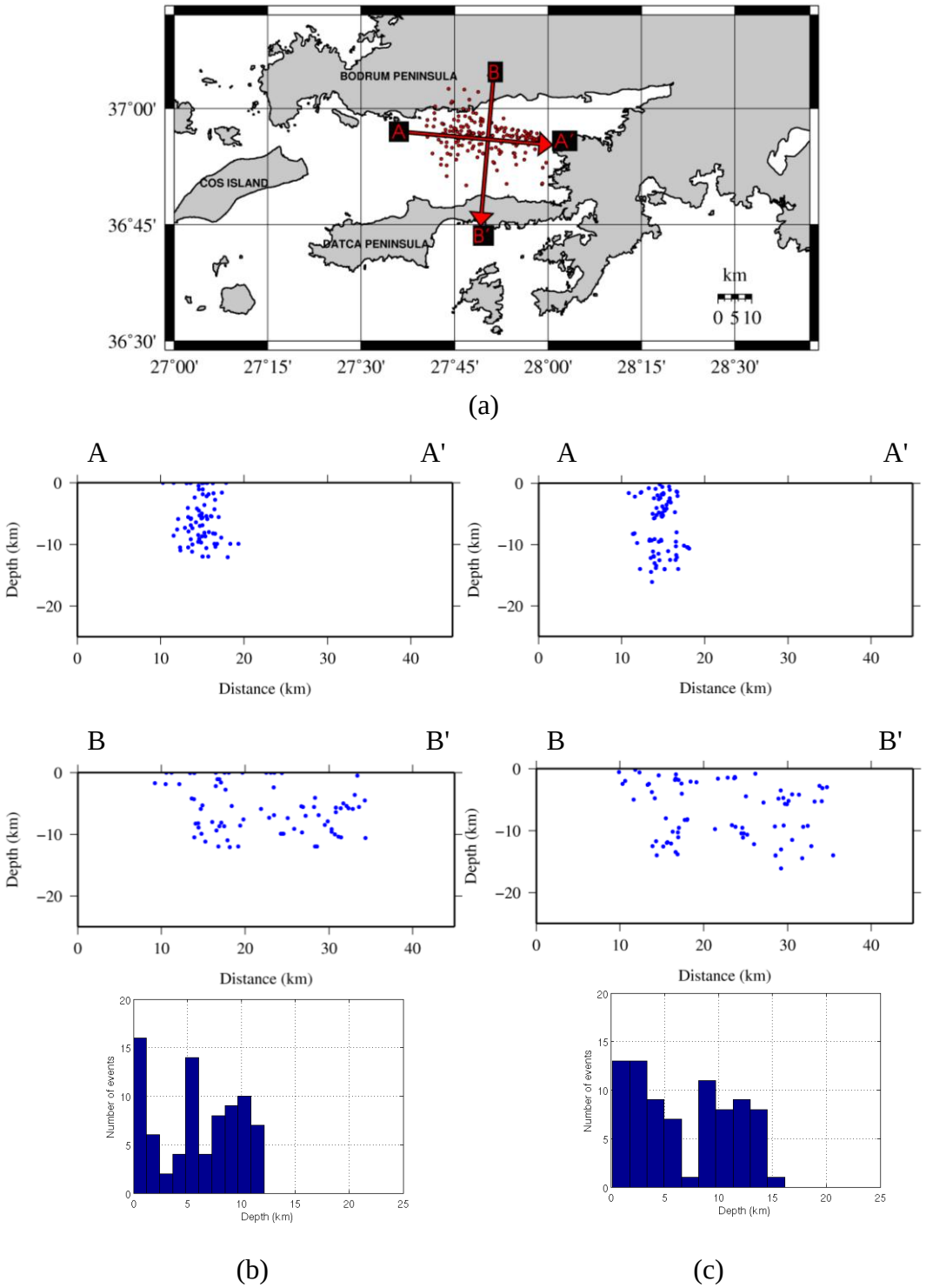

(a)

(b) (c)

Figure A.6. (a) Original locations of the earthquakes (Cluster 2) and profiles; (b) Cross sections view in the strike (Az = 95^0N) and normal to the strike direction (Az = 185^0N) (Original Data) (Cluster 2); (c) Cross sections view in the strike (Az = 95^0N) and normal to the strike direction (Az = 185^0N) (Catalog and Cross-correlation Data) (MAXSEP = 5).

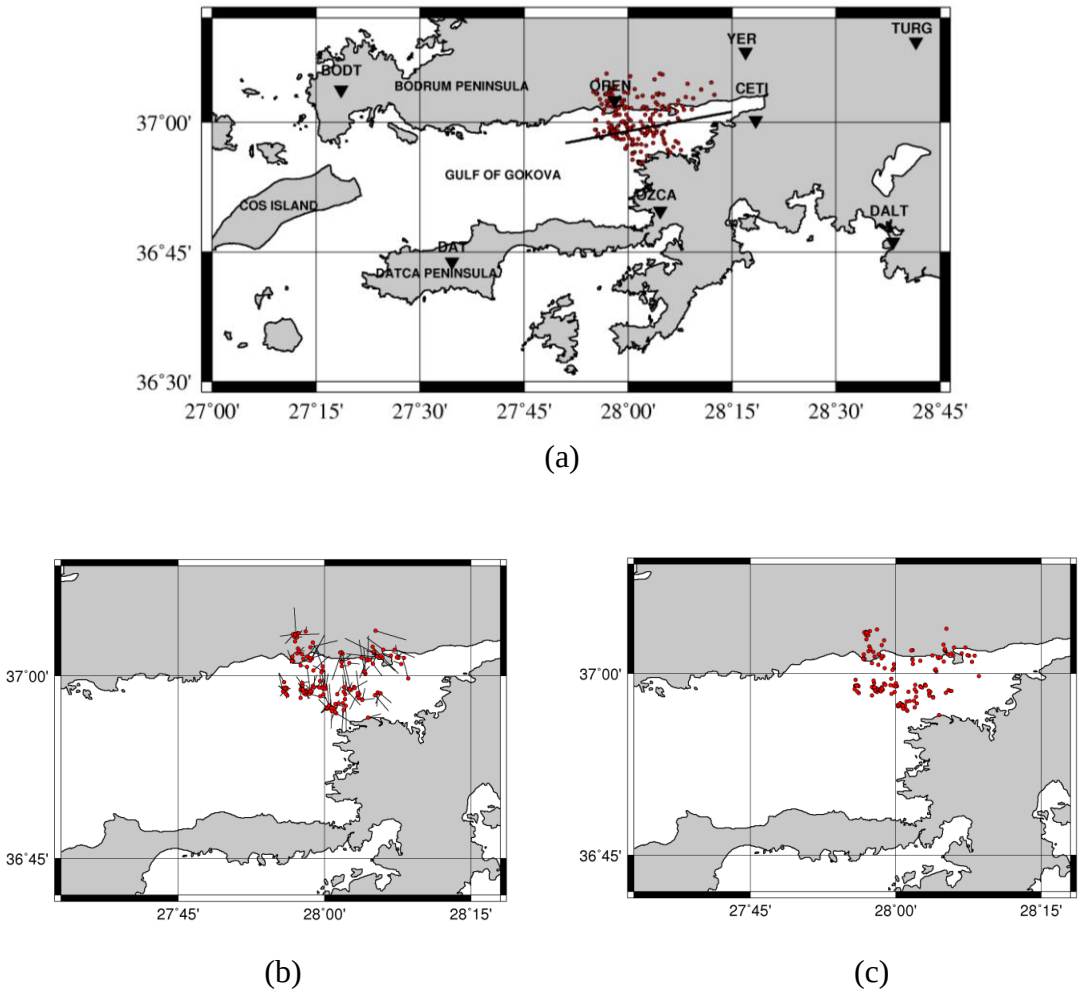

Figure A.7. (a) Original Locations of the Earthquakes of Cluster 3 (HYPO71); (b) The corrections between the original and HYPODD locations (by using Catalog and Cross-correlation Data). The average correction is 1.90 km; (c) Relocated Earthquakes (167 earthquakes) (by using Catalog and Cross-correlation Data) (MAXSEP = 10).

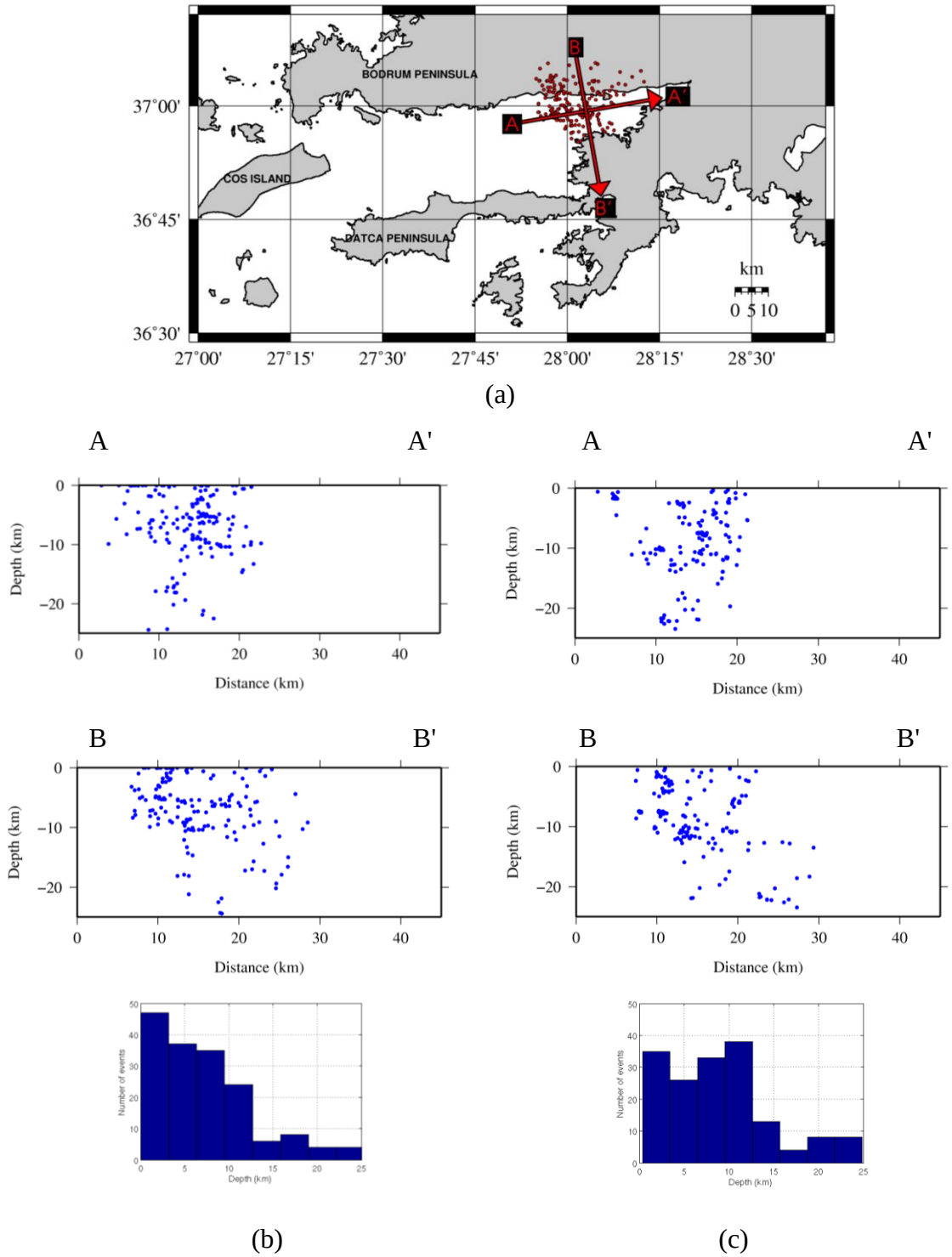

(a)

(b)

(c)

Figure A.8. (a) Original locations of the earthquakes (Cluster 3) and profiles; (b) Cross sections view in the strike (Az = 80^0N) and normal to the strike direction (Az = 170^0N) (Original Data) (Cluster 3); (c) Cross sections view in the strike (Az = 80^0N) and normal to the strike direction (Az = 170^0N) (Catalog and Cross-correlation Data) (MAXSEP = 10).

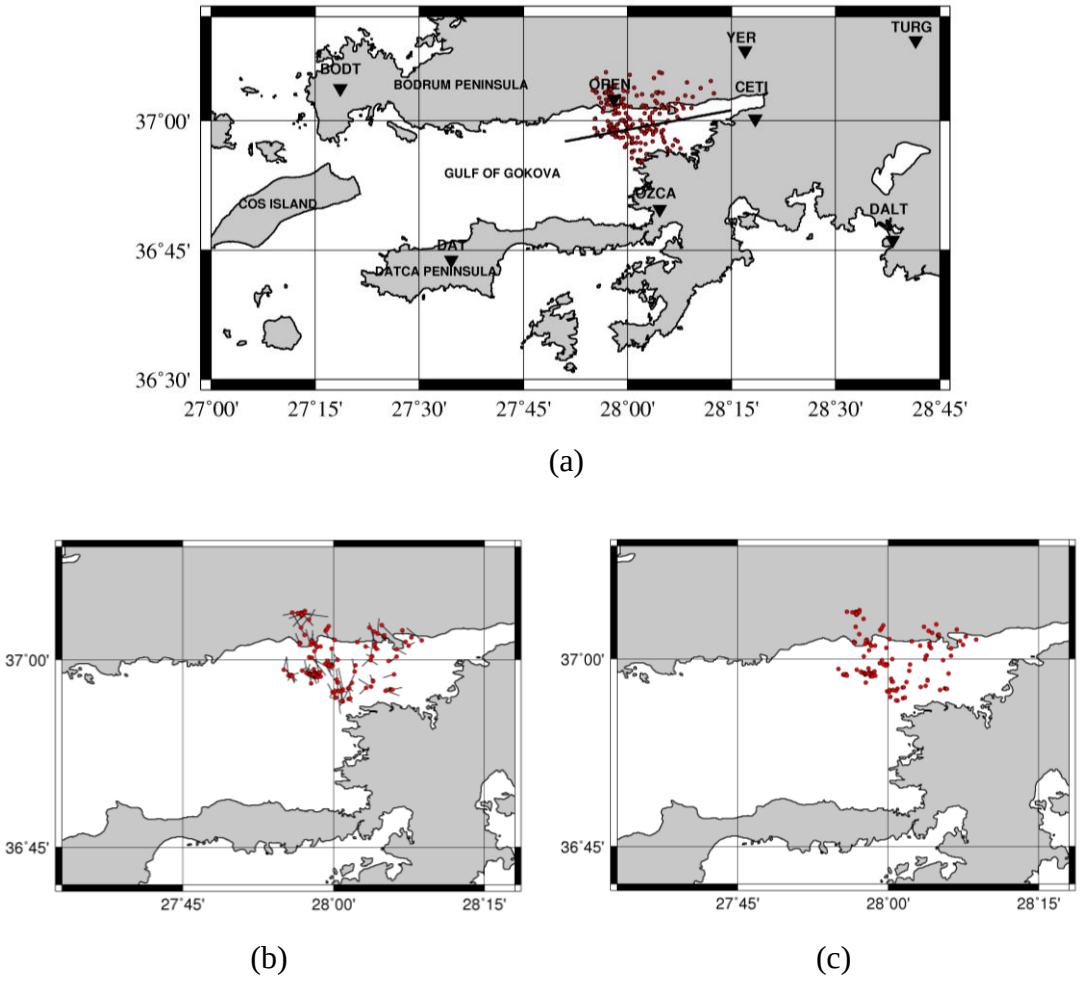

Figure A.9. (a) Original Locations of the Earthquakes of Cluster 3 (HYPO71); (b) The corrections between the original and HYPODD locations (by using Catalog and Cross-correlation Data) The average distance between located (by using HYPO71) and relocated earthquakes is 1.44 km ; (c) Relocated Earthquakes (128 earthquakes) (by using Catalog and Cross-correlation Data) (MAXSEP = 5).

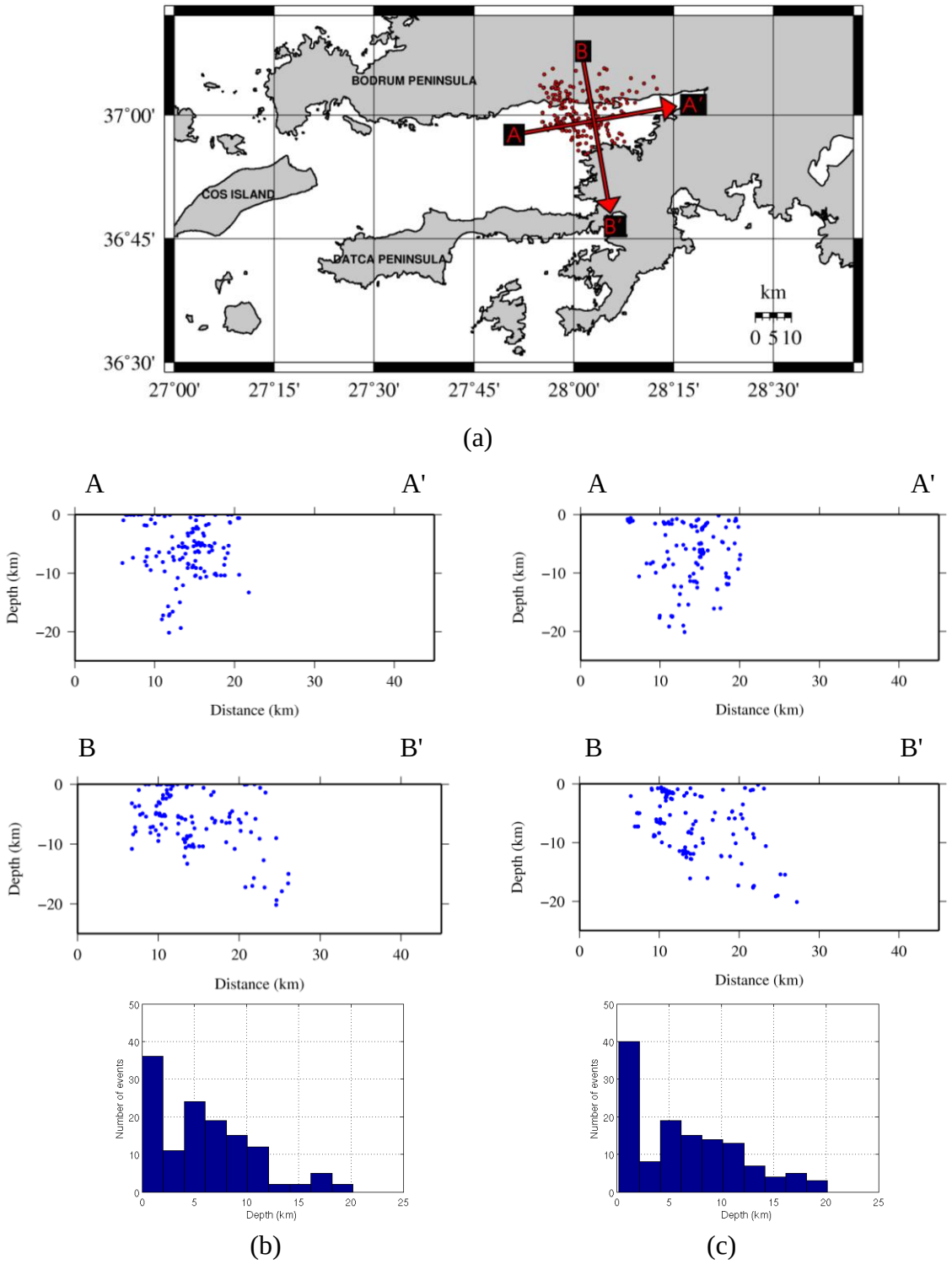

Figure A.10. (a) Original locations of the earthquakes (Cluster 3) and profiles; (b) Cross sections view in the strike (Az = 80^0N) and normal to the strike direction (Az = 170^0N) (Original Data) (Cluster 3); (c) Cross sections view in the strike (Az = 80^0N) and normal to the strike direction (Az = 170^0N) (Catalog and Cross-correlation Data) (MAXSEP = 5).

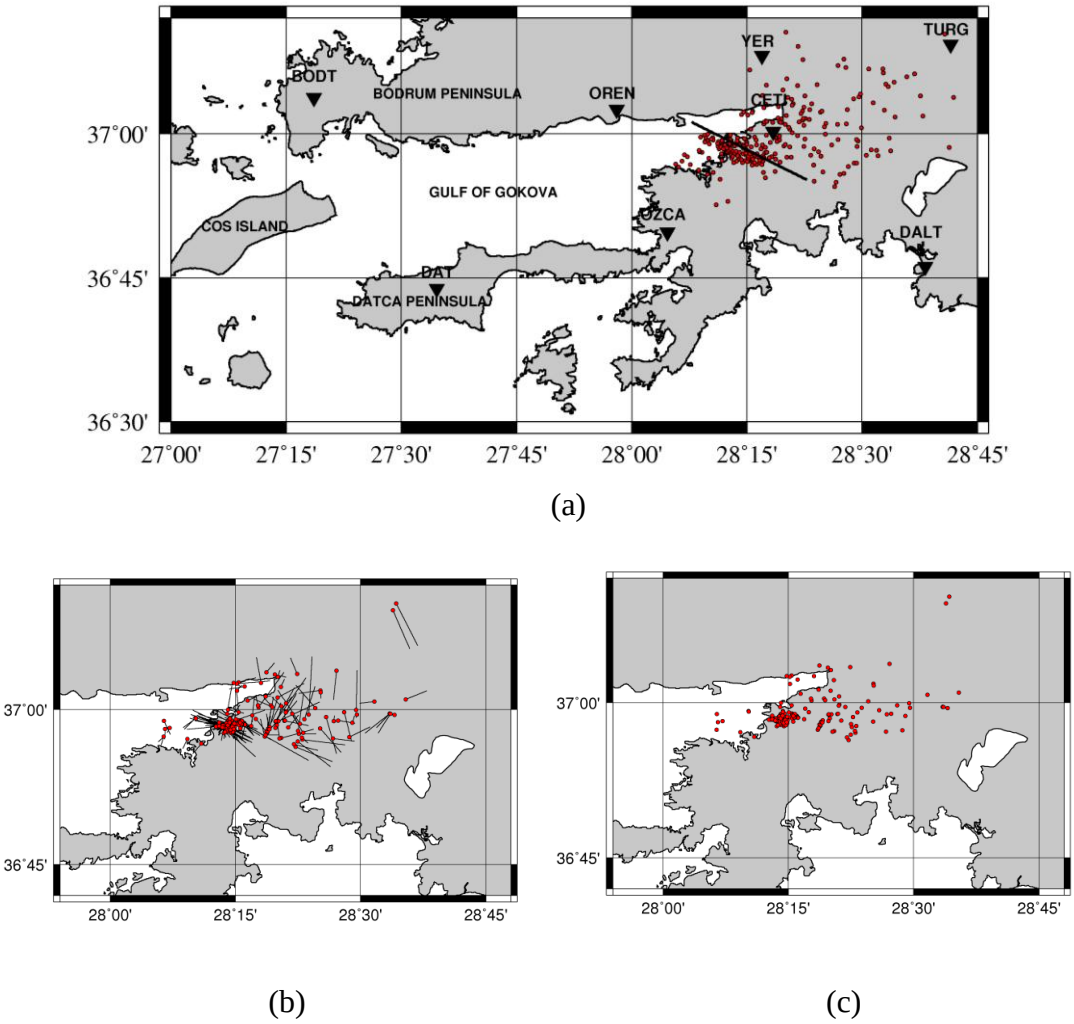

Figure A.11. (a) Original Locations of the Earthquakes of Cluster 4 (HYPO71); (b) The corrections between the original and HYPODD locations (by using Catalog and Cross-correlation Data) The average distance between located (by using HYPO71) and relocated earthquakes is 1.44 km; (c) Relocated Earthquakes (177 earthquakes) (by using Catalog and Cross-correlation Data) (MAXSEP = 10).

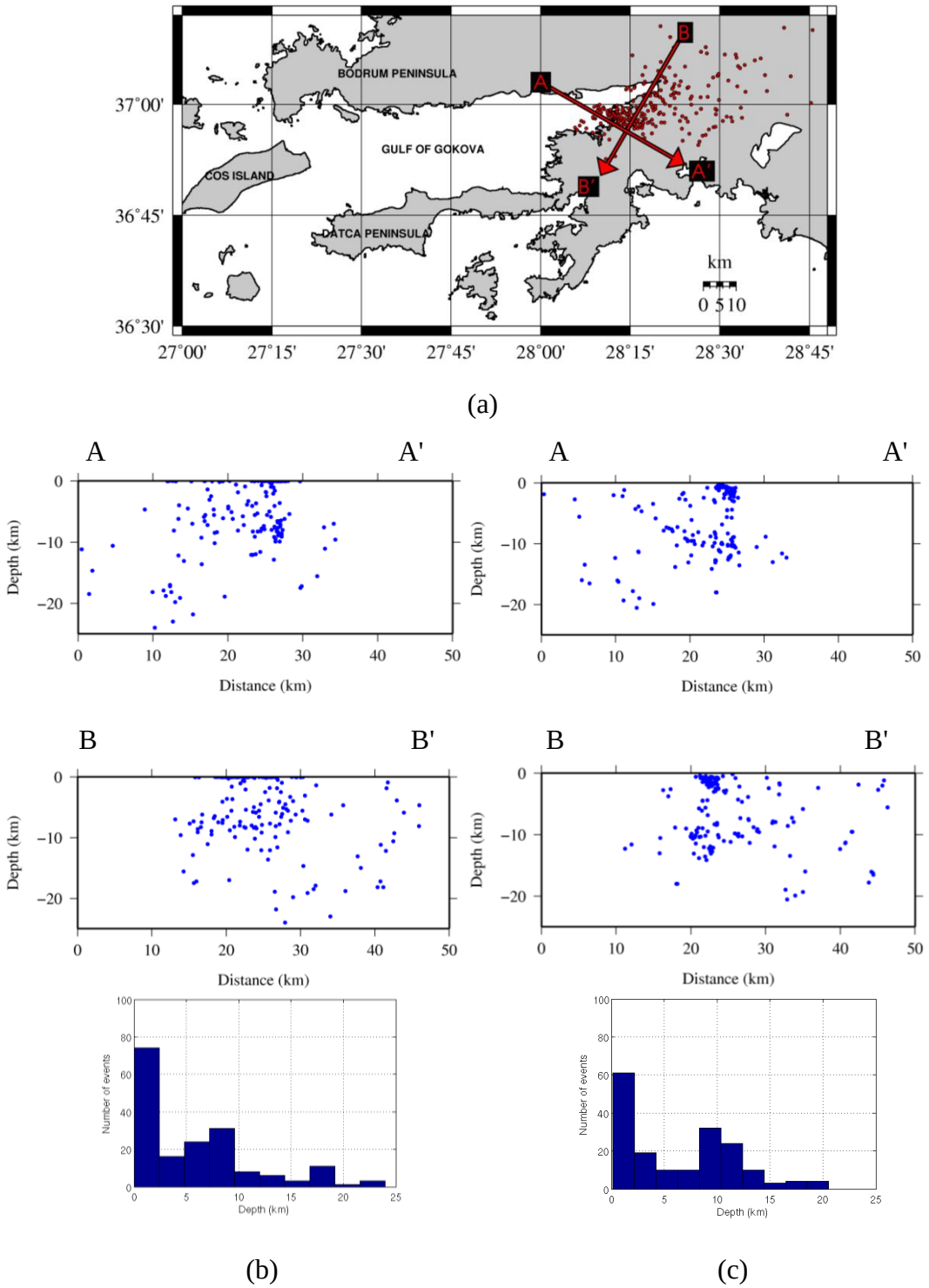

Figure A.12. (a) Original locations of the earthquakes (Cluster 4) and profiles; (b) Cross sections view in the strike (Az = 120^0N) and normal to the strike direction (Az = 210^0N) (Original Data) (Cluster 4); (c) Cross sections view in the strike (Az = 120^0N) and normal to the strike direction (Az = 210^0N) (Catalog and Cross-correlation Data) (MAXSEP = 10).

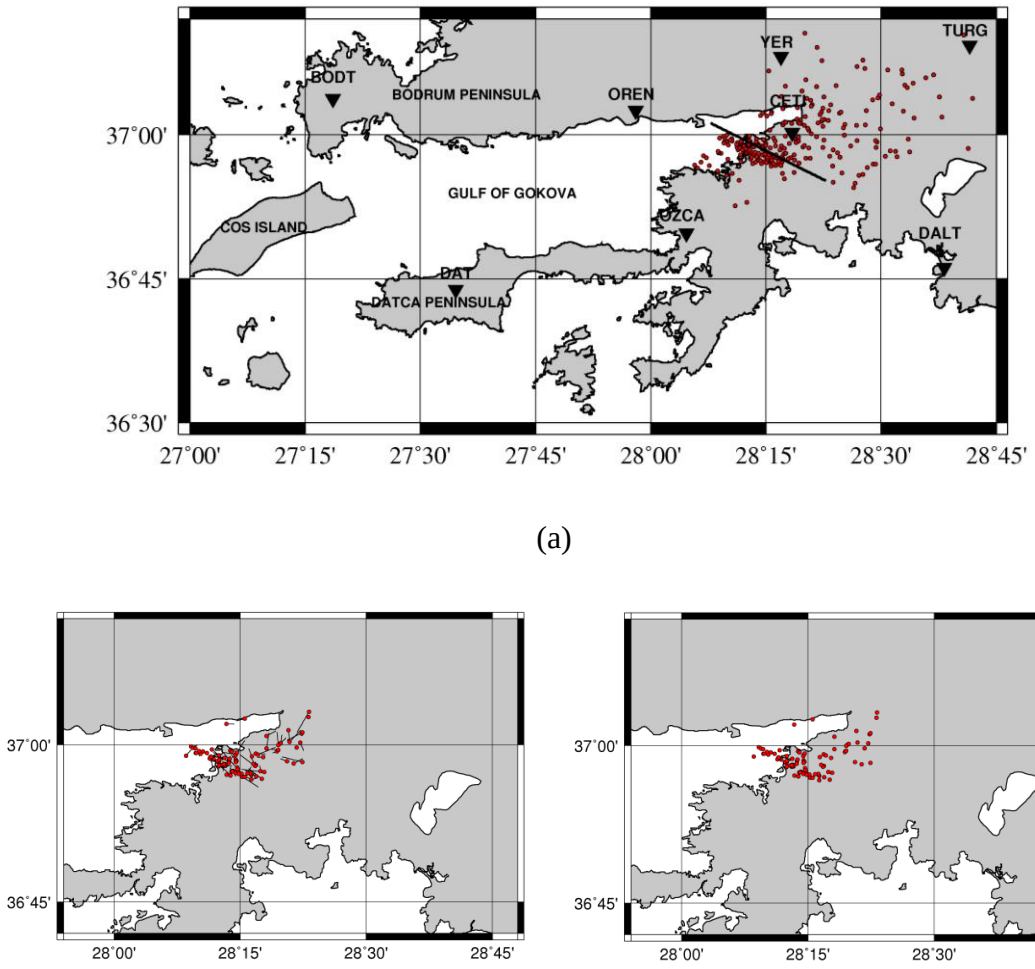

(a)

(b) (c)

Figure A.13. (a) Original Locations of the Earthquakes of Cluster 4 (HYPO71); (b) The corrections between the original and HYPODD locations (by using Catalog and Cross-correlation Data) The average distance between located (by using HYPO71) and relocated earthquakes is 1.43 km ; (c) Relocated Earthquakes (103 earthquakes) (by using Catalog and Cross-correlation Data) (MAXSEP = 5).

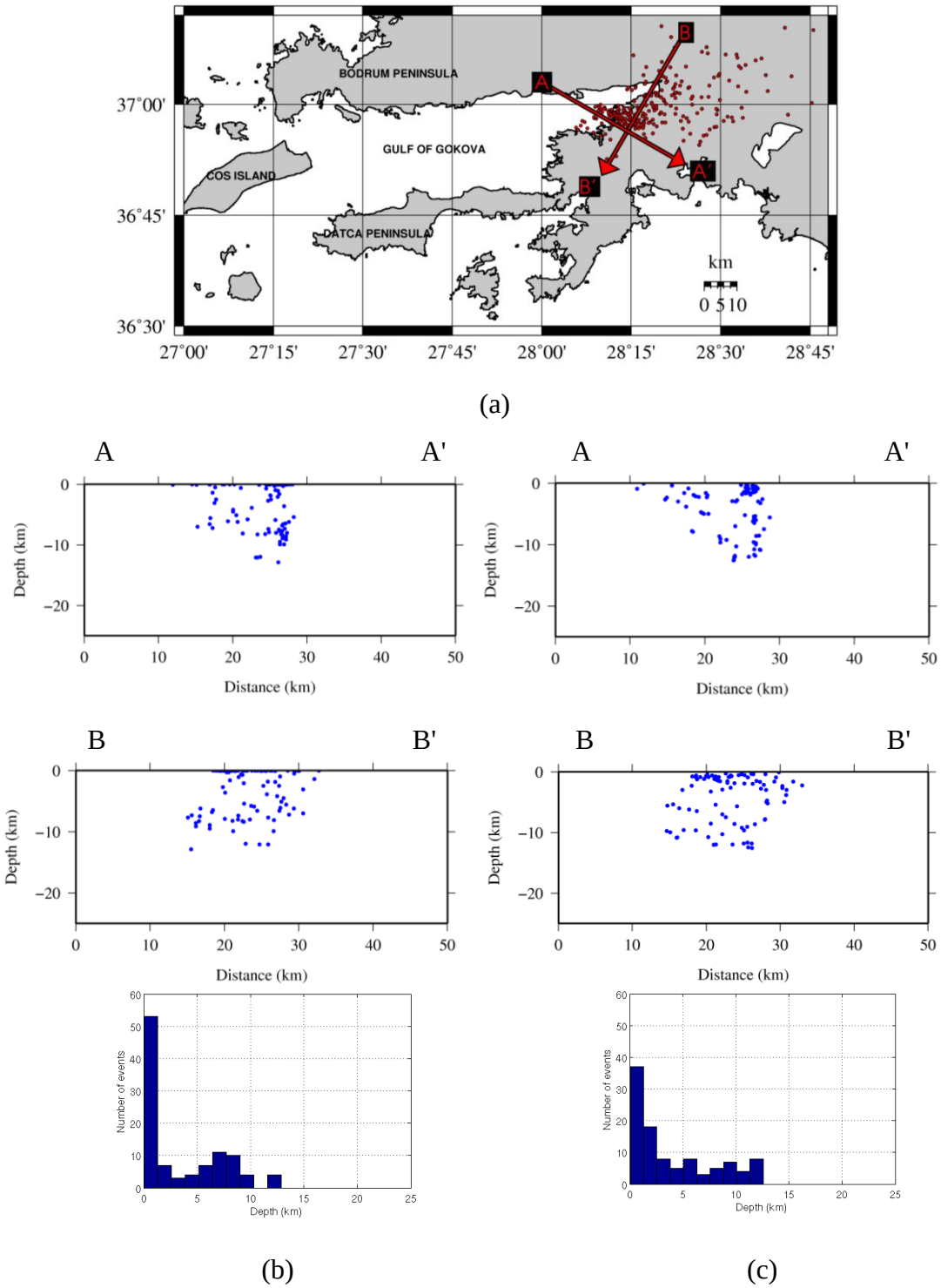

Figure A.14. (a) Original locations of the earthquakes (Cluster 4) and profiles; (b) Cross sections view in the strike (Az = 120^0N) and normal to the strike direction (Original Data) (Az = 210^0N) (Cluster 4); (c) Cross sections view in the strike (Az = 120^0N) and normal to the strike direction (Az = 210^0N) (Catalog and Cross-correlation Data) (MAXSEP = 5).